THE UNIVERSITY OF CHICAGO

UNCOVERING THE MECHANISM OF POTASSIUM CHANNEL FOLDING AND ASSEMBLY

A DISSERTATION SUBMITTED TO
THE FACULTY OF THE DIVISION OF THE BIOLOGICAL SCIENCES
AND THE PRITZKER SCHOOL OF MEDICINE
IN CANDIDACY FOR THE DEGREE OF
DOCTOR OF PHILOSOPHY

INTERDISCIPLINARY SCIENTIST TRAINING PROGRAM:
BIOPHYSICAL SCIENCES

BY
ANDREW VINCENT MOLINA

CHICAGO, ILLINOIS
DECEMBER 2023

to my parents

It must be splendid to command millions of people in great national ventures, to lead a hundred thousand to victory in battle. But it seems to me greater still to discover fundamental truths in a very modest room with very modest means—truths that will still be foundations of human knowledge when the memory of these battles is painstakingly preserved only in the archives of the historian.

Ludwig Boltzmann

A German Professor's Trip to El Dorado, translated by Bertram Schwarzschild

TABLE OF CONTENTS

LIST OF FIGURES

LIST OF TABLES

ACKNOWLEDGMENTS

This work produced many new discoveries about potassium channel folding, assembly, and stability, and generated new techniques to study membrane protein folding, but these successes were only possible due to the guidance and insight of mentors and close colleagues throughout my scientific career, as well as the tremendous support of friends and family leading up to and during graduate school.

I first want to thank my committee and Ph.D. advisors - Drs. Eduardo Perozo, Ka Yee C. Lee, Benoît Roux, and Tobin R. Sosnick - for their insightful and inspiring mentorship and guidance in my personal and professional development as a young scientist. As my undergraduate research advisor, Dr. Lee sparked my interest in pursuing joint scientific and medical careers and introduced me to M.D./Ph.D. programs for the first time. As an undergraduate chemistry major pursuing introductory graduate coursework, taking Dr. Perozo's and Dr. Roux's classes were formative. Dr. Perozo introduced me to the beautiful world of membrane protein biology, and Dr. Roux showed me how elegantly physical chemistry could be applied to biology to understand the detailed workings of proteins and lipids. In graduate school, Drs. Sosnick and Roux provided me with critical guidance for designing, executing, and interpreting what ended up being a very challenging but rewarding project, technically and intellectually. Dr. Sosnick's extensive expertise in protein folding and HDX complemented Dr. Roux's vast knowledge of molecular dynamics and KcsA physiology to produce an optimal scientific environment to support my study of potassium channel folding. Drs. Lee and Perozo supported me through my Ph.D. work as members of my thesis committee, providing invaluable feedback during this project with their backgrounds in lipid membrane biophysics and membrane protein physiology, respectfully, and I am so grateful for the opportunity to work with and learn from such inspiring advisors.

I am also grateful to the University of Chicago's Medical Scientist Training Program and the Biophysical Sciences Graduate Program, not only for helping me find such wonderful

advisors, but also for supporting me throughout my Ph.D. with resources for success in research, grant-writing, and scientific presentation. I am grateful to these programs as well as to Drs. Sosnick and Roux for building such a supportive and diverse community of scientists in graduate and medical school, in my graduate cohorts and my two research groups, many of whom have become my close friends.

Lastly, I would like to thank my friends and family, some of whom traveled long distances to Chicago to hear my thesis defense in person. I am so grateful for my friends' support — in the music we play, food we cook, and places we explore together — during what was an otherwise lonely and difficult time during the COVID-19 pandemic. I am filled with gratitude for the love and support my family has provided, now and in the years leading up to graduate school. Despite being scattered across the world and during a time of illness and loss, they have provided me with unwavering support. Most of all, I would like to thank my parents, Sharon and Vincent, for fostering my strong curiosity for nature, and for teaching me the importance of science and art from a young age. I learned from their open-mindedness and perseverance in the face of adversity, qualities which sustained me through the difficulties of my dissertation work and continue to inspire me to pursue science, medicine, and personal relationships with honesty, tenacity, and compassion.

ABSTRACT

Potassium channels are membrane proteins critical for electrochemical regulation and function in almost all animal cells. In humans, many diseases are associated with mutations in potassium channels, including life-threatening arrhythmias such as Long-QT Syndrome. The process of potassium channel folding and oligomerization is disrupted in many genetic misfolding diseases but remains poorly understood. Outstanding questions concern the structure of folding intermediates, the sequential events involving selectivity filter folding and pore helix insertion to produce the native tetramer, thermodynamic characterization, and the role and generalizability of a protein-dense phase. We have extensively studied the *in vitro* folding behavior of KcsA, a robust model system for ion channel folding for many human potassium channels such as hERG and Kv1.2. Here we characterize a novel tetrameric species under thermal denaturation with circular dichroism, tryptophan fluorescence, and SDS-PAGE. This state consists of a non-native bundle of transmembrane helices with displaced and dynamic pore helices, which we demonstrate to be metastable using our *Upside* force field. We also present results from hydrogen-deuterium exchange mass spectrometry (HDX-MS) that demonstrate the extensive stabilization of the KcsA tetramer compared to the monomer. Most notably, we adapted HDX pulse-labeling to membrane protein folding in liposomes to observe site-resolved changes in hydrogen bond formation and stability during oligomerization for the first time. We observe rapid formation of secondary structure in the transmembrane glycine zipper and the inner half of the pore helix, followed by slower folding of the selectivity filter, turret, and outer half of the pore helix on the same slow timescales of tetramer formation. In the context of our previous work, this suggests that these slow-folding structures act as an architectural "keystone" that is assembled last to stabilize the structure into its native fold.

CHAPTER 1

INTRODUCTION

1.1 The protein folding problem

The protein folding problem, first formally posed in 1936, is one of the most discussed topics in science since the release of AlphaFold2 in 2021.[25,122,126,169] The unprecedented success of this program prompted some to claim that the protein folding problem had been "solved," but in reality this problem encapsulates a wide range of very different questions, none of which have been completely resolved, and many of which remain elusive. Current perspectives on the protein folding problem can be split into two main questions: (1) Can we predict the 3-dimensional structures of a protein given its 1-dimensional amino acid sequence, and (2) what are the underlying forces that shape the energy landscape of protein motions?

The first question — structure prediction — is often approached with top-down methods, most recently with machine learning (ML), as the goal is to build a model that is most predictive of a correct protein structure. These approaches consider minimal inputs, always the 1-dimensional amino acid sequence and subsets of experimentally-solved structures in the Protein Data Bank (PDB), but sometimes additional information like related amino acid sequences. This information is then fed into a neural network-based model as in AlphaFold2 or RoseTTAFold or a language model like RGN2, an output structure is predicted, evaluated, and iteratively refined.[5,27,84]

However, in many of these approaches it is assumed that the underlying physics is too complicated and poorly-understood to be incorporated into an efficient structure-prediction model, and that it is preferable for a machine-learning algorithm to learn significant patterns within the PDB training data that are not necessarily based in physics. There is precedent for top-down approaches as these machine-learning algorithms vastly outperform more physics-based bottom-up models in structure-prediction tasks in both accuracy and

speed. In fact, in the 2020 Critical Assessment of protein Structure Prediction (CASP14) competition, the top ten performing algorithms incorporated deep learning models, and the 26$^{\text{th}}$ best method was the highest-performing non-neural network-based method, which implemented a random forest rather than a purely physics-based model.[139] Despite the unprecedented success of AlphaFold2, which was the overall best-performing model in CASP14, problems remain in the structure-prediction problem: multiple sequence alignment (MSA)-based methods including AlphaFold2 have reduced accuracy for proteins that lack known homologues, and currently are unable to accurately predict the effect of mutational perturbations.[16,134] Language-based models produce more accurate predictions for these cases, but still perform more poorly than AlphaFold2 when an MSA is available.[27,116] Ultimately, these remaining problems with current structure-prediction methods maintain experimental structure determination as an essential part of modern biology, and it is not obvious if future development of these ML-based methods will be able to make experimental methods obsolete without a full understanding of the underlying physics of protein folding.

Therefore it is important to address the second component of the protein-folding problem — protein folding from first principles — to understand the detailed dynamic processes, mechanisms, and driving forces behind protein folding. While a complete solution to this problem would necessarily solve the structure prediction problem unambiguously, solving the protein folding problem from first principles is also critical for (1) understanding the basis of many genetic diseases, (2) designing new folds of functional proteins with no known homologous sequences, and (3) filling the conceptual gap in the Central Dogma of Molecular Biology between translation and functional protein biogenesis.

Many serious diseases are caused by protein misfolding including Alzheimer's disease, prion disesases, Parkinson's disease, Creutzfeldt–Jakob disease, type 2 diabetes mellitus, and cystic fibrosis, and often lead to pathology through amyloidosis.[24,129] Even among diseases that do not produce amyloids, a large percentage of all genetic diseases, particularly

those arising from missense mutations or short in-frame insertions or deletions, are ultimately protein-folding diseases.[14,80] Current approaches to predicting protein misfolding and pathology caused by missense mutations must rely on a physics-based understanding of protein folding, since MSA-based methods poorly predict effects of point mutations on protein stability.[16,134] However, more recent studies suggest that AlphaFold2 could improve its prediction of mutational effects on structure by predicting multiple structures without using structural templates, and measuring the effective strain at the site of mutation rather than pLDDT or RMSD.[113]

Many protein engineers seek to build new proteins from scratch that have novel functions not found in nature. To do this, they often seek to define new folds. This *de novo* protein design is very challenging for MSA-based methods like AlphaFold2 if these newly-defined folds lack significant sequence homology with existing proteins, and may require protein engineers to incorporate physics-based considerations into their design process.[60,121,138]

Lastly, while the Central Dogma of Molecular Biology posits that all of the information required to fold a protein is contained in its 1-dimensional sequence of amino acids, this is increasingly accepted to be an oversimplification. The final functional forms of proteins is determined not just by amino acid sequence, but also by the highly-tuned physical and chemical environment surrounding it as it folds and is trafficked to its final destination: Aqueous or lipidic solvents, salt concentrations, temperature, cofactors, chaperones, and regulatory enzymes and proteases are among the many physical determinants of protein folding. Current top-down structure prediction models handle the genuine conformational diversity of proteins poorly, and most do not incorporate any chemical or physical information about the solvent conditions or protein thermodynamics in their inputs because they do not explicitly predict the stability of their generated structures.

1.2 Membrane protein folding

Most studies of protein folding have been centered on the folding of small, water-soluble proteins. This is because of their high levels of expression in bacterial purification systems, susceptibility to chaotropic denaturants, ease of measurement by techniques such as small angle x-ray scattering (SAXS), circular dichroism (CD) spectroscopy, and hydrogen-deuterium exchange (HDX) coupled with mass spectrometry (MS) or nuclear magnetic resonance (NMR). Many small, water-soluble proteins often have a long shelf-life and resistance to aggregation.

However, membrane proteins are also critical components of cellular biology, essential for signaling, transport, movement, and homeostasis. While membrane proteins only account for 20 to 30% of the proteome, they are targets of around 60% of pharmaceutical drugs.[133,165] Many protein misfolding diseases involve membrane proteins like cystic fibrosis, retinitis pigmentosa, Charcot-Marie-Tooth disease, and long-QT arrhythmias, and therefore the study of their folding is important for medicine as well as basic biology.[153,160]

Studying membrane protein folding is challenging for many reasons: (1) They are often expressed in very low yields, often from animal cell lines that are difficult to culture. (2) Membrane proteins often have very short shelf-life and aggregate quickly after purification, requiring experiments to be short and carried out immediately after purification.[12] (3) They are often regulated by diverse lipid membranes, which may contribute to large artifacts and debilitating signal-to-noise problems when studied with traditional methods like CD and HDX. The lipid requirement of membrane protein folding also necessitates large computational resources to properly simulate membrane proteins embedded in large membranes of explicit lipids with molecular dynamics (MD) simulations. (4) The unfolded state, or disordered state ensemble (DSE) of membrane proteins is much complex than that of water-soluble proteins, and often is highly dependent on the mode of denaturation used to approximate the DSE.[51,53] Additionally, as we show in this work, many denaturants commonly used to study water-soluble proteins do not perturb certain small, stable membrane

proteins like the potassium channel KcsA.[12]

Integral membrane proteins can be grouped into two main categories: (1) alpha-helical membrane proteins, found throughout animal membranes and the inner membrane of prokaryotic organisms, and (2) beta barrel membrane proteins, found in the outer membranes of prokaryotic organisms, chloroplasts, and mitochondria.

Some beta barrel membrane proteins can be folded *in vitro* from a urea-denatured state into lipid membranes, much like water-soluble proteins.[13,39,43] In cells, the folding machinery of these proteins is much more complex, as they must be extruded as an unfolded chain through pores in the inner membrane into the periplasm, after which they are inserted and folded into the outer membrane with the help of a large complex of specialized machinery including chaperones.[23,74,137]

Alpha helical membrane proteins, which are the focus of this work, are more difficult to fold *in vitro*. Bacteriorhodopsin (bR) monomers can be folded from an SDS-partially denaturated state into membranes, and monomers of potassium channels KcsA and KvAP can be refolded from SDS-solubilized monomers into native tetramers in lipid membranes.[42,79,104,114,173,174] From their studies of bR, in which they refolded separate, alpha-helical proteolytic fragments of bR into lipids to produce a state optically indistinguishable from the native state and capable of binding retinal, Popot and Engelman proposed a "2-stage model" of alpha helical membrane protein folding: (1) Transmembrane helices insert into the membrane, followed by (2) helical packing into the native structure.[142] A decade later they amended this model into a "3-stage model" of folding, adding an additional step at the end of the 2-stage model in which prosthetic groups, ligands, and additional structural elements like short helices insert into the transmembrane helical bundle to form the native structure.[49]

Due to the known diversity of the DSE of membrane proteins, and with new methods to study membrane protein folding in purified systems and cotranslationally, the Popot and Engelman models are now accepted as oversimplified. These modern methods include par-

tial chemical denaturation, often with SDS or urea, mutational ψ analysis, directed pulling experiments, often with AFM or optical or magnetic tweezers, and steric trapping experiments.[35,53,82,91,120,128,136,158,177] These methods are often coupled with computational analyses including MD simulations to resolve more molecular detail.[30,51,53,54,111,184] Altogether, these techniques allow researchers to control the folded state of a membrane protein and estimate folding and unfolding rates as well as thermodynamic parameters. They have also revealed the great complexity in membrane protein DSEs, which are often highly dependent on the mode of denaturation or refolding and the system in which the membrane protein is reconstituted (e.g. detergent micelles, mixed micelles, nanodiscs, bicelles, liposomes, or cell membranes).[31,53,68,77,156] Further, recent advances in hydrogen-deuterium exchange mass spectrometry, including those presented in Chapter 5, are now being applied to membrane proteins. A more detailed review of these advances is given in Chapter 2. In cells, integral membrane proteins are inserted into the lipid bilayer cotranslationally via a ribosome-docked translocon, often with many ribosomes on a single mRNA transcript, and many require additional chaperones to partition into the membrane efficiently and with the correct topology.[56,99,164,176,181,182,186] The separation of membrane insertion and formation of tertiary contacts proposed by the Popot and Engelman models is being additionally challenged by the knowledge of cotranslational membrane protein folding. Several groups including the Deutsch and von Heijne labs are able to measure the force required to arrest peptide formation in the exit tunnel of the ribosome. They find significant secondary structure is formed in the exit tunnel and is retained upon passage into the translocon, suggesting that many helices are already formed and available for tertiary structure formation upon exiting the translocon.[36,37,40,54]

Despite these modern methodological advances to study helical membrane protein folding *in vitro* and *in vivo*, relatively few studies focus on the folding and assembly processes associated with helical membrane protein oligomerization. Dimerization studies of ClC-ec1

and Fluc channels by subunit capture, single-molecule photobleaching, and coarse-grained molecular dynamics (CG-MD) simulations suggest a central role of the lipid membrane in driving dimerization.[20–22,50] Studies of higher-order oligomers are often limited to the study of single pass transmembrane helix association.[33,166] However, unfolding experiments have studied the contribution of oligomeric structure to protein stability in larger, more complex proteins.[154,178,190]

Potassium channels are class of multi-pass alpha helical membrane protein comprising four independent subunits whose assembly into a tetramer has been studied in detail. Soon after solving the structures of prokaryotic potassium channel KcsA (K channel of streptomyces A) from *Streptomyces lividans* and KvAP, a voltage-gated channel from *Aeropyrum pernix*, the lab of Dr. Roderick MacKinnon began to study the folding of these channels. They found that KcsA could be folded into native tetramers in lipids from a semi-synthesized state, combining a recombinant peptide (residues 1 to 73) with a synethetic peptide (residues 74 to 125).[173] They also found that wild type (WT) KcsA requires lipids for refolding to the native tetramer, and that KcsA binds anionic lipids at an interfacial binding site between monomers near the lipid-water interface. Anionic lipid binding was not required for folding, but was essential for potassium conductance.[174] The González-Ros group has extensively studied KcsA unfolding, and has also observed lipid-dependent refolding from trifluoroethanol (TFE) denatured states.[8,9,18] The lab of Dr. Ben de Kruijff measured the efficiency of KcsA folding in the absence and presence of the signal recognition particle as well as components of translocon machinery, but find that KcsA can be refolded into native tetramers in the absence of any translocon.[38] Studies of the closely-related potassium channel KvAP have been conducted by the Valiyaveetil group and reveal a strong temperature and lipid-dependence on tetramerization rate. They also find that the KvAP monomer inserts rapidly from SDS micelles into membranes, and that, unlike KcsA, the cytosolic domain of KvAP is required for tetrameric structure to form.[42,114]

1.3 A model for potassium channel pore domain folding

We have chosen to further study KcsA, as it is a robust model for the folding of the pore domain of many potassium channels like hERG and Kv1.2. KcsA is a homotetrameric channel consisting of four multi-pass alpha helical transmembrane monomers surrounding a central pore. Starting from the N-terminus, KcsA begins with a amphipathic peripheral membrane M0 helix. This is followed by a transmembrane helix, TM1, a water-exposed turret loop, a short and highly conserved pore helix, followed by an even shorter selectivity filter. After a short loop, the protein reenters the membrane as a kinked transmembrane helix TM2, which forms the walls of the water-filled cavity in the center of the tetramer, capped by the highly charged intracellular gate and, at the C-terminus, the cytosolic domain. **Figure 1.1** shows many of these components, including the lipid-exposed surface of the monomer, which notably contains many polar residues.

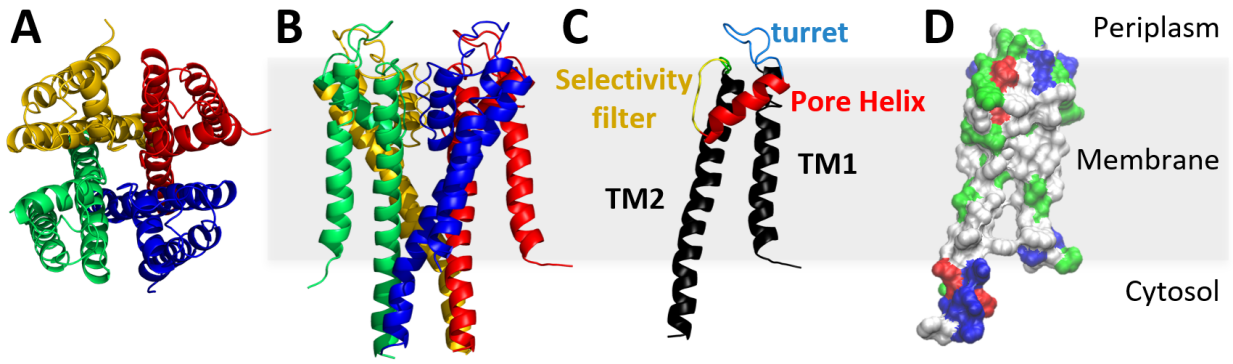

Figure 1.1: KcsA Transmembrane Domain [Protein Data Bank (PDB) ID 3EFF]. **A,** and **B.** Top, side views. **C.** Monomer: TM helices TM1, TM2, pore helix, turret, and selectivity filter. **D.** Surface residues (polar, basic, and acidic residues are colored green, red, and blue, respectively). Figure adapted from Song et al., *PNAS* (2021).

We have built upon the work of MacKinnon and Valiyaveetil, and more extensively characterized the folding and tetramerization process of SDS-solubililzed KcsA monomers inserted into azolectin (soy) small unilamellar vesicles (SUVs). We found that: (1) KcsA rapidly inserts from monomers into a protein-dense phase within the membrane, (2) heterogeneous folding kinetics to the native tetramer ensue, with the amount of flux down

misfolding pathways controllable using an engineered topology-maintaining disulfide bond, and (3) tetramerization rate is irrespective of monomer concentration in free solution.[158] Outstanding questions concern the identification of the rate-limiting step, the structure of folding intermediates, the role of a protein-dense phase, and thermodynamic characterization of channel folding.

With Förster resonance energy transfer (FRET) spectroscopy, we have observed the formation of a protein-dense phase, initially consisting of monomers rapidly inserting into the lipid membrane from a detergent-solubilized state. The dense phase is maintained throughout tetramer formation, suggesting that monomers in the dense phase are dynamic and undergo rearrangements and diffusion before folding into tetramers.[158] It is well established that native tetramers of KcsA form large, supramolecular clusters that may be involved in cooperative gating.[9,58,70,124,148,179] In fact, protein clustering within and peripheral to the membrane is emerging as a general phenomenon in biology, and may have implications ranging from cooperative gating of ion channels to assembly of active complexes in immune signaling.[10,41,140,161,187] It is difficult to study the biophysical bases of these supramolecular membrane protein clusters, because few existing models for membrane protein phase separation bridge the gap between the molecular detail necessary to study any site-specific protein-protein interactions and the macro-scale material properties of the protein and lipid phases necessary to interpret the long-range behavior of these clusters in the context of cells.[2] However, several groups, including the lab of Dr. Sarah Veatch are quickly bridging this gap between macro-scale phase separation at the membrane and detailed molecular models.[92,152,155] Our observation of a protein-dense phase forming early during channel formation is a novel observation of membrane protein clustering, though it remains unclear if this phase has any function in the folding process, or even exists in real cells at all. However, a thorough investigation into the importance of the protein-dense phase in KcsA folding will be left for future studies.

In this dissertation, I was instead interested in studying the site-resolved structural changes associated with KcsA folding and unfolding. In other words, we sought to answer: What structures are most important for the stability of the natively-folded KcsA tetramer, and what parts of the structure fold or unfold first? How unfolded are different structures within the KcsA monomer, and how much stability do these same structures gain in the tetramer? Can we characterize the site-resolved dynamics of secondary-structure formation during KcsA folding and tetramerization?

To answer these difficult questions, we need to integrate a wide variety of optical, biochemical, and computational techniques for detailed folding and stability measurements, and we need a theoretical framework for approaching these problems. Any process of potassium channel folding starts with membrane insertion of the monomers, either *in vitro* from a detergent-solubilized state or *in vivo* using cellular insertion machinery. This is a very flexible and highly dynamic state.[158] The monomers can then follow one of three possible paths: (1) A "native assembly" model, in which each monomer independently folds into a structure with native-like contacts and stability, followed by a tetramerization step of native-like monomers, (2) "keystone" model, in which the transmembrane helices form a tetrameric bundle first, followed by insertion and folding of pore helices and selectivity filters (the "keystone"), and (3) a "cooperative" folding model in which transmebrane helices form a tetrameric bundle simultaneous to pore helix and selectivity filter insertion and folding. This theoretical framework is summarized by the model in **Figure 1.2**.

Note that these models are likely oversimplified, but serve as a useful theoretical framework to contextualize our folding and unfolding studies of KcsA. Additionally, while these models can apply to the pore domain folding of most potassium channels, they does not include the folding of cytosolic or any voltage sensing domains.

In Chapter 3, we study conformational changes of the KcsA tetramer under different modes of denaturation. We find that the stability of KcsA is determined by the presence of

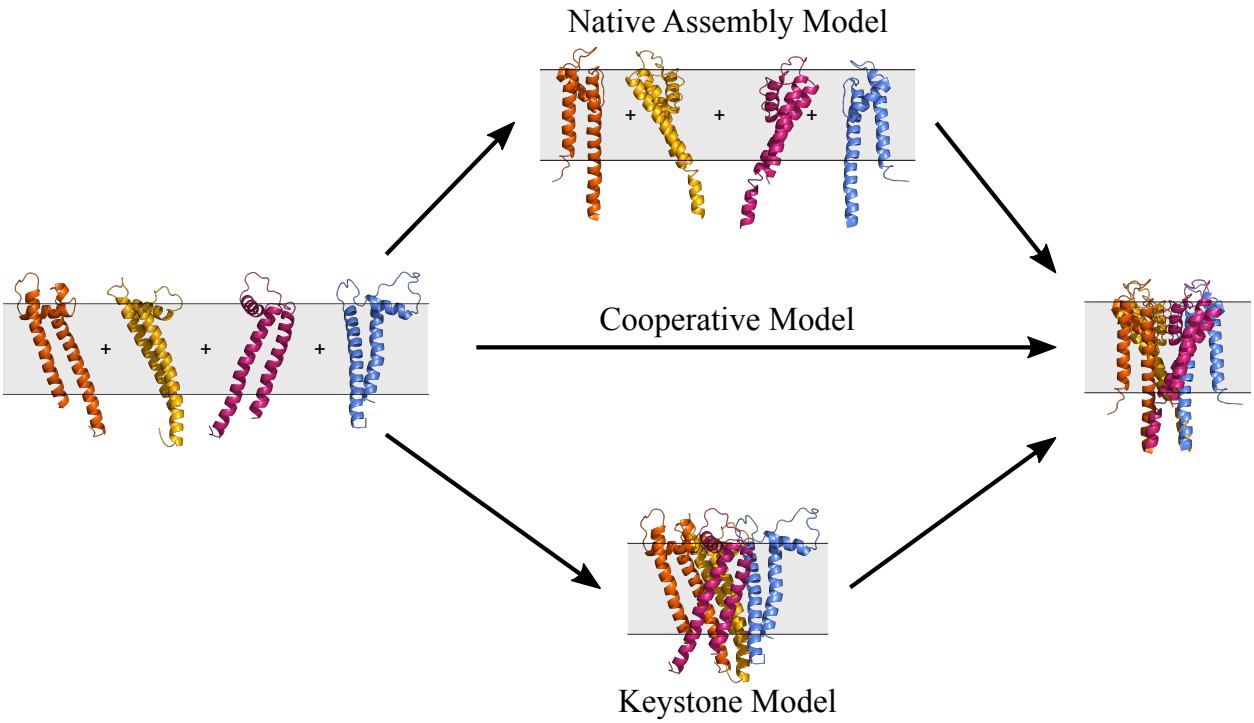

Figure 1.2: 3 Models for Potassium Channel Pore Domain Folding and Assembly

lipid or detergent, monovalent cations, and surprisingly, the choice of experimental buffer. Under thermal denaturation, we observe a sequential and irreversible unfolding pathway starting with displacement and unfolding of the pore helices, followed by disassembly of the tetramer, and ultimately monomer aggregation. We also characterize a novel state of KcsA observed at 50°C constisting of a tetrameric transmembrane helix bundle with displaced and dynamic pore helices that we observe to be metastable by CG-MD and resembles the intermediate state in the "keystone" model of folding. In Chapter 4, we measure the native-state HDX of KcsA monomers and tetramers in DDM micelles, in the presence and absence of potassium ions, and with chaotropic denaturant. We find that the tetramer of KcsA is extremely stable, especially in relation to the structured, but less stable KcsA monomer. Urea was observed to disrupt only a few locations on the tetramer, including destabilization of TM1 and the loop to TM2, and unexpected stabilization of the C-terminal end of the M0 helix. Equally unexpected was the absence of tetramer stabilization measured in high

potassium conditions. In the context of KcsA assembly, the large difference in stability between monomeric and native tetrameric states argues against the "native assembly" model. In Chapter 5, we adapt HDX pulse-labeling to study the folding and oligomerization of a membrane protein in liposomes with peptide-level resolution for the first time. We observe rapid folding of TM2 and the inner half of the pore helix, followed by slower folding of the outer half of the pore helix and attached selectivity filter and turret. By SDS-PAGE, we observe that native tetramers are formed on the same timescales as the slow-folding components measured by pulse-labeling. Pulse-labeling experiments, as well as native-state HDX measurements of the KcsA monomer, required a novel purification of a folding-competent, monomeric form of KcsA in DDM, which we report in Chapter 2. Altogether, unfolding experiments and CG-MD are suggestive of the "keystone" model for folding, while native-state HDX argues against the "native assembly" model. However, we remain agnostic to the resemblance of the real folding pathway to either the "keystone" or "cooperative" folding models since we are not yet able to measure the rate of transmembrane helix bundle formation or inter-monomeric pore helix contacts from these methods alone. However, the observation that the pore helix, selectivity filter, and turret fold on the same timescales as native tetramer formation suggest that these structures can be considered the "keystone" component. As in an architectural arch, these structures form last, locking the tetramer into its stable, native fold.

CHAPTER 2

MATERIALS AND METHODS

2.1 Introduction to HDX

HDX is an integral tool for studying protein folding and dynamics with high spatial and temporal resolution. Compared to other methods to probe protein stability and solvent accessibility that involve making mutations for the attachment of large chemical labels, HDX is non-perturbative: It requires no mutations, it can probe the backbone stability of potentially all non-proline residues in the protein simultaneously, and the backbone hydrogen exchange reaction that it takes advantage of is a naturally-occurring process for all proteins with their surrounding water. All applications of HDX involve the labeling of backbone amide protons by deuterium, from heavy water. This can occur as an acid- or, more commonly, base-catalyzed reaction. There are different ways to determine what part of the protein was labeled: (1) nuclear magnetic resonance (NMR), in which the rates of decay of site-resolved peaks resulting from deuterium labeling are measured, or (2) mass spectrometry (MS), in which the protein is proteolyzed into many peptide fragments whose mass shifts upon deuterium labeling are measured by mass spectrometry. In this work, we couple HDX to MS and measure deuterium content of KcsA peptides by the average m/z shift of their mass distributions upon labeling. **Figure 2.1** shows representative spectra of peptide VAGITSFGLVTAAL in the KcsA monomer from undeuterated (magenta) to full uptake (green).

In any HDX experiment, deuterium can only exchange with the amide hydrogen if that hydrogen is not actively participating in a hydrogen bond. Taking advantage of this, there are two main kinds of experiments that can be conducted to measure the folded state of that backbone amide under different conditions: native-state HDX and HDX pulse-labeling. Native-state HDX measures equilibrium backbone dynamics by applying deuterium pulses of varying lengths to a protein sample in equilibrium. A protein at equilibrium is not static.

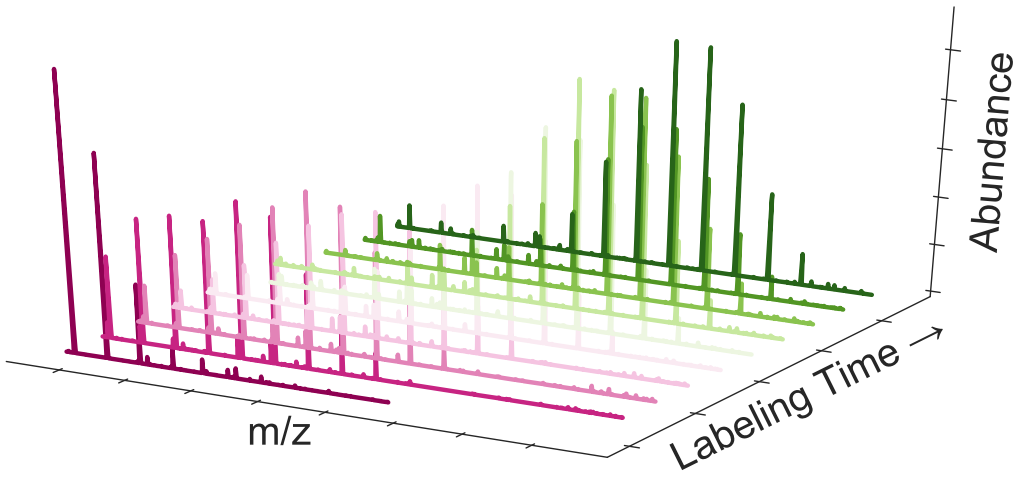

Figure 2.1: Mass spectra of TM2 peptide VAGITSFGLVTAAL from native-state HDX of KcsA monomer in DDM, from undeuterated (magenta) to full uptake at 24 hours (green). The undeuterated mass distribution reflects the natural isotopic distribution in an unlabeled peptide, whereas the fully labeled mass distribution is binomially distributed.

Rather, it is undergoing thermal fluctuations that transiently break and reform the backbone hydrogen bond structures. The probability of these structures breaking is inversely related to the equilibrium stability of that structure. In other words, if a backbone amide can only pick up a deuterium at long labeling times during a native-state experiment, then that amide is very stably folded compared to a less stable amide that is only rarely hydrogen bonded and can therefore pick up a deuterium quickly, at short labeling times. In an HDX pulse-labeling experiment, the duration of deuterium pulse is held constant but the protein is undergoing a non-equilibrium process. This can be protein folding, binding, or changing conforational state. In pulse-labeling, changes in deuterium occupancy of an amide group represent changes in the folded state of that amide over the course of the non-equilibrium process. A schematic comparing a typical native-state experiment to a pulse-labeled experiment for KcsA is shown in **Figure 2.2**.

The equilibrium expression governing hydrogen-deuterium exchange for a given part of

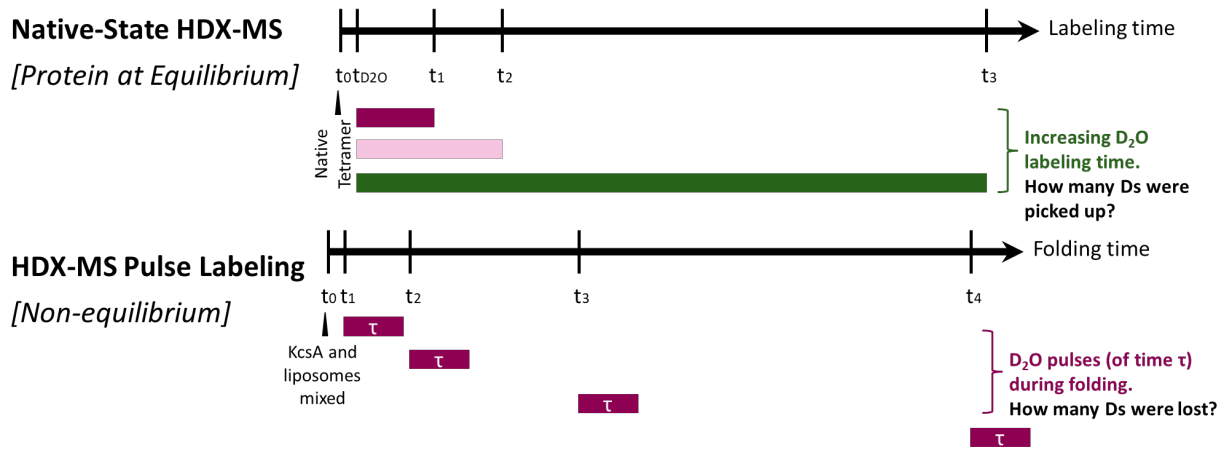

Figure 2.2: Schematic depiction of native-state versus pulse-labeled HDX-MS experiments.

a protein is given by Equation 2.1:

$$\text{Folded} \underset{k_{\text{fold}}}{\overset{k_{\text{unfold}}}{\rightleftharpoons}} \text{Unfolded} \xrightarrow[k_{\text{intrinsic}}]{\text{D}_2\text{O}} \text{Exchanged} \tag{2.1}$$

Generally, the observed hydrogen-deuterium exchange rate, k_{HDX}, of an amide hydrogen is given by

$$k_{\text{HDX}} = \frac{k_{\text{unfold}}\, k_{\text{intrinsic}}}{k_{\text{unfold}} + k_{\text{fold}} + k_{\text{intrinsic}}} \tag{2.2}$$

In what is called the EX2 limit, $k_{\text{fold}} \gg k_{\text{intrinsic}}$, and given $K_{\text{eq,folding}} \equiv k_{\text{fold}}/k_{\text{unfold}}$, Equation 2.2 simplifies to

$$k_{\text{HDX}} = \frac{k_{\text{unfold}}\, k_{\text{intrinsic}}}{k_{\text{unfold}} + k_{\text{fold}}} \sim \frac{k_{\text{intrinsic}}}{K_{\text{eq,folding}}} \tag{2.3}$$

We can estimate the free energy change, ΔG_{fold}, associated with forming a backbone hydrogen bond with this amide hydrogen by measuring the protection factor, $k_{\text{intrinsic}}/k_{\text{HDX}}$.

$$\Delta G_{\text{fold}} = -RT \ln(K_{\text{eq,folding}}) \sim -RT \ln \left(\frac{k_{\text{intrinsic}}}{k_{\text{HDX}}} \right) \tag{2.4}$$

In the EX1 limit, $k_{\text{fold}} \ll k_{\text{intrinsic}}$, and Equation 2.2 simplifies to

$$k_{\text{HDX}} \sim k_{\text{unfold}} \tag{2.5}$$

In this way, conducting HDX in the EX2 limit yields thermodynamic information about the folding/unfolding equilibrium while an EX1 HDX experiment produces kinetic information about changes in hydrogen-bond structure during a non-equilibrium folding or unfolding process. Therefore, native-state HDX often makes use of the EX2 limit to measure hydrogen bond stabilities in a protein at equilibrium. Pulse-labeling HDX experiments are less clearly in the EX2 or EX1 regime, and often different parts of a protein will exhibit EX2 or EX1 behavior during the same folding or unfolding process.

In Chapter 4, we measure native-state HDX of the KcsA monomer and tetramer in DDM in the presence of different ions and denaturants. We observe extreme stability in the tetramer, with incomplete uptake in almost the entire protein after 24 hours of labeling in pD 8.5 deuterium buffer at 25°C. However, we measure complete uptake in a single part of the tetramer, the M0 helix, from no deuterium uptake at 1 s to saturated labeling around 10,000 s (**Figure 2.3**). In one peptide from the M0 helix, LARLVKL, we have chosen to represent this saturated deuteration level, which remains around 4 deuterium atoms through at least 24 hours in labeling, as our upper labeling limit, the "all-D" reference state. This peptide never reaches the theoretical limit of 5 deuterium atoms because of a phenomenon called "back-exchange" in which deuterated backbone amides can exchange their deuterium back to protium from bulk water during proteolysis or desalting. There is also a potential

for "forward-exchange" arising from new deuterium atoms being picked up by an unlabeled backbone amide from residual deuterium during these same processes, but in LARLVKL, we observe almost no forward-exchange. We can normalize the uptake curve of this peptide to the "all-D" level, and fit the curves to a single or double exponential fit of the following form, where A, B, and C are scaling constants, and k_{HDX} is the measured exchange rate for a single exponential fit, while k_{HDX1} and k_{HDX2} are the measured exchange rates for a double exponential fit:

$$\text{Single Exponential Fit} : \#\text{Deuterium} = C\left(1 - Ae^{-k_{\mathrm{HDX}}\cdot t}\right)$$
$$\text{Double Exponential Fit} : \#\text{Deuterium} = C\left(1 - Ae^{-k_{\mathrm{HDX1}}\cdot t} - Be^{-k_{\mathrm{HDX2}}\cdot t}\right)$$

A single exponential fit would be most appropriate if, for example, the entire peptide exchanged cooperatively (i.e. when it unfolds, it unfolds all together, and all amide protons are equally likely to exchange), but from **Figure 2.3**, it appears that a double exponential fit is most appropriate, suggesting that this peptide exchanges in two halves, with the faster half exchanging at $k_{\mathrm{HDX1}} \sim 30/s$ and the slower half exchanging at $k_{\mathrm{HDX2}} \sim 0.0009/s$. However, since we don't know which rates correspond to which residues, we cannot estimate the $k_{\mathrm{intrinsic}}$ corresponding to these exchange rates, so we cannot calculate free energies of folding for each half. However, we know that the single exponential fit, with $k_{\mathrm{HDX}} \sim 0.001/s$, represents the average exchange of the entire peptide LARLVKL for which we can estimate $k_{\mathrm{intrinsic}} = 470/s$.[6,28,130] Assuming we are exchanging in the EX2 limit, then by Equation 2.4, the free energy associated with folding this peptide is $\Delta G_{\mathrm{fold}} \sim -8$ kcal/mol. Since the rest of the KcsA tetramer in DDM was not observed to reach "all-D" by 24 hours, it is likely that much of the protein has an even greater stability than the M0 helix, with $\Delta G_{\mathrm{fold}} < -8$ kcal/mol.

Pulse-labeling experiments in Chapter 5 exhibited mostly EX2-like behavior, though

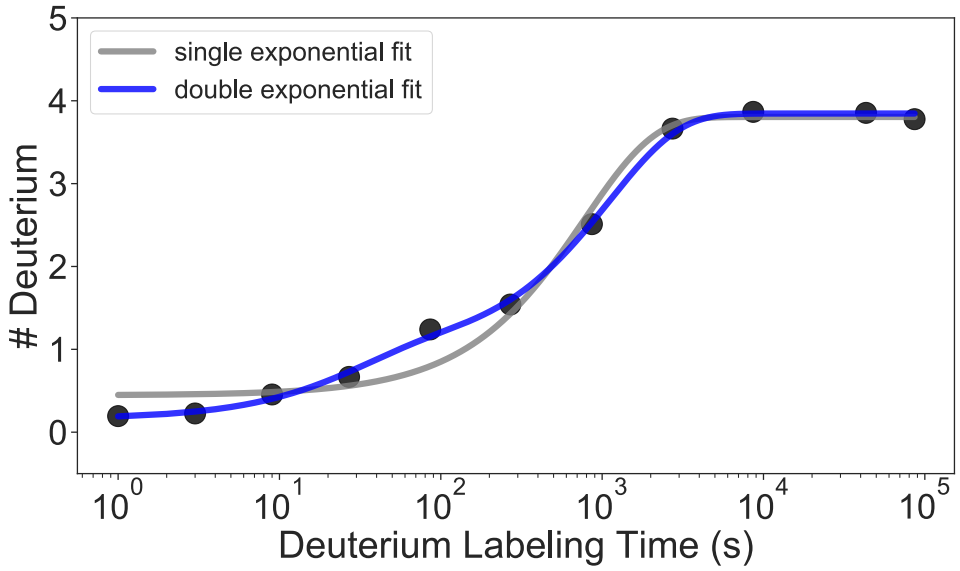

Figure 2.3: HDX-MS uptake curves for M0 helix peptide "LARLVKL" showing single and double exponential fits.

interpretation of the observed bimodality in some peptides is discussed in detail in Section 5.3.

2.2 Development of a new HDX-MS technique

The vast majority of both native-state and pulse-labeling HDX-MS studies have focused on water-soluble proteins, with current development focused on increasing the resolution of HDX-MS data by improving peptide coverage and developing new analysis methods of MS and MS-MS labeled spectra.[66,78,86,87,183]

However, the development of HDX techniques for membrane proteins significantly lags behind that of water-soluble proteins. This is because the presence of membranes and membrane mimetics pose many additional challenges related to lipid removal, ion suppression, stability against chemical denaturation, and generally poor digestion efficiency of integral membrane proteins, aside from low protein yield during expression and high tendency to form protein aggregates outside of lipids and detergents. Additionally, while the same general methodologies work for HDX on most water-soluble proteins, HDX methods must be

optimized individually for each membrane protein and each membrane mimetic system.[110] These considerations are discussed for HDX pulse-labeling of KcsA in detail in Chapter 5.

To our knowledge, the first application of HDX to a membrane protein was in 2004, in which detergent-solubilized microsomal glutathione transferase 1 was found to have significant movement of transmembrane helices and reorganization of its cytosolic domain upon glutathione binding with native-state HDX coupled to crystallography.[17] This was followed by many other membrane protein HDX studies from detergent-solubilized states. These focused in particular on conformational changes in transporters and G-protein coupled receptors (GPCRs).[19,47,48,57,102,115,118,191] Notably, HDX has also been applied to ATP-driven conformational dynamics of the prokaryotic translocon machinery SecYEG-SecA.[30] Several groups including our own have begun to study HDX of membrane proteins in lipids. Different self-assembled lipid structures — bicelles, nanodics, SMALPs, and liposomes — require different protocols for lipid removal and proteolysis.[1,44,69,83,112,144] One study even used HDX to study conformational changes of the γ-rotor shaft of ATP synthase in liposomes under a proton gradient across a membrane in liposomes.[172] This is notable because the lipid load from liposomes is higher than that of bicelles, nanodiscs, or SMALPs, so the required lipid removal before MS analysis is harder. However, this work focused on water-soluble domains of ATP synthase, and we found that their methods were insufficient to resolve transmembrane peptide signal from KcsA in liposomes in our own experiments. Lastly, our group has begun developing HDX methods for *in vivo* applications, and we have measured deuterium uptake of a beta barrel in the outer membrane of live *e. coli* cells.[101]

While some of these studies have observed limited EX1 behavior, almost all existing studies of membrane protein HDX consist of native-state HDX measurements in the EX2 limit. To our knowledge, only a single study has successfully conducted pulse-labeling of a membrane protein in lipid bilayers.[89] This study folds bR monomers from an SDS-partially denatured state into bicelles. They observe significant changes in deuterium incorporation

during monomer refolding, but because they are limited to whole-protein measurements, it remains unknown where this deuterium incorporation occurs within bR. Here, we adapted HDX-MS pulse-labeling for site-resolved membrane protein dynamics in liposomes. We have optimized a method for on and off-column digestion with pepsin and FPXIII (fungal pepsin from *Aspergillus saitoi*, type XIII) and efficient lipid removal using a suspension of BSA-blocked ZrO_2 beads, which are used during mechanical agitation and sample frothing. With this method, we can now observe changes in hydrogen-bonded structure and dynamics in a membrane protein undergoing tetramerization with peptide-level resolution.

We report this optimized protocol here, along with all other materials and methods used in this work.

2.3 Materials

Chemicals were purchased from Sigma-Aldrich (St Louis, Missouri) unless otherwise noted. All detergents were purchased from Anatrace (Maumee, OH), and all lipids were purchased from Avanti Polar Lipids (Alabaster, Alabama).

2.4 HDX pulse-labeling of KcsA folding in liposomes with peptide-level resolution

KcsA folding was initiated by mixing 2 μL KcsA Δ125 monomer (35 μM in 50 mM Na-Phosphate pH 7.5, 100 mM NaCl, 1 mM DDM) with 2 μL azolectin SUVs (prepared as described below) for various folding times, t_{fold}, at room temperature, 25°C. We then added 26 μL of pulse buffer (20 mM Tris pD 7.0, 8.0, or 9.0, 100 mM NaCl, 1 mM DDM) for a 6 s pulse duration, $\tau_{\text{pulse}} = 6s$. 30 μL quench buffer, consisting of 600 mM glycine pH 2.5, 100 mM NaCl, 3 M urea, 1 M thiourea, and 0.4% DDM was added to stop the labeling reaction. To start soluble protease digestion, 2 μL of pepsin (Sigma-Aldrich, reference no.

P6887, with optical density 6 in 100 mM sodium citrate, pH 4.4) was added, and incubated for 4 minutes at room temperature. At this point, 4 μL of approximately 190 mg/mL ZrO_2 (Sigma-Aldrich, reference no. 55261-U, and blocked with bovine serum albumen, BSA) were added. Critically, the sample was vigorously frothed by pipetting up and down with high flow for 1 minute at room temperature. The sample, now foamy, was transferred to a spin filter (0.45 μm pore), and spun at approximately 15,000 r.c.f. for 30 s at 2°C. This removed the bubbles and lipid-bound ZrO_2 from the sample. Samples were immediately flash frozen in a bath of dry ice and EtOH and stored at -80°C until liquid chromatography mass spectrometry (LC-MS) analysis at a later time. Since all mixing timepoints were on the order of seconds, all reactions were conducted by hand. These steps are summarized in Chapter 5 in **Figure 5.1**.

Samples were thawed on ice and 50 μL was immediately injected into the LC sample loop, which had been filled with 200 μL of chase buffer (same buffer as quench buffer) immediately prior. The sample and chase buffer were then run at 0.1 mL/min with isocratic buffer (0.1% FA pH'd to 2.5 with TFA) through a hand-packed 1:1 pepsin:FPXIII (fungal pepsin from *Aspergillus saitoi*, type XIII) column for on-column proteolysis for 210 s. Peptides were collected on a Targa Piccolo C8 trap column for 150 s of desalting in isocratic buffer. Peptides were then eluted at 20 μL/min over a Targa C18 analytical column (5 μm beads) with a gradient of 10% MeOH (containing 0.1% FA, against 90% of water containing 0.05% TFA) at 0 minutes to 90% MeOH at 23 minutes. Peptides were collected from 3 to 22 minutes over this gradient and directed towards the HESI-II (Thermo Fisher Scientific) probe attached to a Thermo Q203 Exactive mass spectrometer. Note that DDM eluted after 23 minutes, so it was important to divert the detergent away from the MS and into the waste for long-term maintenance of the MS. After 23 minutes, 4 sawtooth gradients from 10% MeOH to 90% MeOH were used to clean the trap and analytical columns. Meanwhile, the protease column was cleaned with 6 column volumes of clean mix (5% iPrOH, 5% ACN, 20% acetic acid, 70%

water). All chambers of the LC are maintained at approximately 6°C except for the protease column chamber at 20°C.

Critically, the ZrO_2 resin was incubated with 3% BSA (in 50 mM Na-Phosphate, 100 mM NaCl, pH 7.5) for at least an hour, followed by 5 cycles of gentle washing in isocratic buffer to remove excess weakly-bound BSA, each time letting the resin settle by gravity and eluting off the supernatant. BSA-bound ZrO_2 lasted for approximately 2 hours before the BSA was no longer sufficiently blocking the resin, leaving unblocked sites to bind KcsA peptides, and leading to massive reduction in peptide signal.

Undeuterated measurements were carried out with the same protocols listed above (even including lipids), except water was used instead of deuterium buffer. These same undeuterated conditions were used for MS-MS fragmentation experiments, for which peptides were identified by searching against the entire BL21 proteome, with KcsA and potential protein contaminants manually added to the search list. SearchGUI with X! Tandem, MS Amanda, and Comet algorithms was used for peptide identification, and identified peptides were imported into HDExaminer (Sierra Analytics, Modesto, CA). Analysis of deuterated and undeuterated MS runs was conducted with HDExaminer, which identified m/z envelopes, calculated their centers of mass, and quantified changes in deuterium incorporation between pulse-labeling timepoints. All peptide maps were generated by ExMS2.[87]

Note that residual lipids not removed by ZrO_2 caused non-monotonic shifts in retention times of as much as 1 minute over tens of runs. Compared to runs with no lipids, the retention time of the peptide was shifted by an even greater amount. Therefore, for any given peptide, mass spectra were integrated over the same range of retention times relative to the maximum total ionic current (TIC) for that peptide in that run. This resulted in retention time integration ranges that differed significantly between runs, but was consistent with respect to the maximum TIC.

Note also that our 0 s folding timepoint was conducted by mixing pulse buffer and lipids

before adding protein and quenching 6 s later. We originally attempted to measure the uptake of KcsA monomers in DDM under equilibrium conditions for 6 s, but since the presence of lipids in other experiments affected the retention times of peptides so dramatically, it was hard to choose comparable retention time integration bounds between experiments with and without lipids, so we chose to measure the 0 s folding timepoint in lipids as well.

This is a highly-optimized protocol, with the compositions of all buffers, 2-step proteolysis, chase buffer, and manual frothing of the quenched sample containing ZrO_2 beads all being critical for consistent, high-signal recovery of the 11 peptides we studied across many folding times. Any other conditions we tried produced almost 0 resolved peptides. We believe the manual frothing of sample with ZrO_2 was critical for forming many air-detergent-lipid interfaces while simultaneously providing rapid and strong shear forces to disturb the liposome structure and extract the partially-digested protein into DDM. Curiously, vortexing and sonication of the sample did not produce the same effect, as vortexing may have been too gentle a perturbation, and sonication likely caused BSA to fall off of the ZrO_2 beads, leading them to bind not only to phospholipid headgroups but also to peptide fragments and partially-digested protein. This caused an almost complete reduction in peptide signal.

2.5 Native-state HDX of KcsA monomers and tetramers in DDM

All native-state HDX experiments in this work were measured from protein stocks in 20 mM Tris pH 7.5, 100 mM NaCl, and 1 mM DDM, and all protein concentrations are reported per monomer.

Deuterium labeling was initiated by incubating KcsA with deuterium buffer for various labeling times at room temperature, 25°C. For monomer measurements, 2 μL of 19.5 μM protein were mixed with 28 μL deuterium buffer (pD 8.5). For tetramer measurements in NaCl, 6 μL of 88 μM KcsA was mixed with 24 μL of deuterium buffer (pD 8.5), whereas for measurements in KCl, 6 μL of 88 μM KcsA was first mixed with 2 μL 1 M KCl for 5

minutes before initiating labeling with 24 μL of deuterium buffer (pD 8.5). For both NaCl and KCl measurements in 4 M urea, 3 μL of 98 μM KcsA was first incubated with 3 μL equilibration buffer (20 mM Tris pH 7.5, 100 mM NaCl, 1 mM DDM, 4 M urea, and only in the KCl/urea experiment, 300 mM KCl) for 1.5 minutes, followed by labeling with 24 μL deuterium buffer (pD 8.5, 4 M urea, and only in the KCl/urea experiment, 150 mM KCl). In every experiment, HDX was then quenched at room temperature by adding 30 μL of quench buffer. For monomer experiments this contained 600 mM glycine pH 2.5, 8 M urea, and 0.4% DDM, while all tetramer experiments used a quench buffer with 600 mM glycine pH 2.5, 4 M urea, and 0.4% DDM. Monomer samples were then spin filtered (0.2 or 0.45 μm pore) at 2°C for 30 s, and 50 μL was injected into the LC with 200 μL of chase buffer (600 mM glycine pH 2.5, 4 M urea, 0.4% DDM) behind the sample in the injection loop. To quenched tetramer samples, 10 μL of soluble pepsin (O.D. 2 in 100 mM sodium citrate, pH 4.4) was added and digested without mixing for 5 minutes at room temperature. These samples were then spin filtered and injected with chase buffer in the same manner as monomer samples.

Both monomeric and tetrameric samples then underwent online digestion on a POROS hand-packed 1:1 pepsin:FPXIII column at 20°C under 0.1 mL/min flow of isocratic buffer (0.1% FA pH'd to 2.5 with TFA) for 210 s. All samples were desalted on a POROS hand-packed R2 trap column for 150 s. Peptides were eluted over a Targa C18 analytical reverse-phase column (5 μm beads) with a 2-buffer gradient scheme (with 20 μL/min flow) consisting of a ramp from 10% acetonitrile (ACN) (containing 0.1% FA, against 90% water containing 0.05% TFA) at 0 minutes to 50% ACN at 14 minutes, to 90% ACN at 15 minutes, and remaining at 90% ACN until 18 minutes. Peptides were collected from 5 minutes to 16 minutes along this scheme, and after 18 minutes, 5 sawtooth gradients from 10% ACN to 90% ACN cleaned the trap and analytical columns. Meanwhile, the protease column was cleaned with 6 column volumes of clean mix (5% iPrOH, 5% ACN, 20% acetic acid, 70% water) between injections. All chambers of the LC were maintained at approximately 6°C

except for the protease column chamber at 20°C. Eluted peptides underwent electrospray ionization with the HESI-II (Thermo Fisher Scientific) probe attached to a Thermo Q203 Exactive mass spectrometer.

Undeuterated measurements were carried out with the same protocols listed above, except water was used instead of deuterium buffer. These same undeuterated conditions were used for MS-MS fragmentation experiments, for which peptides were identified by searching against the entire BL21 proteome, with KcsA and potential protein contaminants being manually added to the search list. SearchGUI with X! Tandem, MS Amanda, and Comet algorithms was used for peptide identification, and identified peptides were imported into HDExaminer (Sierra Analytics, Modesto, CA). Analysis of deuterated and undeuterated MS runs was conducted with HDExaminer, which identified m/z envelopes, calculated their centers of mass, and quantified changes in deuterium uptake between native-state labeling timepoints. For any given peptide, mass spectra were integrated over the same range of retention times in the LC.

We were not able to obtain a maximally-deuterated "all-D" control due to KcsA's high protection by detergent and high propensity to aggregate without detergent, even in 8 M urea. However, many peptides in our monomeric native-state HDX experiments were observed to reach a saturated deuterium level at long labeling timepoints. We treated those as our all-D control. On the other hand, to control for possible deuteration picked up after quenching (i.e., "forward-exchange"), we mixed deuterium buffer and quench buffer together first before adding the protein sample to this mixture, and then followed the same protocol as above. We found the effect of "foward-exchange" to be negligible.

Lastly, as in our HDX pulse-labeling method, this is a highly-optimized protocol, so removing any component of quench or chase buffer or reducing preolysis conditions led to a drastically reduced peptide signal. This is likely because KcsA is so small and stable, making it very hard to digest. Further, without chase buffer, the peptides of KcsA are too sticky to

ever reach the R2 trap column, and are never detected.

2.6 Gentle purification of folding-competent KcsA monomers in DDM

Expression and purification of KcsA tetramers in *e. coli* is adapted from previous work from the Roux Lab, with a few notable differences.[150] Instead of purification in DM, we used DDM in every purification buffer. Note that detergent exchange from DM to DDM is very tricky and often resulted in a severe drop in yield due to KcsA precipitation. Therefore, our membrane extraction/solubilization buffer contained 20 mM Tris pH 7.5, 0.15 M KCl, and 30 mM DDM (soluble grade). Instead of affinity tag purification on Ni-NTA, we used cobalt resin instead, which we found reduced impurities. Our cobalt column wash buffer consisted of 20 mM Tris, pH 7.5, 0.15 M KCl, 1 mM DDM (soluble grade), and 20 mM imidazole. We eluted our sample off the column with 20 mM Tris, pH 7.5, 0.15 M KCl, 1 mM DDM (soluble grade), and 300 mM imidazole. After chymotrypsin treatment to remove the His tag as described previously, we finally purified the DDM-solubilized KcsA tetramer by passing it over a Superdex 200 Increase 10/300 GL size exclusion column in either 20 mM Tris pH 7.5 or 50 mM Na-Phosphate pH 7.5, 100 mM NaCl, and 1 mM DDM (analytical grade). This protocol produces between 2 and 4 mg of tetramer per liter of *e. coli* culture. Tetramers in Tris or phosphate buffer were used for melting experiments, while those used for native-state HDX were full-length and did not undergo chymotrypsin treatment.

To produce folding-competent monomers from this tetramer stock, we unfolded the tetramers and removed DDM by TCA precipitation followed by acetone washes as previously reported.[158] We resolubilized the unfolded, precipitated monomers in 0.5% SDS (in 50 mM Na-Phosphate pH 7.5 and 100 mM NaCl). We performed slow dialysis with Slide-A-Lyzer MINI Dialysis Devices of 10K MWCO (Thermo Fisher, Waltham, MA) into purification buffer (containing 50 mM Na-Phosphate pH 7.5, 100 mM NaCl, and 1 mM DDM). Dialysis

took place with gentle rocking at room temperature for 4 days, followed by a single pass through a 2 mL, 7K MWCO, Zeba desalting spin column in purification buffer to remove any remaining SDS. Samples were flash frozen in a bath of dry ice and EtOH, and stored at -80°C. These DDM-solubilized KcsA monomers are refoldable upon thawing and mixing with SUVs.

If we attempted to switch detergents from SDS to DDM too quickly, either with a desalting spin column or by size exclusion chromatography, we observed a yield loss of up to around 98% in mass. We also tried to exchange detergent by reattaching full-length KcsA monomers (which we had not subjected to chymotrypsin treatment) to Ni-NTA resin, to wash with consecutively higher concentrations of DDM. However, the SDS-denatured state of KcsA monomers was unable to bind efficiently to the Ni-NTA. The small amount of KcsA that was bound and detergent-exchanged in this way appeared to be misfolded, because it could no longer reform tetramers when mixed with lipid membranes. Therefore, despite achieving a monomeric KcsA species in DDM, the purification was too harsh, and the monomer was no longer folding-competent. While detergent exchange by dialysis is very slow, it is gentle enough to produce monomeric species that can refold properly.

Purification of KcsA monomers in DDM has previously been reported by a different method, with a slow, stepwise temperature ramp to unfold the tetramer gently enough to maintain solubility of the monomer.[94] However, we have yet to evaluate if this method produces refoldable monomers.

2.7 Liposome preparation

Small unilamellar vesicle (SUV) liposomes were prepared from azolectin (541602 Soy Extract Polar, Avanti). Lipids were dissolved in chloroform in a glass vial, dried overnight in a vacuum desiccator, and rehydrated the next day using neutral phosphate buffer (50 mM NaPi, 100 mM NaCl, 1 mM DDM) to a final lipid concentration of 10 mg/mL. Rehydration

was accomplished by vortexing for 5 to 15 minutes at room temperature. The lipid suspension was then subject to 5 rapid freeze/thaw cycles (using a dry ice/EtOH bath to freeze, and a 60°C water bath to thaw), followed by extrusion 51 times (using an Avanti extrusion kit) through a membrane with 100 nm pores at approximately 50°C. The resulting SUVs were cooled to room temperature before use in an experiment, and incubated under Ar gas for long-term storage (for 1 to 2 weeks).

2.8 *In vitro* refolding of KcsA from DDM into liposomes

Refolding of DDM-solubilized KcsA Δ125 monomers was initiated by mixing with azolectin SUVs. This was done at various monomer to lipid ratios across different experiments. For HDX pulse-labeling in Chapter 5, folding was initiated at a ratio of 1:300. Refolding experiments in NaCl and KCl, in which tetramerization was measured by SDS-PAGE in Chapter 5, were carried out at a ratio of 1:700, while melts of refolded KcsA in Chapter 3 were carried out at 1:1000. We have observed previously that the refolding rate of Δ125 monomers was independent of monomer concentration in bulk solution.[158]

For the SDS-PAGE tetramerization assay in **Figure 5.8**, 10 μL of lipid/protein refolding mixture was quenched with 20 μL 10% SDS (in 50 mM NaPi, 100 mM NaCl), and run on a 4-20% Tris-Glycine gel with non-reducing loading buffer as previously reported.[158] These gels were stained with a silver staining kit (Thermo Fisher, Waltham, MA), imaged using a Bio-Rad ChemiDoc Imaging system, and band intensities were quantified using Bio-Rad Image Lab software. These SDS-PAGE-based tetramerization curves were fit to a single exponential function with scipy.optimize.curve_fit to estimate folding time constants, τ_{fold}, with A and C as fit scaling constants.

$$\%\text{Tetramer}(t) = C\left(1 - Ae^{-t/\tau_{\text{fold}}}\right)$$

2.9 KcsA denaturation experiments: thermal denaturation, TFE denaturation, urea, and SDS ramps

KcsA Δ125 tetramers were purified in either 20 mM Tris pH 7.5 or 50 mM sodium phosphate (NaPi) pH 7.5, both containing 100 mM NaCl and 1 mM DDM. For thermal denaturation experiments measured by SDS-PAGE, six fractions of tetramer were simultaneously incubated for 30 minutes at each measured temperature using a PCR thermocycler, with a 7^{th} fraction incubated at room temperature, 25°C. Following incubation, samples were run on a 4-20% Tris-Glycine gel with non-reducing loading buffer without boiling samples. For chemical denaturation experiments, purification buffer (50 mM NaPi pH 7.5, 100 mM NaCl, 1 mM DDM) was mixed in different ratios with 10 M Urea or 10% SDS (both dissolved in purification buffer) or 100% TFE to a final volume of 20 uM. This was briefly mixed with 5 μL of native tetramer sample, incubated for 5 minutes at 25°C, and run on SDS-PAGE following the same protocol used for thermal denaturation samples. For comparison between Tris and phosphate buffer thermal stability, KcsA purified in Tris was buffer-exchanged into phosphate using a 2 mL, 7K MWCO, Zeba desalting spin column, and vice versa.

Reconstituted proteoliposomes were produced by incubating purified KcsA tetramers with azolectin SUVs (prepared as described above) at a ratio of approximately 1 monomer to 1000 lipid molecules (assuming an average molecular weight of a lipid of 800 g/mol) for 11 hours at room temperature. Refolded samples were produced by mixing azolectin SUVs with purified KcsA monomers at a ratio of around 1 monomer to 1000 lipid molecules for approximately 20 hours at room temperature. To remove excess DDM in both reconstituted and refolded proteoliposomes, BioBeads were added to a final concentration of about 40 mg/mL and incubated with gentle rotation for another 11 hours at room temperature. Biobeads were removed by spin filtration at 13.4 r.c.f. through a spin filter (0.45 μm pore). Thermal and chemical denaturation measurements were carried out as described above for DDM-solubilized KcsA tetramers.

SDS-PAGE gels were stained either with AcquaStain Protein Gel Blue Stain or with a silver staining kit (Thermo Fisher, Waltham, MA) and imaged using a Bio-Rad ChemiDoc Imaging system. Band intensities were quantified using Bio-Rad Image Lab software, and fit to the following form with scipy.optimize.curve_fit to estimate melting temperatures, T_m, witht A and C as fit scaling constants.

$$\%\text{Tetramer}(T) = C\left(1 - \frac{1}{1 + e^{-A(T-T_m)}}\right)$$

2.10 *Upside* simulations

Structures of KcsA lacking the M0 helix were prepared from PDB ID 3EFF. KcsA structures including the M0 helix, both WT and KcsA-Gly_{20} were prepared from AlphaFold2's Google Collaboratory notebook (https://github.com/sokrypton/ColabFold) to predict the structure of full-length KcsA tetramer. For WT, the full-length sequence was input as a homotetramer, whereas for KcsA-Gly_{20}, residues E51 through T85 were replaced with a string of 20 adjacent Gly residues and input as a homotetramer. All structures of KcsA were positioned in a 38 Å membrane manually using Swiss PDB Viewer (http://www.expasy.org/spdbv/).

The *Upside* force field 2.1 was implemented with an implicit 38 Å membrane potential as previously reported, with solvent-accessible surface calculated at each frame to determine residue water or lipid positioning.[51,184] For relaxation simulations of KcsA-Gly_{20}, relaxation was carried out in 4 replicates at T=0.85 kT and showed rapid equilibration within 250 frames (**Figure 3.10B**). One of the four replicates was not included here because the cytoplasmic helix of one monomer got stuck in an unrealistic pose, peripheral to the membrane surface, never encountering the other cytoplasmic helices. For melting simulations of KcsA Δ125 WT, 28 evenly-spaced temperature replicates between T=0.8 and 1.1 kT were used, with a replica exchange interval of 10 frames between exchange attempts. These simulations were achieved within 36 hr wall times with replicates distributed among Intel(R) Xeon(R) CPU

E5-2680 v4 single cores on The University of Chicago's Midway2 computing cluster.

2.11 Tryptophan fluorescence in SUVs

Tryptophan fluorescence of KcsA in SUVs was measured on a HORIBA Fluorolog-3 spectrophotometer (Flurolog-3 Yobin Yvon-Horiba; Synergy Neo HST, BioTek). Tryptophan excitation was conducted with 296 nm light with 1 nm slits. Fluorescence emission was collected at 90° to the excitation path, with a wavelength scan from 311 to 400 nm, 10 nm slits, 0.1 s integration time, and a monochromator grating (with 1200 lines/mm and 330 nm blaze wavelength) to reduce scattering artifacts from liposomes. The temperature scan was conducted with an increment of 1°C, with tolerance of 1°C and an equilibration time of 6 min at each measured temperature. Emission counts were normalized to the lamp intensity as S1/R1. This work was conducted in The University of Chicago Biophysics Core Facility (RRID:SCR_017915).

For the analysis of fluorescence melting curves in **Figure 3.8**, both NaCl and KCl traces were normalized to the maximum emission at 330 nm. While scattering effects were not explicitly taken into account for each individual spectrum, the SUV samples in potassium and sodium were taken from the same stock, so a comparison of the two conditions is valid, as the scattering effects in both would be corrected by the same linear offset.[125]

Samples for melting experiments were contained in a square micro fluorometer cuvette with a teflon stopper top and FCA3 thermal adaptor (spectrosil quartz, 0.315mL, Catalog #23-3, 45-Q-3 from Starna Cells, Atascadero, CA). Samples were filled to the top of the cuvette and capped tightly with the teflon stopper to prevent boiling at temperatures over 100°C.

2.12 Simultaneous circular dichroism and tryptophan fluorescence

CD and tryptophan fluorescence were measured simultaneously on a Jasco J-715 CD Spectrophotometer, customized with a second photomultiplier tube (PMT) orthogonal to the incident light path to measure fluorescence (**Figure 2.4A**). Constant-temperature CD spectra were measured with a data pitch of 1 nm, 10 to 20 nm/min wavelength scan speed, 4 s response time, and a band width of 1 nm. Temperature ramps were measured with 226 nm incident circularly-polarized light, with a 5 nm bandwidth. Fast temperature ramps were collected with a data pitch of 1.0°C, temperature slope of 1°C/min, and 4 s response time, while slow temperature ramps were collected with data pitch 1.0°C, temperature slope of 7°C/hr, and a 16 s response time. In the fluorescence arm of the light path, a high-pass filter (over 330 nm) was used to remove scattering artifacts, and the fluorescence PMT gain was manually set to 0.020 at the start of each experiment. Samples were contained in a square micro cuvette with a teflon stopper top and FCA3 thermal adaptor as described above.

A representative CD trace of KcsA Δ125 is shown in **Figure 2.4B**, with high tension (HT) overlaid.

2.13 Protein-dense phase microscopy

Total internal reflection fluorescence microscopy (TIRFM) was conducted on a Leica GSD/TIRFM. KcsA Δ125 monomers solubilized in SDS (0.5% SDS, 20 mM Tris pH 7.0, 100 mM NaCl) and labeled with Alexa-594 thioreactive dye at KcsA residue 86 (L86C) were rapidly mixed with giant unilamellar vesicles (GUVs), deposited on a glass-bottomed microwell dish (MatTek, Ashland, MA), and imaged under TIRF conditions. This workflow is diagrammed in **Figure 2.5A**. Azolectin GUVs were prepared from 3 cycles of rapid freezing of SUVs (preparation described previously) in dry-ice/EtOH followed by thawing slowly on ice.[72] TIRFM was performed in the Integrated Light Microscopy Core at University of Chicago, which

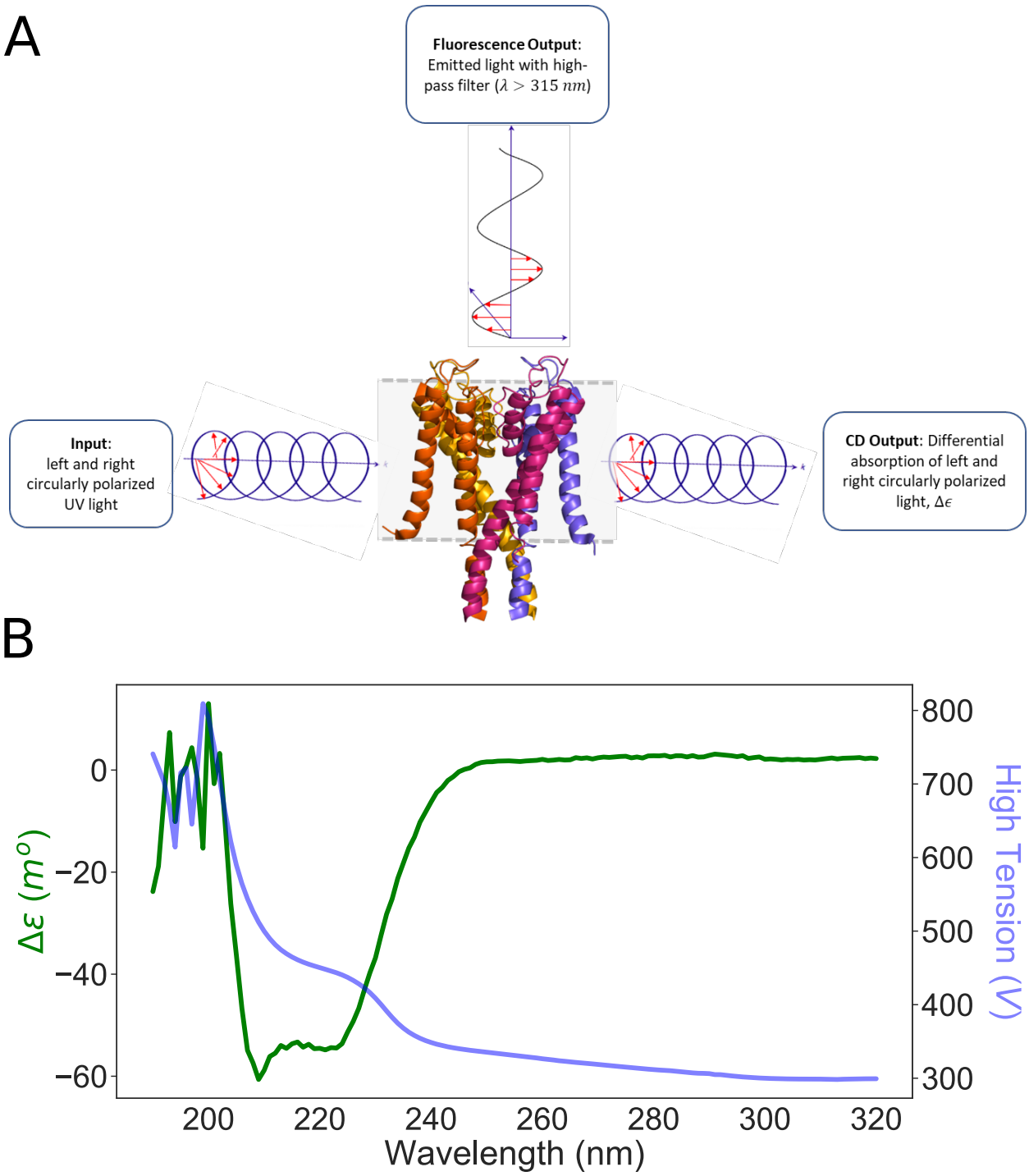

Figure 2.4: Simultaneous CD and Trp Fluorescence. **A.** Light paths for CD and Trp fluorescence measurements in our customized Jasco J-715 Spectrophotometer. **B.** CD spectrum of 8μM KcsA Δ125 overlaid with HT.

receives financial support from the Cancer Center Support Grant (P30CA014599). RRID: SCR_019197.

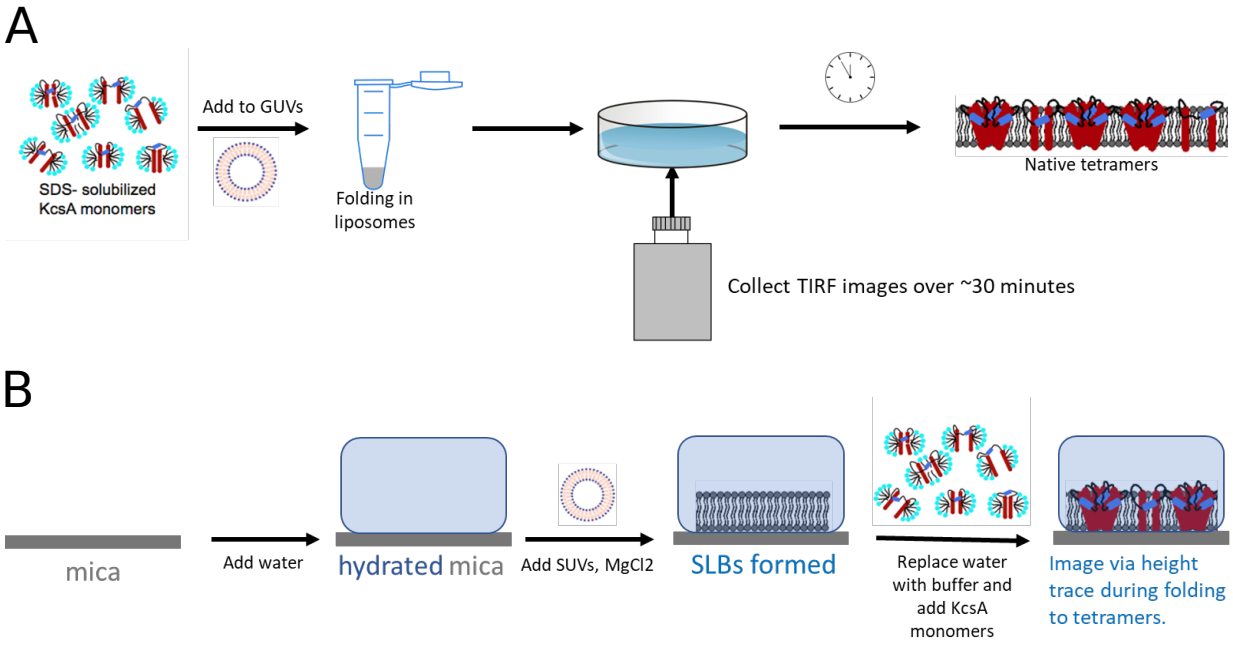

Figure 2.5: Protein-dense phase microscopy workflows. **A.** Method for folding KcsA while imaging with TIRFM. **B.** Production of SLB on mica substrate, followed by insertion and folding of KcsA with fluid-cell AFM.

Fluid-cell atomic force microscopy (AFM) was conducted on the Asylum Cypher AFM. Supported lipid bilayers (SLBs) were produced as previously reported by the Lee Group, except that azolectin SUVs in Tris buffer (20mM Tris pH 7.0, 100 mM NaCl) were used in this work instead of SUVs of purified lipids.[71] After SLBs were deposited on the mica substrate, the system was rinsed with additional Tris buffer to remove non-attached membranes. This was followed by introduction of KcsA Δ125 monomers in SDS (0.5% SDS, 20 mM Tris pH 7.0, 100 mM NaCl). Height-trace images were captured by tapping-mode AFM at 25°C before SLB formation, after SLB formation, and after KcsA incorporation. A schematic of this workflow is shown in **Figure 2.5B**. This work made use of the shared facilities at the University of Chicago Materials Research Science and Engineering Center, supported by National Science Foundation under award number DMR-2011854.

CHAPTER 3

POTASSIUM CHANNEL UNFOLDING IDENTIFIES A NOVEL NON-NATIVE TETRAMERIC SPECIES OF KCSA

The folding of a multimeric helical membrane protein necessitates several key processes: (1) formation of secondary structure in the membrane, (2) folding of water-exposed chains, (3) the clustering and stabilization of transmembrane helix bundles, (4) establishment of correct orientation of N- and C-termini in relation to the membrane, (5) the formation of multimers from monomers, and occasionally (6) the binding of ligands or prosthetic groups and/or (7) the formation of a water-filled pore. Processes (1) through (5) are often grouped together conceptually to define a given membrane protein topology, whereas (6) and (7) more specific to ion channels, transporters, and pumps.[180]

In studying the folding and multimeric assembly of KcsA, it is important to evaluate the contribution of each of these processes to the stability of monomeric and tetrameric states of the channel as well as intermediate states that may be traversed during folding. From an energetic perspective, we can consider the monomer, tetramer, and observable intermediates as minima on an energy hypersurface in the space of all protein conformations. It is notable that functional states of the protein, such as open, closed, and inactivated states of an ion channel, are also observable local minima on the same energy surface. Perturbations such as changes in solvent conditions (e.g. lipid composition in the membrane, and pH, ion, and ligand concentration in the aqueous solvent), temperature, protein density, and changes in electric or chemical potential across the membrane affect the depths of the state-defining wells, the heights of the barriers between states, and the frequency with which the protein samples these states.

To characterize the monomeric and tetrameric states, which are the endpoints of KcsA assembly, as well as any folding intermediates, it is important to be able to physically perturb the folded state of the protein. We also want observables to report protein structural

information under these perturbations. We can determine barrier heights by measuring the kinetic rates of tetramerization and the (free energy) well depths of each state by measuring the relative populations of protein in each well. Here we choose to do the latter, and measure the relative stabilities of monomeric and tetrameric KcsA as well as that of a putative folding intermediate observed during denaturation. Our structural observables are (1) tetrameric state as measured by sodium dodecyl sulfate–polyacrylamide gel electrophoresis (SDS-PAGE), (2) alpha-helical content measured by CD and HDX, and (3) solvent accessibility of native tryptophans as measured by fluorescence. To aid interpretability, we compare these experimental observations to model structures generated by the AlphaFold2 structure-prediction algorithm and our *Upside* coarse-grained molecular dynamics (MD) package.[85] This approach is powerful not only because it allows for thermodynamic characterization of monomeric and tetrameric states, but also because it can isolate intermediate states that might be difficult to identify during folding but are nonetheless accessible to the protein as it folds and unfolds.

In this chapter, we characterize the structural changes associated with KcsA unfolding and identify a novel tetrameric species. This state consists of a tetrameric bundle of transmembrane helices lacking a natively-folded pore helix and selectivity filter. We observe that this tetrameric species is metastable by structural prediction and CG-MD simulations, but exhibits much greater suceptibility to denaturants than the native tetramer. While we were unable to observe refolding from this state in preliminary experiments, this work suggests that the hypothesized intermediate in the "keystone model" of KcsA folding is a real, metastable state accessible during channel unfolding.

3.1 Denaturation of KcsA depends on ion concentration, lipids, pH, and buffer condition.

To understand structural differences between the KcsA monomer, tetramer, and any intermediates, we needed to control the relative populations of monomeric and tetrameric channels at equilibrium. To do this, we started with the natively-folded KcsA tetramer and investigated structural changes upon channel denaturation.

This required a method to unfold KcsA in a controlled manner as we monitored structural properties of the protein under different unfolding conditions. Finding such a method proved to be nontrivial, as common denaturants like urea and SDS, used for similar studies in cytosolic proteins, proved to be ineffective at significantly perturbing KcsA. In fact, the native KcsA tetramer, solubilized in either n-Dodecyl-β-D-maltoside (DDM) detergent or reconstituted in azolectin small unilamellar vesicles (SUVs), was unperturbed by up to 8 M urea or 8% SDS (**Figure 3.1**).

Only heat-induced denaturation and the organic solvent 2,2,2-Trifluoroethanol (TFE) were observed to break the tetrameric structure of the native KcsA channel, with melting temperatures measured to be $61.07 \pm 0.87\,^{o}$C in DDM and $92.53 \pm 1.00\,^{o}$C in azolectin SUVs, and the TFE denaturation midpoint concentrations, $[\text{TFE}]_{1/2}$, to be 22.64 ± 0.14 %TFE in DDM and 30.01 ± 0.56 %TFE in SUVs. (**Figure 3.1**).

Stabilization of KcsA is observed not only in the presence of lipids, but also in the presence of K^+ ions (**Figure 3.2**). More surprisingly, KcsA was found to be stabilized in Tris buffer compared to phosphate buffer both in DDM micelles and lipid vesicles. This effect was confirmed by exchanging channels, originally purified in one buffer, into the other buffer and remeasuring their melting temperatures. We found that the final buffer identity, rather than the initial buffer from protein purification, determined the protein stability (**Figure 3.3**). The stabilization of KcsA by potassium ions that we observe is well established, and is thought to derive from the higher binding energy to the selectivity filter of potassium, cesium,

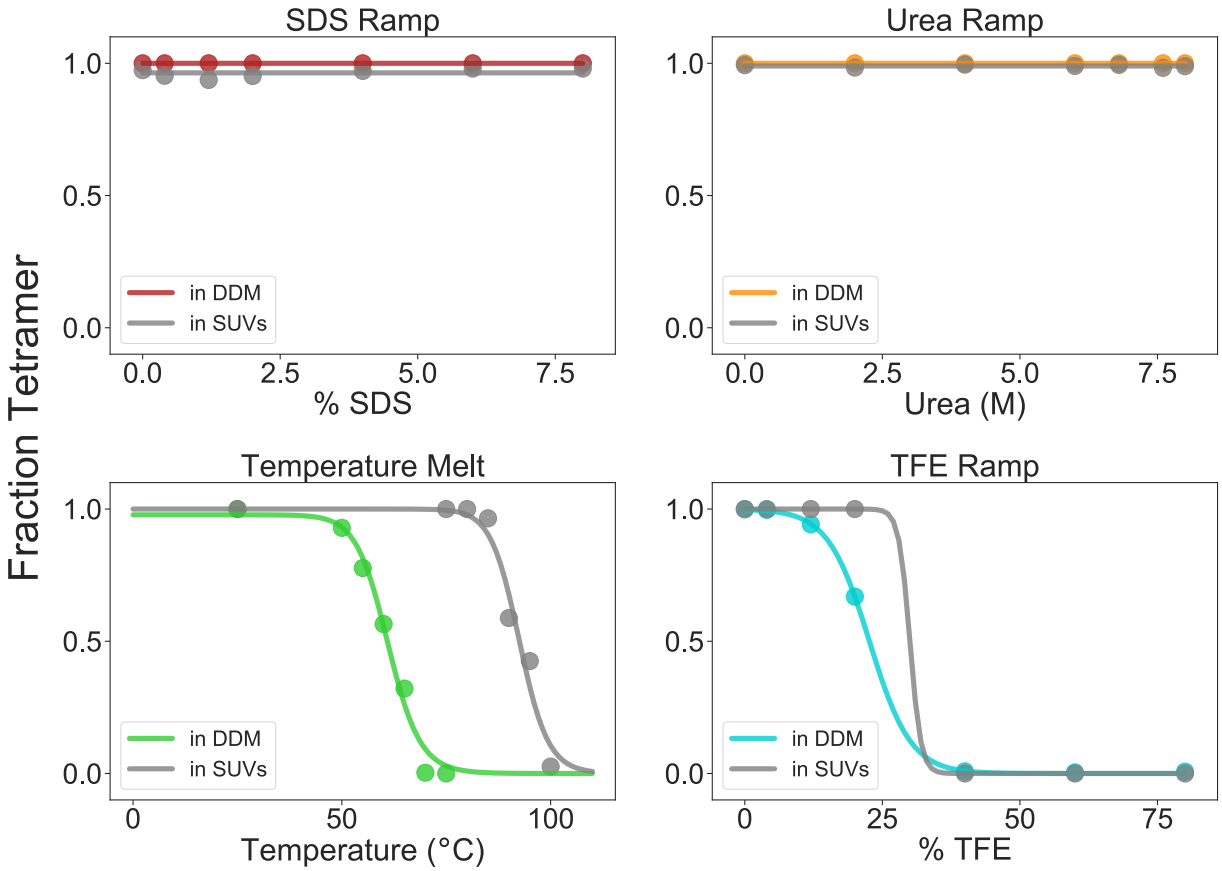

Figure 3.1: Natively-folded KcsA Δ125 can be unfolded by heat and TFE, but not by commonly-used denaturants SDS or urea, as measured by SDS-PAGE melting curves.

and rubidium ions compared to sodium ions.[59,103,145–147] Similarly, the stabilization of KcsA by lipids is well-known.[175]

In contrast, the effect of buffer identity on protein stability is poorly studied, but there is evidence that different buffers, even at the same pH, adsorb differently to the surface of a protein. This is believed to be the result of differential buffer hydration and in one study has been linked to buffer-dependent perturbations of protein liquid-liquid phase separation (LLPS).[15] Tris buffer was not a subject of that study, but is known to have a significant temperature-dependence of its buffering capacity, lowering the pH of a solution by approximately 0.03 pH units per 1°C increase in temperature.[46] KcsA is a pH-gated channel with highly charged water-exposed residues in its intracellular gate that undergo large conforma-

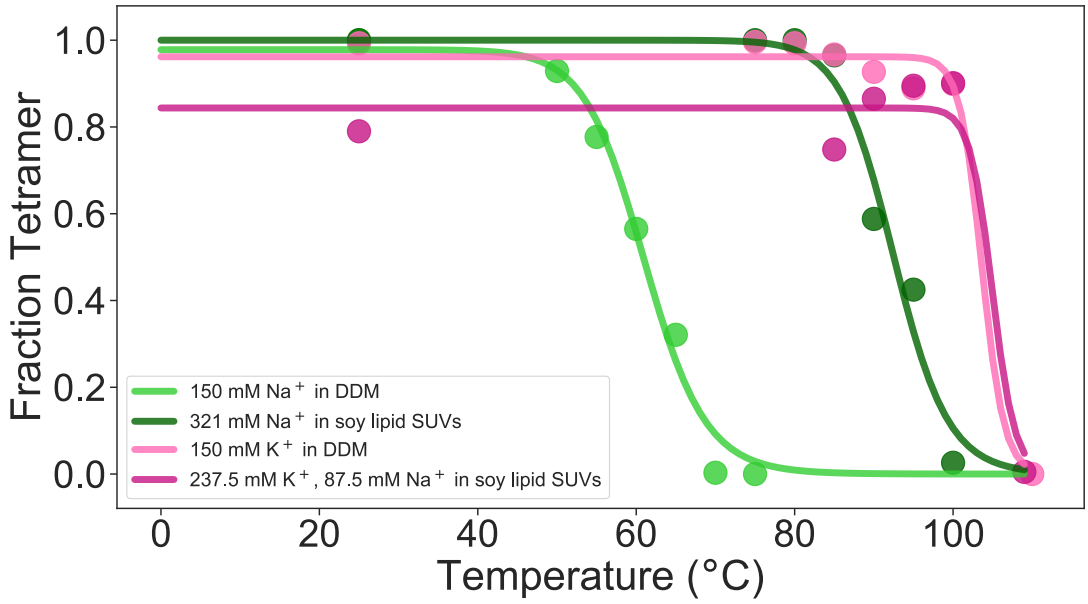

Figure 3.2: KcsA Δ125 melting curves from SDS-PAGE demonstrate stabilization in K^+ and lipids.

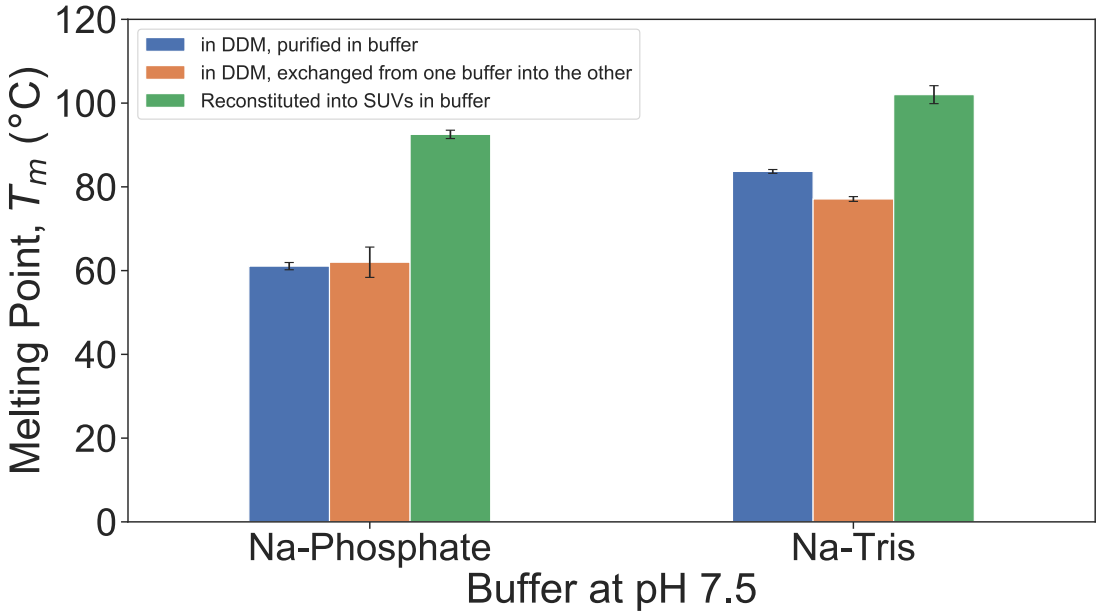

Figure 3.3: Comparison of estimated T_m values of thermal melts of KcsA Δ125 at pH 7.5 in Tris and Phosphate buffers showing channel stabilization in Tris.

tional changes at low pH, so we hypothesized that the decrease in pH of Tris at increasing temperatures may be stabilizing the channel. Upon testing the stability of KcsA in a low-pH (pH 2.6) phosphate buffer, we observed that tetramers in DDM are unstable at temperatures as low as 25°C, ruling out channel stabilization by acidic conditions.

Having ruled out pH-effects, we speculate that the observed stabilization by Tris may derive from a hydration-based effect similar to that proposed by the LLPS study. This may lead to different degrees of adsorption to the water-exposed monomeric interfaces, perhaps lining the water-exposed faces of the selectivity filter or the TM2 inter-monomeric contacts in the water cavity near the glycine zipper. It is also possible that the observed stabilization by Tris is a result of a high-temperature degradation byproduct of Tris, formaldehyde, which can react with tyrosine residues near inter-monomeric contacts and lead to chemical fixation and stabilization of the KcsA tetramer.[159,167] It is notable that, while Tris stabilizes KcsA in SUVs, the effect is much smaller than the observed stabilization in DDM micelles, suggesting that the buffers could be interacting with the detergent micelle more than the liposome. It is also possible that the stabilizing effects of lipids are stronger than those from buffer interactions. Additional experiments are required to fully evaluate the effect of buffer composition on membrane protein stability.

Irrespective of buffer choice, we found that heat and TFE denaturation are effective for perturbing the structure of natively-folded KcsA.

3.2 Tryptophan fluorescence, circular dichroism, and SDS-PAGE identify a non-native tetrameric species.

Denaturation curves of KcsA by SDS-PAGE are useful in that they report the fraction of tetrameric species under different conditions, however this assay is difficult to interpret structurally. It is possible that non-native tetrameric, trimeric, or dimeric species exist at sampled denaturation conditions, but are destabilized by SDS-PAGE and run as monomers

on the gel. Therefore, it is necessary to measure KcsA denaturation with more structurally-specific methods.

Taking advantage of the extremely helical structure of KcsA and the abundance of native tryptophan residues on each monomer, we can measure simultaneous CD absorbance and tryptophan fluorescence spectra under different denaturation conditions to observe changes in KcsA secondary structure and tryptophan solvent accessibility. This allows us to detect more detailed structural changes and observe any non-native intermediate species that could not be captured by SDS-PAGE.

Upon slow thermal denaturation, we observed several distinct unfolding transitions in CD (226 nm) and tryptophan fluorescence in DDM-solubilized KcsA (**Figure 3.4**). The differential absorbance ($\Delta\varepsilon$) of 226 nm left- and right- circularly polarized incident light is commonly used as an alpha-helical signature in CD, and its monotonic increase towards zero from 40°C to 110°C indicates that KcsA is losing significant secondary structure during the thermal melt.[61] Tryptophan fluorescence, excited with the same 226 nm incident light and measured orthogonally along with CD absorbance, displayed a monotonic decrease over the same temperature range, characteristic of solvent quenching. Structurally, all five native tryptophan residues of KcsA are located near the lipid-water interface (**Figure 3.8A**), so a decrease in tryptophan fluorescence suggests that there is an increase in water exposure of these native fluorophores with increasing temperature. The sharpest changes in CD absorbance and fluorescence correspond well to a tetramer melting transition measured by SDS-PAGE. Therefore, there is a significant loss of alpha-helical secondary structure and increased solvent exposure of native tryptophan residues as the KcsA tetramer is unfolded and dissociated into monomers. Since three of the native tryptophan residues are at the ends of transmembrane helices, these likely remain fairly stable during thermal denaturation as long as the membrane or detergent structure remains intact, and any significant changes in fluorescence come from the two adjacent tryptophan residues in the pore helix, W67 and

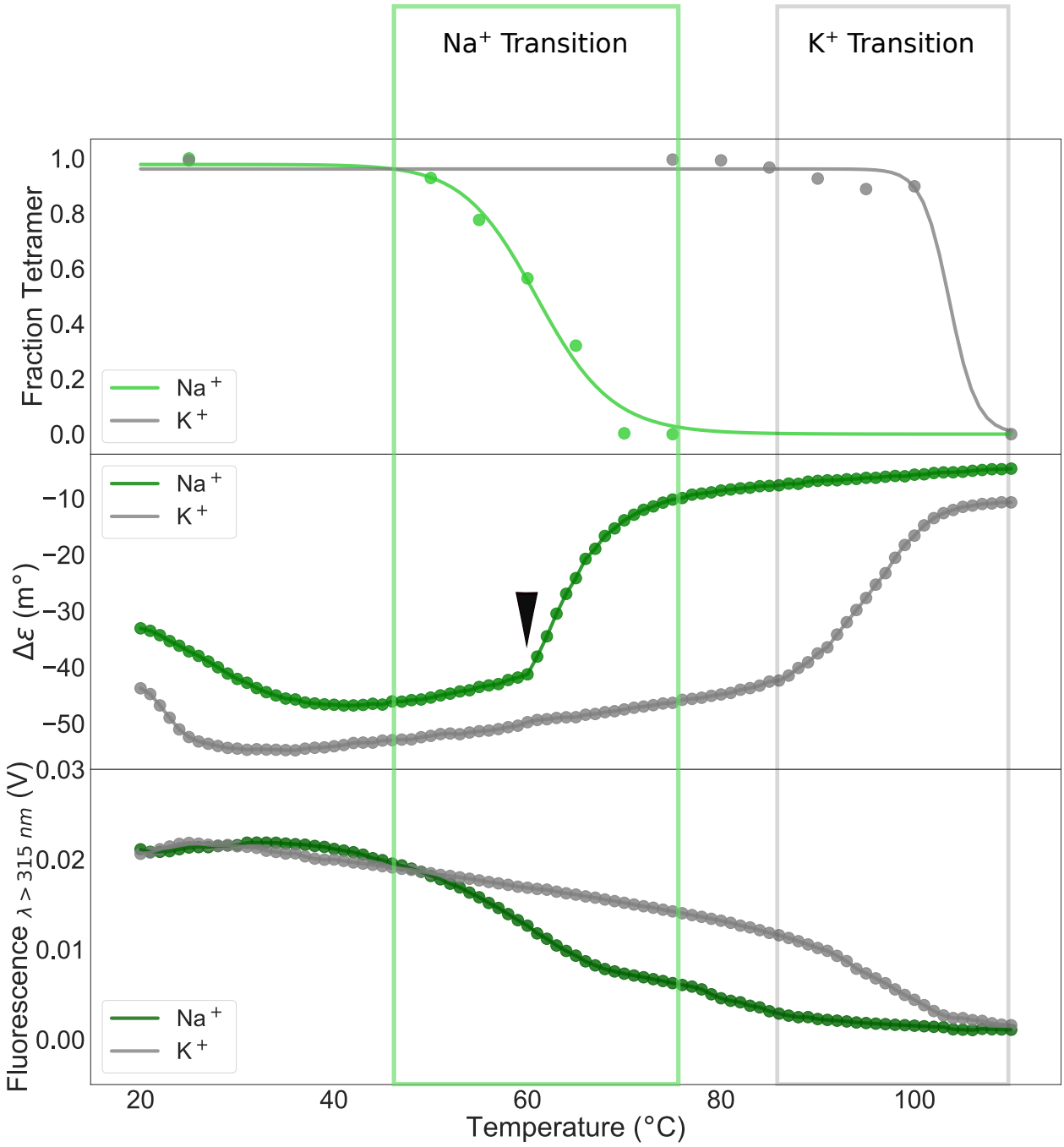

Figure 3.4: Simultaneous measurements of CD absorbance and tryptophan fluorescence over a thermal melt of KcsA from 20°C to 110°C overlaid with the tetramer disassembly curve from SDS-PAGE. All structural transitions in potassium (grey box) occur at higher temperatures than those in sodium (green box), whereas only in sodium is there an abrupt loss of secondary structure during tetramer disassembly (black wedge).

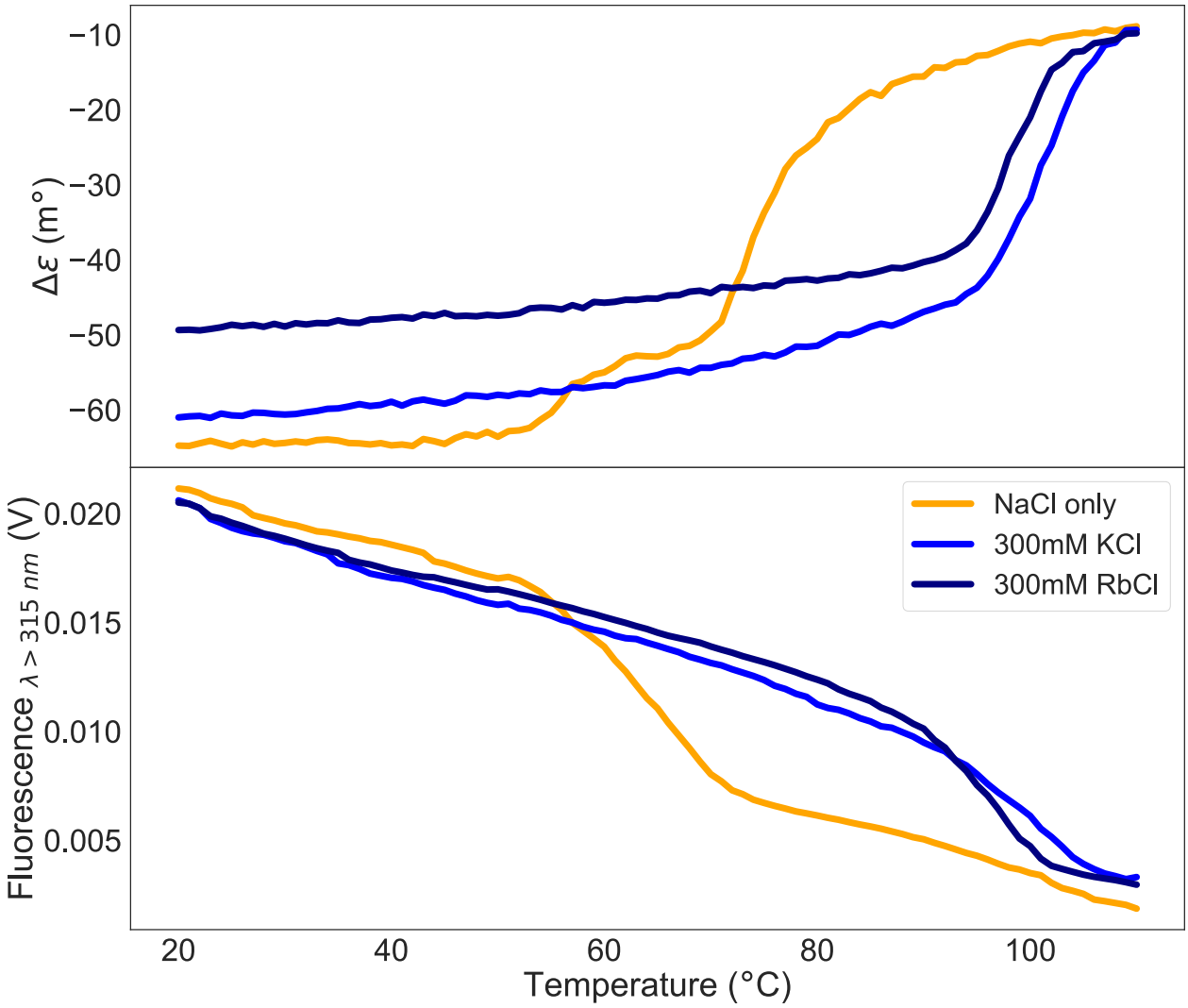

Figure 3.5: Potassium and rubidium ions stabilize the CD and tryptophan fluorescence melting curves of KcsA.

W68. Accordingly, the large decrease in tryptophan fluorescence upon KcsA melting could correspond to the pore helix losing its native contacts and popping out into free water. At high temperatures (around 100°C), we expect that the detergent structure is no longer intact, so fluorescence changes at high temperatures may reflect changes in solvent accessibility of all five tryptophan residues.

Notably we observed the same stabilization by CD, tryptophan fluorescence, and SDS-PAGE associated with potassium binding (**Figure 3.4** green and grey boxes). **Figure 3.5**

demonstrates the same behavior with rubidium ions, which stabilize the channel almost as much as potassium, and can be similarly measured by CD and tryptophan fluorescence. This is in agreement with measured binding energies of potassium and rubidium to KcsA.[103]. Note that while all of the melting transitions in **Figure 3.5** are at higher temperatures than those measured in **Figure 3.4**, the former experiment applied a temperature ramp with a 10 times greater slope and was likely too fast to fully equilibrate at each measured temperature. Therefore we only refer to this latter experiment for qualitative comparison of KcsA stabilization by different ions. To ensure that the ion-based stabilization of KcsA was due to specific ion binding and not a discrepancy or contamination of the experimental buffers, we measured the CD melting curves of an unrelated, water-soluble protein, cytochrome c (Cyt C) from horse heart using the same buffers as our KcsA melts. Cyt C contains no such selectivity filter, and as we expected, had no observable ion dependence on its thermal stability (**Figure 3.6**) supporting the interpretation that the observed increase in thermal stability in KcsA is due to specific cation binding.

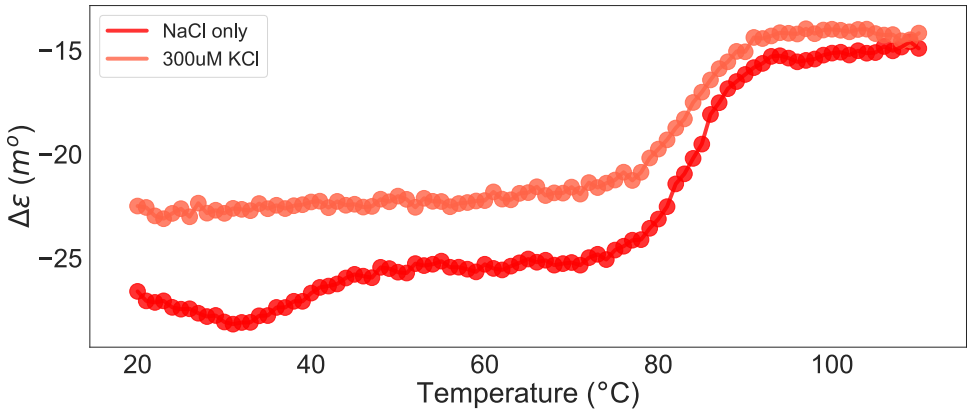

Figure 3.6: Cytochrome C from horse heart shows no ion dependence in its CD melting curves.

Because of the marked differences in tetramer stability measured by SDS-PAGE, alpha helical content measured by CD, and tryptophan solvent accessibility measured by fluorescence resulting from different binding ions, we can conclude that the selectivity filter and attached pore helix contribute greatly to the stability of native KcsA.

While the melting transition tracked by SDS-PAGE and tryptophan fluorescence is smooth, there is a surprisingly abrupt increase in CD absorbance over the same temperature range (black wedge in **Figure 3.4**). This sharp change in CD behavior around 60°C occurs when approximately half of the tetrameric species has dissociated, and suggests that DDM-solubilized KcsA only begins to lose secondary structure around halfway through the tetramer disassembly process. Because tryptophan fluorescence is already becoming quenched below 60°C, at temperatures when the tetramer is beginning to dissociate, but before any significant loss in helical content, we infer that the tetramer disassembly does not necessitate pore helix unfolding. Potentially, pore helix displacement at T $<$ 60°C is sufficient to destabilize the tetramer, but above 60°C the pore helix begins to unfold, further biasing a displaced state and destabilizing the tetramer even more so that by 75°C, almost the entire population of KcsA is monomeric, with displaced and unfolded pore helices.

For completeness, we considered that 60°C may represent a critical point in the phase transition from DDM-solubilized KcsA to protein aggregate, as supported by a spike in the simultaneous high tension measurement, possibly due to light scattering off of protein aggregates. (**Figure 3.7**). As in **Figure 3.5**, this high tension measurement was conducted

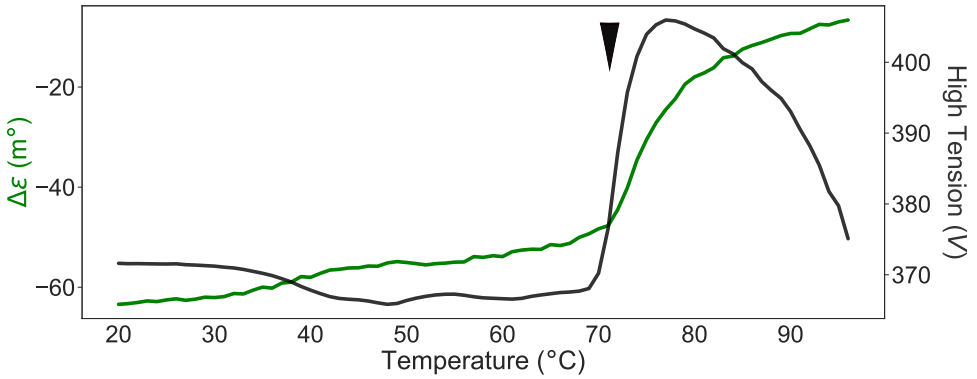

Figure 3.7: There is a spike in high tension when KcsA begins to lose alpha helical structure (black wedge).

over a fast temperature ramp during which the sample was likely not fully equilibrated with the heat bath, leading to artifactually high estimates of transition temperatures. If 60°C is

a critical temperature, then it is possible that the loss of secondary structure during KcsA melting is more continuous (and simultaneous with pore helix displacement) throughout the tetramer dissociation transition, but at 60°C there is enough unfolded pore helix in solution to rapidly precipitate the protein, leading to the rapid loss of CD absorbance and the increase in high tension.

The same trends in unfolding behavior were observed in lipids by a measurement of tryptophan fluorescence for a temperature ramp of KcsA reconstituted into azolectin SUVs and excited with 296 nm light (**Figure 3.8**). In the presence of only sodium, the pore helix is displaced at lower temperatures than in potassium. Notably, however, in lipids there is a large separation in temperature between tryptophan fluorescence transitions and tetramer disassembly. This is most prominent in the presence of sodium alone, where the fluorescence transition occurs between 40 and 60°C, whereas tetramer dissociation occurs at 80 to 100°C. Assuming fluorescence changes are mostly the result of pore helix movements, this suggests that the pore helices are fully displaced before the tetramer dissociates during KcsA melting in membranes. Interestingly, pore helix displacement occurs at nearly the same temperatures in lipids and DDM, even though the tetramer disassembles only at much higher temperatures in lipids than DDM. This suggests that lipids do not contribute much to the stability of the pore helix, but they do contribute greatly to the stability of the tetramer. This also implies the existence of a non-native tetrameric species in lipids between 60 and 80°C consisting of a tetrameric transmembrane helix bundle with pore helices displaced into the water.

The existence of such a non-native tetrameric state produced during unfolding raises several questions: Can we characterize the stability of this state, and is it an intermediate in folding?

To study the stability of this state, we equilibrated a sample of DDM-solubilized KcsA (in NaCl) at 50°C, a mostly tetrameric state in DDM but with some pore helix displacement, and exposed this sample to different amounts chemical denaturants (**Figure 3.9A**). SDS had no

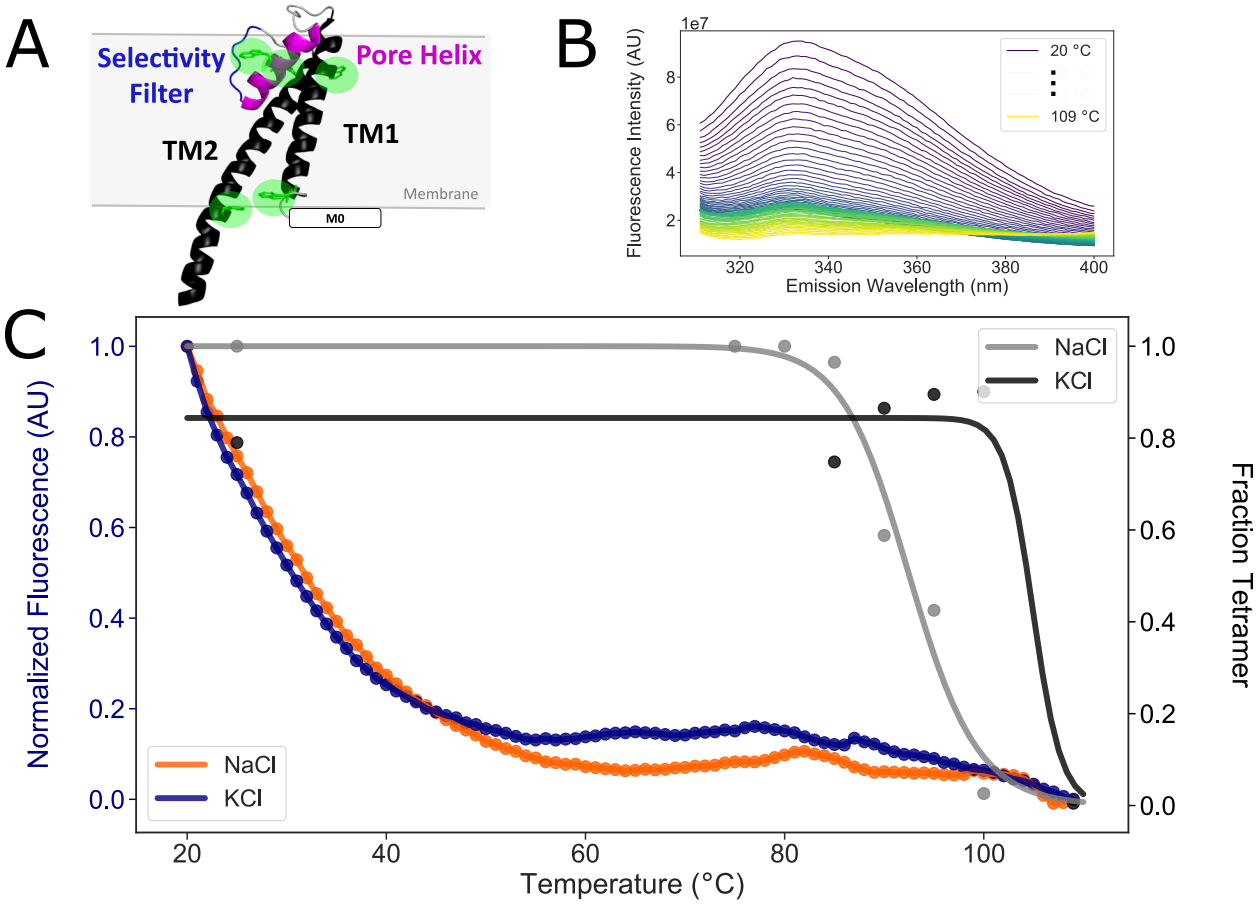

Figure 3.8: Tryptophan fluorescence of KcsA in azolectin SUVs. **A.** Structure of KcsA monomer (PDB 3EFF) highlighting key structural elements and the five native tryptophan residues in green. **B.** Full emission spectra of KcsA reconstituted into azolectin SUVs in 150 mM KCl from 20°C to 109°C. **C.** Fluorescence emission at 330 nm (in NaCl in orange and KCl in blue) shows a structural change in average tryptophan water-accessibility at temperatures where the channel remains tetrameric in lipids (overlaid SDS-PAGE curves in NaCl in grey and KCl in black).

effect on this non-native 50°C state as in the native tetramer, but TFE destabilized this state more than the native tetramer. Most surprising was the effect of urea, which did not perturb the native tetramer, but greatly destabilized the 50°C state. We also examined the effect of these denaturants on the full KcsA melting pathway by thermally denaturing the channel in the presence of a high but constant concentration of these denaturants (**Figure 3.9B**). Again, SDS had no effect on KcsA thermal stability, but urea significantly decreased the thermal stability of the channel. Therefore, destabilizing the pore helix causes destabilization of the entire tetramer.

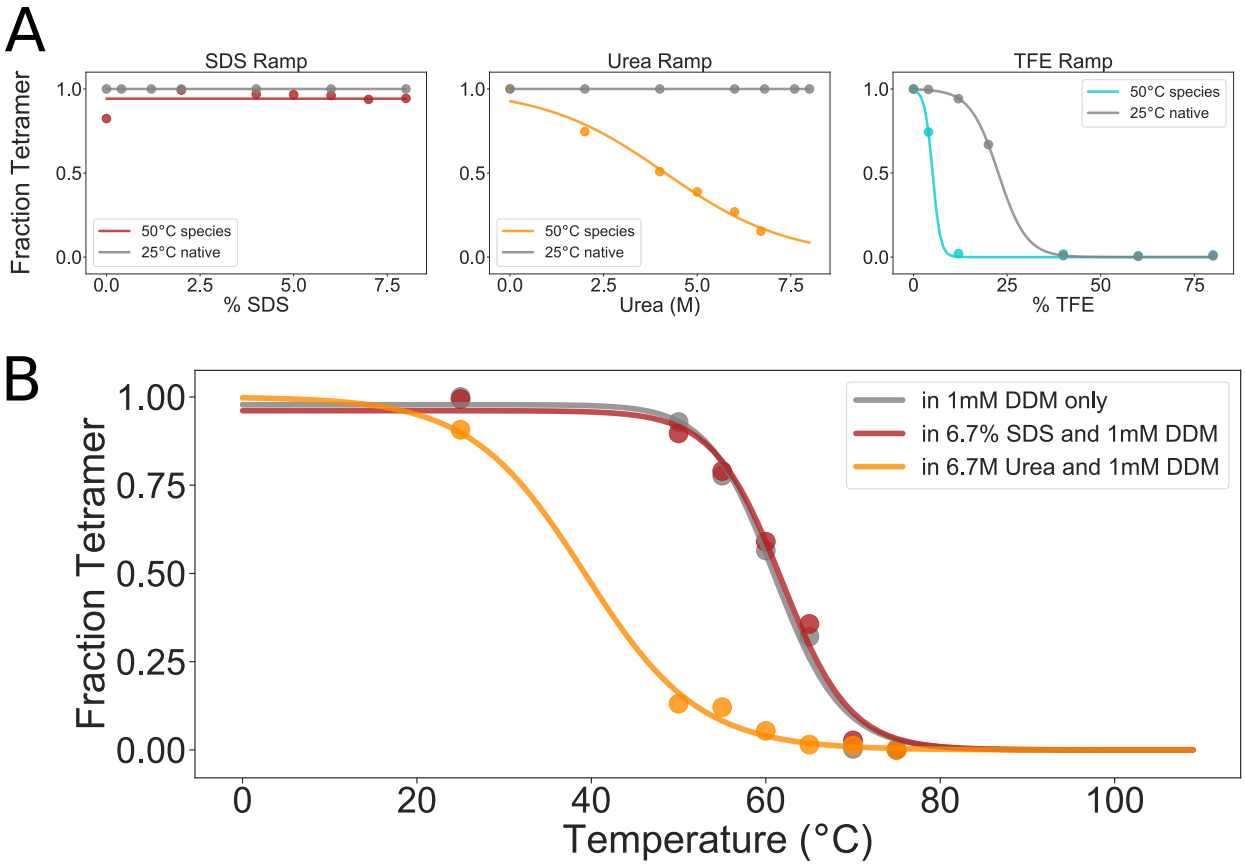

Figure 3.9: Susceptibility of non-native tetrameric species of KcsA to denaturation. **A.** This high-temperature state is destabilized in TFE and urea, but not SDS. **B.** Thermal denaturation of KcsA in 6.7% SDS and 6.7M urea demonstrate no effect of SDS, but significant destabilization by urea.

Overall, these results speak to the very different structural perturbations produced by each denaturant as well as the nature of a novel state of KcsA. Denaturing detergents (e.g., SDS) and lipids act on the stability of transmembrane helices, as observed in the large stabilization of KcsA by lipids. In contrast, urea acts on the water-exposed parts of the membrane protein, only perturbing the stability of KcsA in DDM when the pore helix becomes displaced and more water exposed at 50°C. Heat acts on all protein contacts equally, but may have additional indirect effects on transmembrane helix stability by its potential to alter the bulk material properties of the surrounding lipids and detergent. TFE simultaneously denatures and causes precipitation of KcsA in a similar manner as other alcohols.[157] For membrane proteins specifically, TFE also likely perturbs the membrane or detergent structures, fur-

ther destabilizing a membrane protein. The differential destabilization of helical membrane proteins by different denaturants is well-established but remains poorly understood.[75]

Therefore, we propose a novel species of KcsA consisting of a tetrameric transmembrane helical bundle with displaced, water-accessible pore helices that is uniquely susceptible to urea denaturation but retains tetrameric stability in lipids. This also suggests that both the pore helix and the transmembrane helix bundle are critical for native KcsA tetramer stability.

3.3 Modeling and CG-MD concur that a transmembrane helix bundle can be a metastable unfolding intermediate.

To supplement the experimental characterization of a novel non-native tetrameric state of KcsA, we have used structural modeling and CG-MD to evaluate the theoretical stability of such an state.

If this state truly consists of a transmembrane helix bundle with displaced, water-accessible pore helices as implied by the thermal unfolding experiment in lipids (**Figure 3.8**), then a model of KcsA lacking any pore helix or selectivity filter should be stable with only a transmembrane helix bundle. To test this, we ran an AlphaFold2 homo-tetrameric prediction with an input sequence of full-length KcsA, but with residues E51 through T85 replaced with a 20 residue-long poly-glycine chain which we will call KcsA-Gly_{20}. AlphaFold2 predicted a native-like structure with low per-residue confidence score (pLDDT) throughout the model protein. Given the strange vertical placement of the peripheral M0 helix adjacent and parallel to the transmembrane helices, and the lack of energetic considerations in AlphaFold2's prediction algorithms, we chose to manually relax AlphaFold2's output structure using our *Upside* coarse-grained force field (**Figure 3.10A**). *Upside* was chosen because of its ability to efficiently sample protein dynamics and because of its past success in modeling membrane proteins.[51,85,184] The resulting *Upside* structure, relaxed with the *Upside*

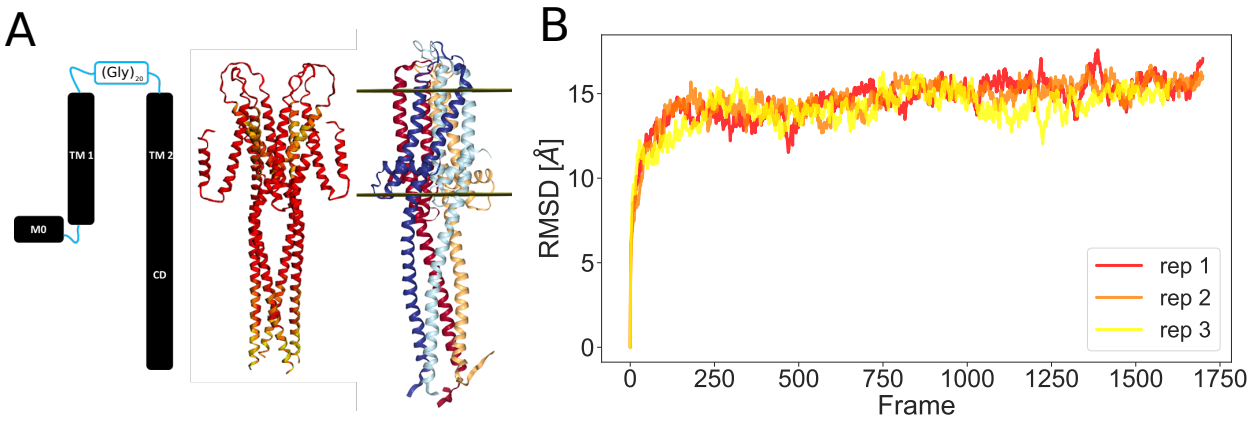

Figure 3.10: KcsA-Gly_{20}. **A.** *left*, Cartoon showing structural elements of KcsA-Gly_{20}, notably replacing the pore helix and selectivity filter with 20 glycine residues, *middle*, AlphaFold2 prediction of KcsA-Gly_{20} structure, *right*, *Upside* Representative relaxation of AlphaFold2 structure showing a bundled transmembrane helix structure. **B.** RMSD over 3 replicates of *Upside* relaxation simulations demonstrate the stability of the bundled tetrameric structure at T=0.85 kT.

2.1 force field with an implicit membrane potential in 3 independent replicates at constant temperature 0.85 kT (corresponding to approximately 25°C), finds a collapsed transmembrane bundle structure lacking a native water-filled cavity. The angle of these bundled transmembrane helices is more perpendicular to the membrane-water interface than in the native structure. This non-native tetrameric species is stable because the structure predicted by AlphaFold2 quickly equilibrates to the same collapsed state (with stable RMSD) within 200 frames in all replicates (**Figure 3.10B**). Note that RMSDs are calculated relative to the initial, unrelaxed starting structure. This stable structure supports our experimental inference that KcsA can form a tetrameric bundle of transmembrane helices, even without a pore helix or selectivity filter.

Can a similar structure be achieved at elevated temperature by a wild-type (WT) KcsA that includes the full pore helix and selectivity filter? To investigate this question, we simulated heat-induced denaturation of the truncated construct of WT KcsA (Δ125) in *Upside* using temperature replica exchange molecular dynamics (REMD) over 28 evenly-spaced replicates from 0.80 to 1.10 kT. In the 1.0 kT replicate we observed a collapsed transmembrane helix bundle in the implicit membrane with completely unfolded and water-

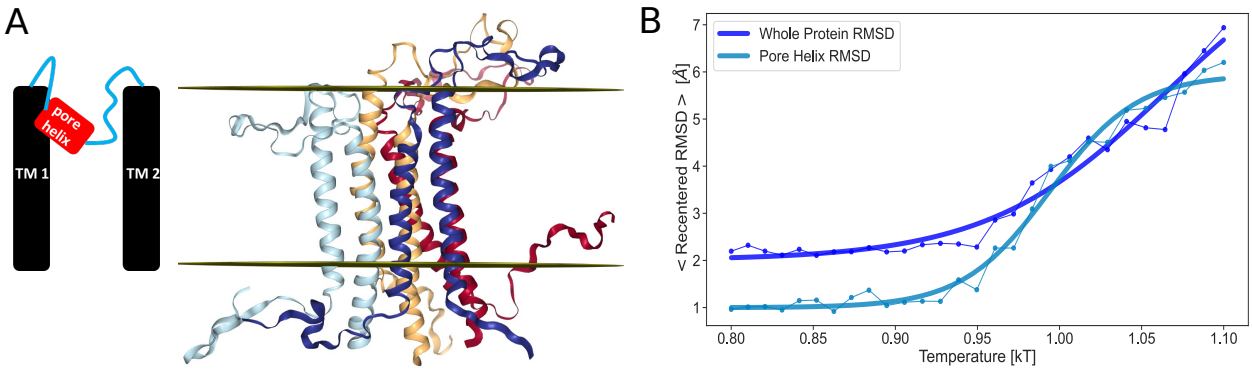

Figure 3.11: *Upside* CD-MD melting of KcsA WT Δ125. **A.** *left*, Cartoon showing main structural elements of protein, *right*, snapshot of non-native tetrameric bundle at 1.0 kT. **B.** Average recentered RMSDs per monomer over 28 temperature replicates show the lower thermal stability of the pore helix compared to the whole protein.

.

exposed pore helices and selectivity filters. As in the relaxed KcsA-Gly_{20} structure, we observed that the transmembrane helices in this collapsed state are more perpendicular to the membrane-water interface and do not surround any water-filled cavity (**Figure 3.11A**). Additionally, we constructed melting curves from the recentered RMSD of alpha carbon (CA) protein coordinates averaged over each monomer for each temperature replicate. Comparing the CA average monomeric RMSDs for the whole protein to those of only the pore helix supports our experimental observations that the pore helix of KcsA melts at lower temperatures (T_m(pore helix) = 1.00 kT) than the those required for the full tetramer disassembly (T_m(whole protein) = 1.06 kT) (**Figure 3.11B**). Note that the unfolded state of the pore helix measured by RMSD in these CG-MD simulations is displaced and no longer helical, so this state likely corresponds to the unfolded state measured by CD rather than that measured by tryptophan fluorescence.

These modeling and CG-MD studies support the plausibility and proposed structure of a non-native tetrameric state of KcsA with displaced pore helices as an unfolding intermediate.

3.4 Discussion: The role of a non-native tetrameric species in KcsA unfolding and folding.

In this chapter, we have studied KcsA denaturation by many methods, observing that only TFE and heat-induced denaturation can dissociate the tetramer. We observed significant stabilization of KcsA by ions including potassium and rubidium that can bind the selectivity filter as well as stabilization by lipids and, most surprisingly, Tris buffer. The observation that urea and SDS have no measured effect on the stability of the KcsA tetramer is consistent with the knowledge that different denaturants work by different mechanisms, and that the physical nature of membrane protein unfolding is fundamentally very different than the unfolding of water-soluble proteins.[75]

We also measured changes in KcsA structure upon thermal melting. Measurement of the tetrameric state by SDS-PAGE, alpha helical content by CD, and solvent-accessibility of the pore helix by trypotphan fluorescence suggest that structural changes upon thermal denaturation are not simultaneous among different parts of the structure. This led us to identify a novel tetrameric species at temperatures high enough to displace the pore helix into aqueous solvent, but low enough to preserve the tetramer.

The stability of this novel species was studied in different denaturants, and its susceptibility to urea denaturation and stabilization by lipids suggests that it has the following structure: a tetrameric, but collapsed bundle of transmembrane helices with displaced and water-exposed pore helices. Lastly, we demonstrated the plausibility of this non-native tetrameric state using AlphaFold2 structure prediction and Upside CG-MD, which confirm the stability of this structure as well as the susceptibility of the pore helix to unfold at lower temperatures than tetramer dissociation.

Altogether these observations suggest a sequential mechanism for KcsA thermal denaturation in DDM: Starting with native KcsA tetramer, pore helices begin to pop out into the surrounding water around 45°C. This is enough to destabilize the tetramer so that monomers

begin to form. At 60°C, the pore helices begin to lose secondary structure, with more being displaced into the water and increased tetramer disassembly. By 75°C, almost all of the pore helices have unfolded and popped out, and almost all species are monomeric. These structural transitions upon KcsA thermal denaturation are summarized by **Figure 3.12**, and are very similar to those proposed for a 2-stage mechanism of TFE-based KcsA denaturation.[8,9,18]

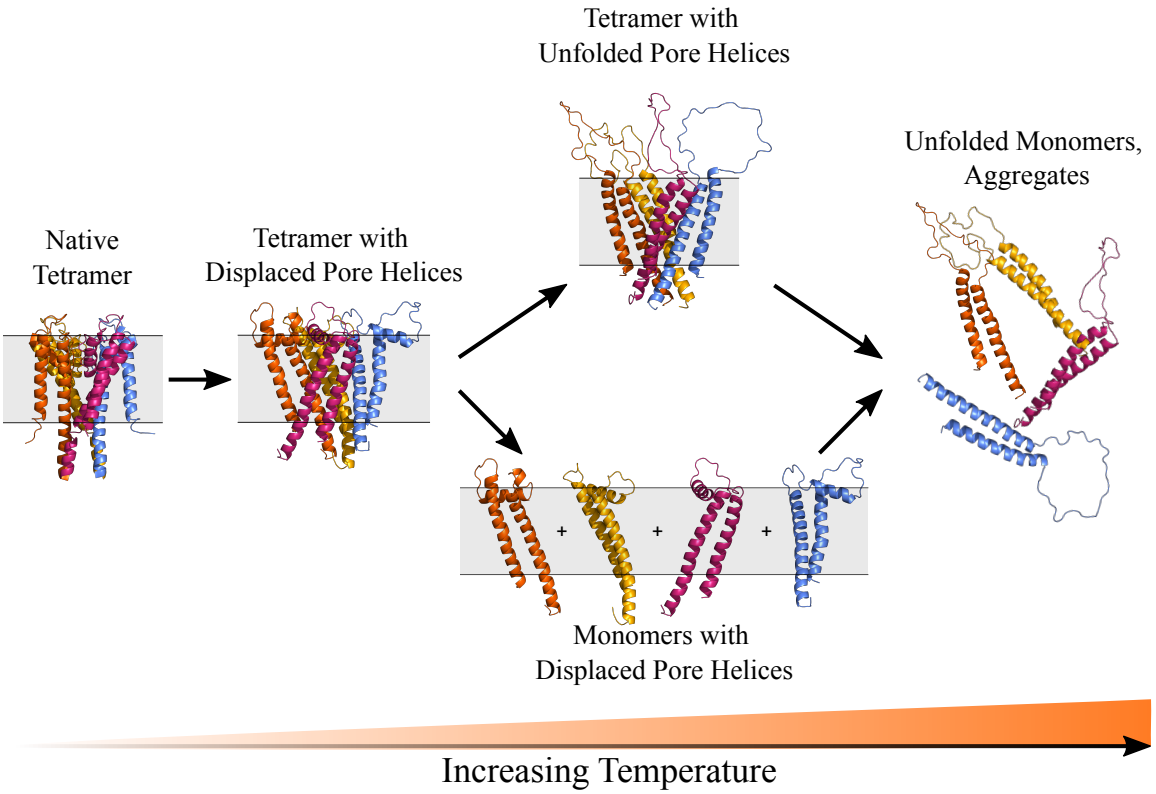

Figure 3.12: Sequential model for KcsA thermal denaturation.

While this non-native tetrameric species is certainly an unfolding intermediate, it is less clear whether this state is accessed during folding and assembly of monomers into tetramers. The structure of this species, with bundled transmembrane helices but displaced and dynamic pore helices, suggests that it could be a reasonable intermediate in the "keystone model" for KcsA folding. However, for this species to be a folding intermediate, the transition to this state from the native tetramer must be reversible. We tested this by measuring

the CD absorbance of KcsA in DDM during a temperature sawtooth, starting at 20°C, heating up to 65°C, cooling down to 20°C, heating up to 110°C, and cooling back to 20°C. We observe irreversibility of KcsA unfolding by CD absorbance during this temperature sawtooth (**Figure 3.13A**). Measuring the full CD spectrum reveals a monotonic loss of

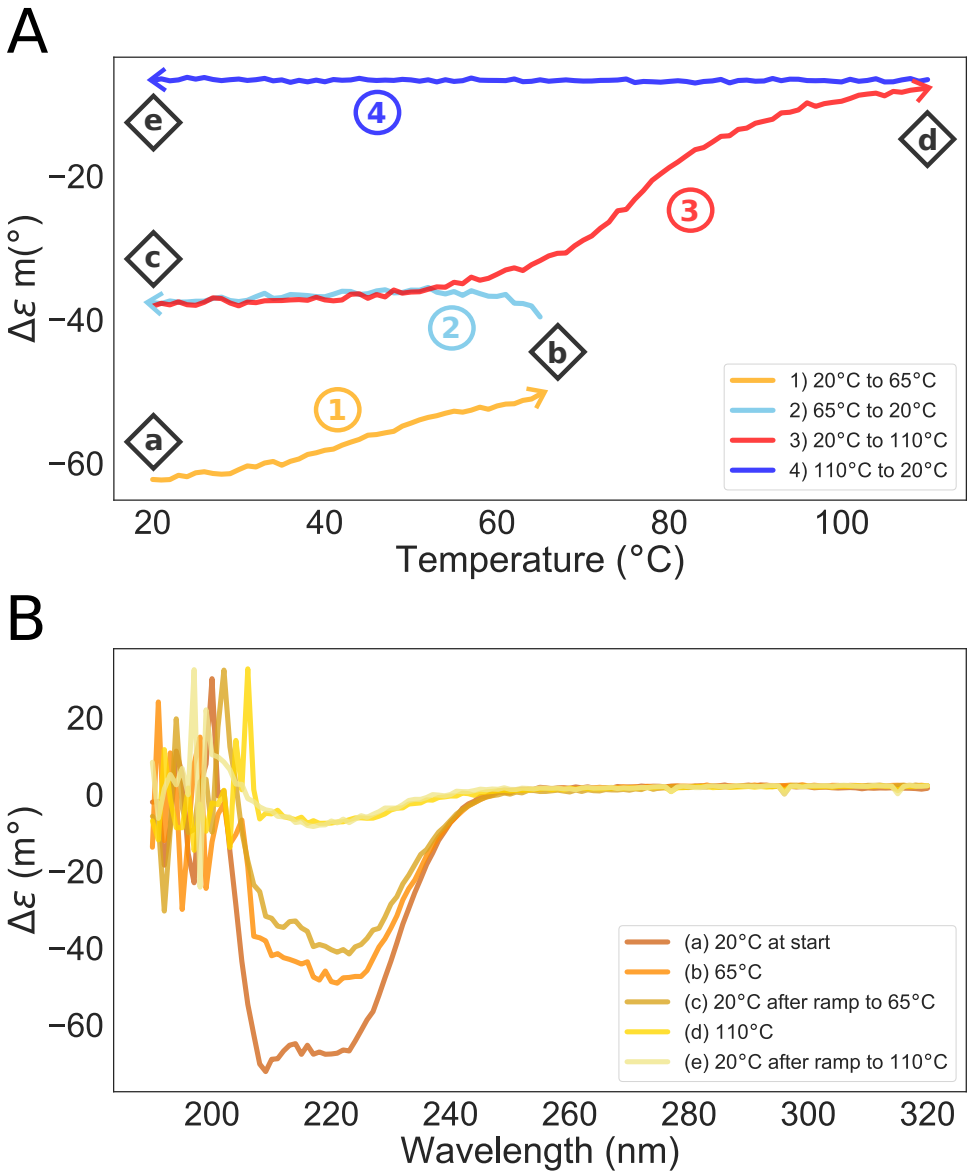

Figure 3.13: Formation of the non-native tetrameric species of KcsA at 65°C is irreversible. **A.** CD absorbance (226 nm) shows irreversible unfolding over a temperature sawtooth from 20°C to 60°C to 20°C to 110°C and back to 20°C. **B.** CD spectra in the far UV demonstrate irreversible loss of secondary structure during the temperature sawtooth. Lettered traces in **B** correspond to sawtooth endpoints in **A**.

secondary structure over the course of the experiment, irrespective of whether the sample

was being heated or cooled (**Figure 3.13B**). This irreversibility suggests that this non-native tetrameric species may not be an intermediate in KcsA folding. However, it should be acknowledged that these temperature changes were all conducted very quickly, and the sample may not have had time to fully equilibrate with the temperature bath. This could explain the large discrepancy in CD signal at 65°C in the first heating and cooling arms of the experiment. Future experiments measuring unfolding reversibility in a more gentle system (slower heating to a lower reversal temperature) and measurement of tetramerization kinetics in the presence of urea (which should destabilize any similar non-native tetrameric state) would be necessary to determine if this species is accessed during KcsA folding and assembly. Curiously, in the published 2-stage TFE-based unfolding model for KcsA, the first stage of unfolding, consisting of both pore helix displacement and tetramer disassembly is observed to be reversible in detergent.[8] However, it has been proposed that thermal denaturation of KcsA is irreversible because of the displacement of detergent molecules from the protein at higher temperatures.[18] In fact, the destabilization of the tetramer in either detergent or lipids at high temperatures may be primarily due to disruption of the membrane or membrane mimetic at these temperatures.

CHAPTER 4

NATIVE-STATE HYDROGEN-DEUTERIUM EXCHANGE DEMONSTRATES THE EXTREME STABILITY OF POTASSIUM CHANNEL KCSA

To understand the structural changes associated with potassium channel tetramerization, we sought to measure the stability and equilibrium dynamics of the KcsA monomer and tetramer, which are the two endpoints of a tetramerization or melting process. We wanted to measure protein stability, not simply of the whole protein as in Chapter 3, but on the level of individual groups of residues throughout the protein. To do this, we optimized experimental conditions for native-state hydrogen-deuterium exchange mass spectrometry (HDX-MS) measurements of KcsA monomers and tetramers in detergent (DDM) micelles.

Native-state HDX-MS is a powerful tool to measure equilibrium protein dynamics and stability by measuring the rate at which backbone amide protons exchange with bulk water. By plunging the protein into deuterated buffer at high pH, which we call the labeling buffer, native protium can exchange with deuterium in a base-catalyzed exchange reaction (at pH > 4). The reaction is then quenched at low pH, the protein is rapidly digested by protease, resulting peptides are desalted and separated by reverse-phase chromatography, and loaded onto a mass spectrometer to measure the mass change of the peptide resulting from any deuterium labeling.

For exchange to occur in a given amino acid, the part of the protein containing that amino acid must unfold, and the proton on that residue's amide nitrogen must swap with a deuterium in the labeling buffer as shown in **Figure 4.1**. In the EX2 limit, when the protein is folding and unfolding in equilibrium, $k_{\text{fold}} \gg k_{\text{intrinsic}}$, the free energy of folding that amino acid, ΔG_{fold}, is related to the measured exchange rate, k_{HDX}, by $\Delta G_{\text{fold}} \sim -RT \ln(k_{\text{intrinsic}}/k_{\text{HDX}})$. Then the relative stabilities of different parts of the protein in the

same equilibrium state can be simultaneously estimated. Alternatively, we can compare the stability of the same part of the protein in multiple different states, $\Delta\Delta G_{\text{fold}}$. We applied this powerful technique to WT KcsA and examined any differences in stability in monomers and tetramers, in the presence of potassium, and in the presence of urea, a denaturant.

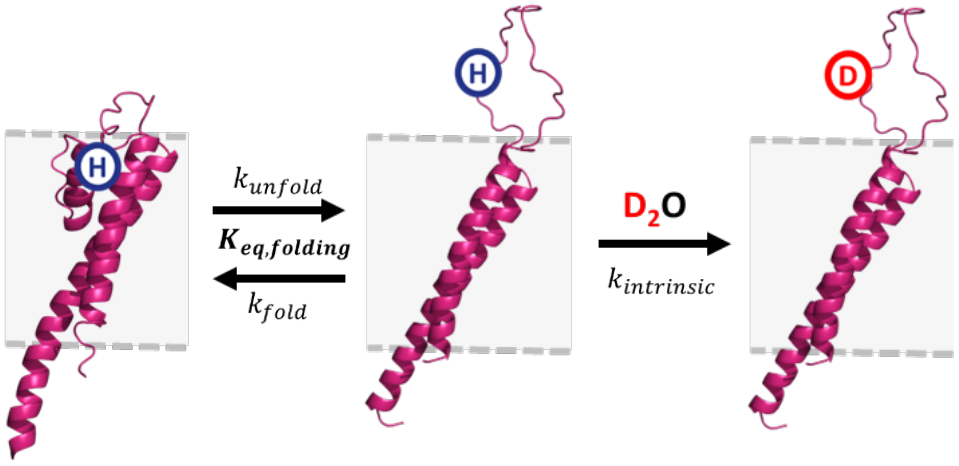

Figure 4.1: Cartoon representation of KcsA Δ125 monomer in equilibrium between folding (k_{fold}) and unfolding (k_{unfold}), and undergoing HDX ($k_{\text{intrinsic}}$) from the unfolded state. In the EX2 limit, the measured HDX rate can be compared to the intrinsic exchange rate, $k_{\text{intrinsic}}$ to estimate the free energy of folding, ΔG_{fold}.

We found that KcsA is structured even in monomeric form, maintaining most of its stability in its transmembrane helices, but becomes much more stable in the tetrameric form in which free energies of folding are too high to be measured. Additionally, to our surprise, the significant stabilization of the KcsA tetramer by potassium, as demonstrated in Chapter 3, was completely unresolvable from native-state HDX, even in the presence of urea, which destabilized only the C-terminal end of KcsA's transmembrane helix 1 (TM1) and the loop between the selectivity filter and transmembrane helix 2 (TM2).

4.1 Native-State HDX of monomeric KcsA is highly structured in DDM.

The extreme stability of tetrameric KcsA, the presence of lipid membranes or membrane mimetics such as DDM, and the inaccessibility of KcsA to protease cleavage made HDX-MS measurements quite difficult. Extensive optimization of protease cleavage conditions and liquid chromatography (LC) gradients, washes, and columns were required for even the most simple HDX-MS measurements of KcsA. Further, we found different optimal conditions for HDX-MS measurements of monomer and tetramer in DDM. Our optimized protocols are described in detail in Chapter 2.

In DDM, we were able to detect 71 unique peptides whose identity we confirmed with secondary fragmentation (MS-MS) measurements. These peptides were derived from all regions of the protein except the N-terminus of the M0 helix, a small segment in the middle of TM1 and a few residues in the middle of TM2 (**Figure 4.2A**). Notably, due to extensive peptide overlap, we were able to achieve single amino-acid resolution for many sites along the KcsA sequence including much of the pore helix and part of the cytosolic domain (**Figure 4.2B**).

We measured HDX in a pD 8.5 deuterium buffer for over 24 hours (**Figure 4.3**). The observed exchange rate in all measured parts of the protein, even in the fastest-exchanging (i.e., least protected) peptides, is orders of magnitude slower than the intrinsic exchange rate at pD 8.5 ($k_{\text{intrinsic}} \sim 500/s$). This suggests that the entire KcsA monomer in DDM is highly structured. Comparing the uptake (%D) of different structural elements of KcsA over the same labeling times allows for a qualitative comparison of stability. It is notable that the cores of transmembrane helices, TM1 and TM2, are much more protected compared to the turret, pore helix, selectivity filter (SF), and loop to TM2. Qualitatively, this suggests that the pore helix, SF, and attached loops are much more water-exposed and less stable compared to the transmembrane helices. TM2 does have higher uptake than TM1, and the

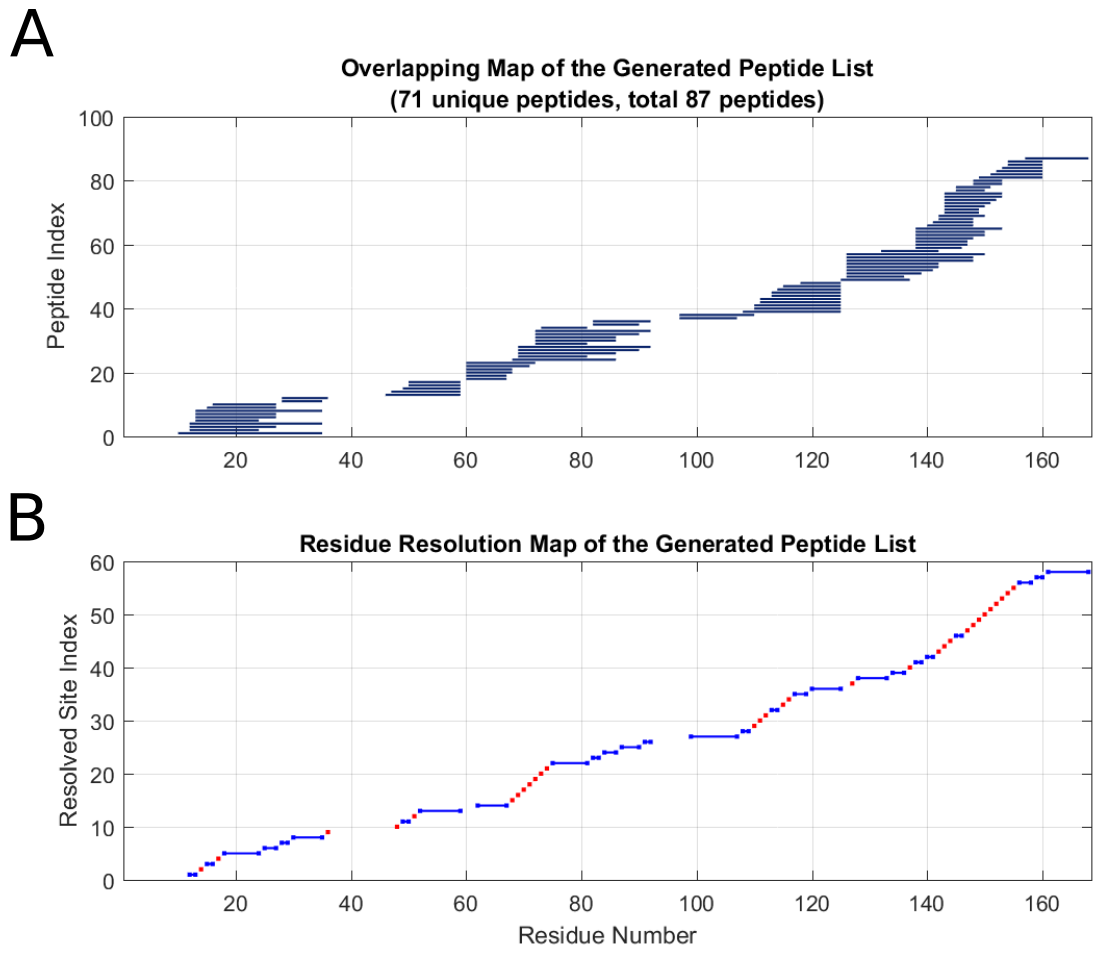

Figure 4.2: Peptide map of full-length KcsA monomer in DDM. **A.** All peptides identified from MS-MS fragmentation spectra (blue bars indicate peptide length and location within the full sequence). **B.** Peptide and residue-level resolution indicated by red dots (single amino-acid resolution) and blue bars (longer peptide resolution), with no bar or dot indicating no coverage in that part of the sequence.

ends of both TM helices have extremely high uptake, suggesting that the core of both TM helices of the KcsA monomer is already structured and buried in the DDM micelle.

While we are defining the KcsA monomer as the "unfolded" endpoint in a folding or unfolding process, native-state HDX suggests that, unlike the unfolded state of cytosolic proteins, which often behave as self-avoiding random walks with no persistent secondary structure, the unfolded, monomeric state of KcsA in DDM already has significant secondary structure. This is consistent with structural studies of the monomer in SDS that show significant structure in TM1 and TM2, but with additional flexibility in TM2 around the

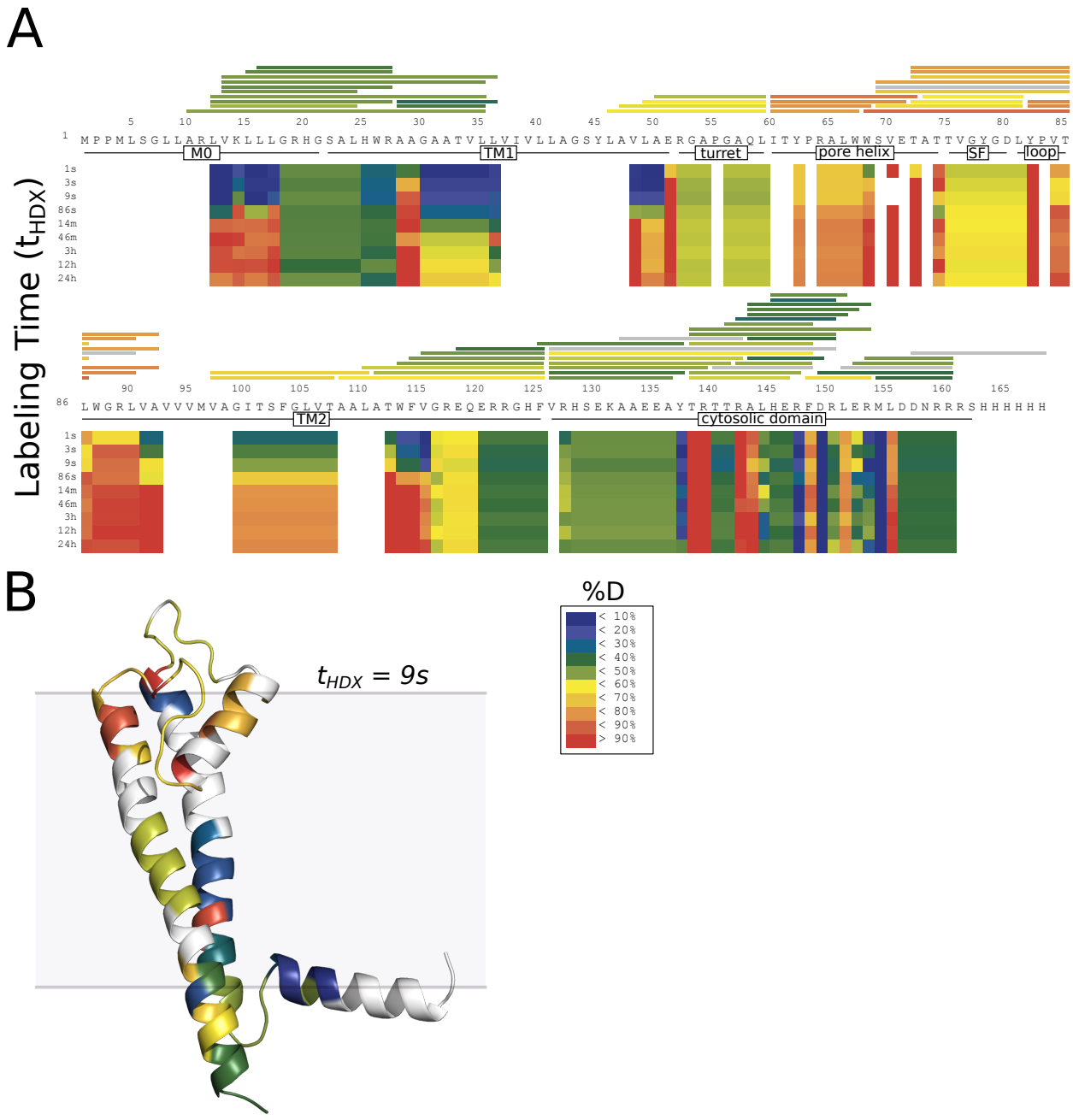

Figure 4.3: Native-State HDX of KcsA Monomer in DDM. **A.** Heatmap showing the percent deuteration throughout the protein. Uptake levels (%D) are plotted on the sequence of the protein, with important structures annotated. Bars over the sequence show all measured overlapping peptides colored by average deuterium uptake. **B.** Cartoon representation of KcsA Δ125 monomer colored by %D at 9s of labeling. White indicates no data.

G99 glycine hinge.[26]

4.2 HDX rates of tetrameric KcsA identify extreme stability.

If one defines the KcsA monomer as the unfolded state, then how does the stability of this protein change in its native tetrameric state? To evaluate this question, we optimized separate proteolysis and LC-MS conditions to maximize peptide coverage and signal for native-state HDX on the KcsA tetramer in DDM. We were able to detect and confirm the identity with MS-MS scans of 89 unique peptides. These cover the entire sequence, except for a large segment in the second half of TM1 (**Figure 4.4A**), with amino-acid resolution for many sites across the sequence, especially in the loop connecting M0 and TM1, turret, pore helix, and cytosolic domain (**Figure 4.4B**).

Deuterium uptake of tetrameric KcsA in DDM was measured at pD 8.5 over 24 hours (**Figure 4.5**). As in the monomer, we observed HDX exchange rates across the tetramer that were many orders of magnitude slower than their equivalent intrinsic exchange rates. However, all parts of the tetramer demonstrated large increases in protection compared to the monomer, except in the M0 helix. In fact, we measured almost no deuterium uptake across much of the protein within 24 hours, even in the turret, pore helix, SF, and loop to TM2. In the tetramer, TM2 is much more protected than TM1, whereas the relative stabilities of these structures are reversed in the monomer. Because of the extremely high protection in the tetramer, and because samples were prone to aggregation during labeling conditions longer than 24 hours, we could not quantify ΔG_{fold} for most of the tetramer, except for the least stable part of the channel, peptide LARLVKL spanning residues 9 to 15 in the M0 helix, which was estimated to have $\Delta G_{\text{fold}} \sim -8$ kcal/mol. Since the rest of the tetramer had even less uptake, it is likely that these regions are more stable than the M0 helix, with $\Delta G_{\text{fold}} < -8$ kcal/mol.

A more direct of comparison of stability between the monomer and tetramer can be ob-

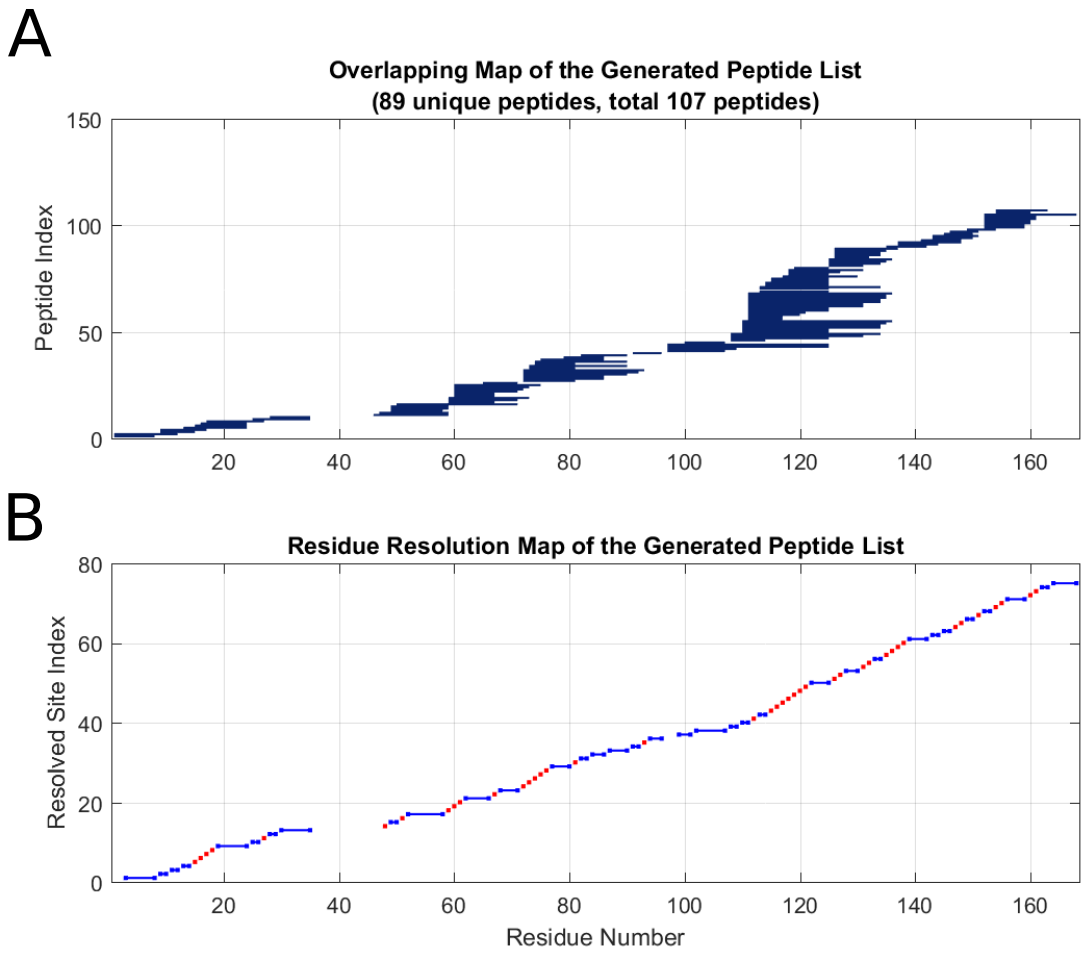

Figure 4.4: Peptide map of full-length KcsA tetramer in DDM. **A.** All peptides identified from MS-MS fragmentation spectra (blue bars indicate peptide length and location within the full sequence). **B.** Peptide and residue-level resolution indicated by red dots (single amino-acid resolution) and blue bars (longer peptide resolution), with no bar or dot indicating no coverage in that part of the sequence.

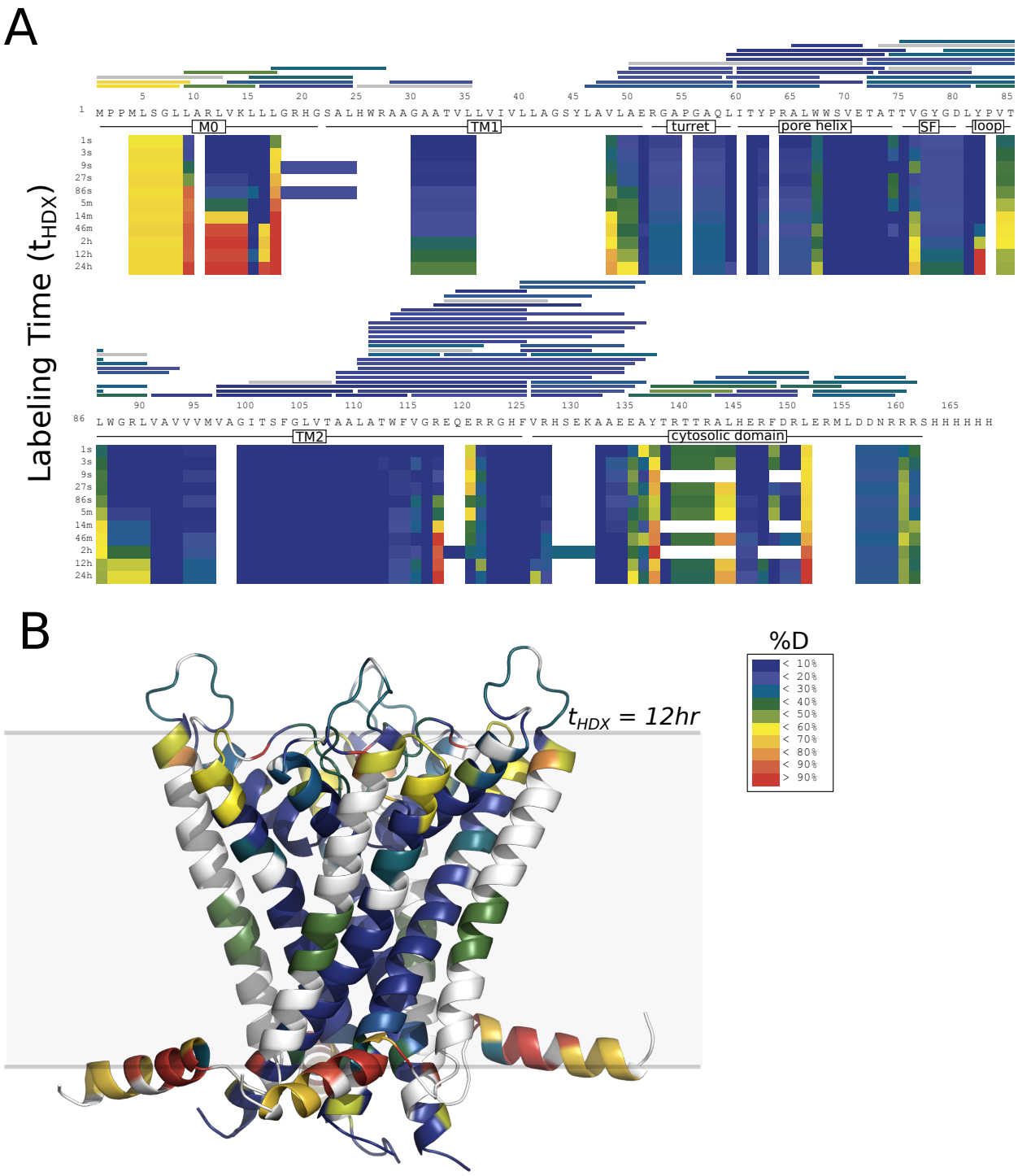

Figure 4.5: Native-State HDX of KcsA Tetramer in DDM. **A.** Heatmap showing the percent deuteration throughout the protein. Uptake levels (%D) are plotted on the sequence of the protein, with important structures annotated. Bars over the sequence show all measured overlapping peptides colored by average deuterium uptake. **B.** Cartoon representation of KcsA Δ125 tetramer colored by %D at 12 hr of labeling. White indicates no data.

served on the level of individual peptides. Examining the individual deuterium uptake curves of the peptides AAGAATVL, residues 28 to 35 from TM1, ITYPRALWWSVE, residues 60 to 71 in the pore helix, and VAGITSFGLVT, residues 97 to 107 in TM2, we again see that all three parts of the protein are very protected compared to $k_{\text{intrinsic}}$ (**Figure 4.6**). In all peptides, the exchange curves in the tetramer are right-shifted significantly from those in the monomer, again highlighting the extensive stabilization of the native tetramer.

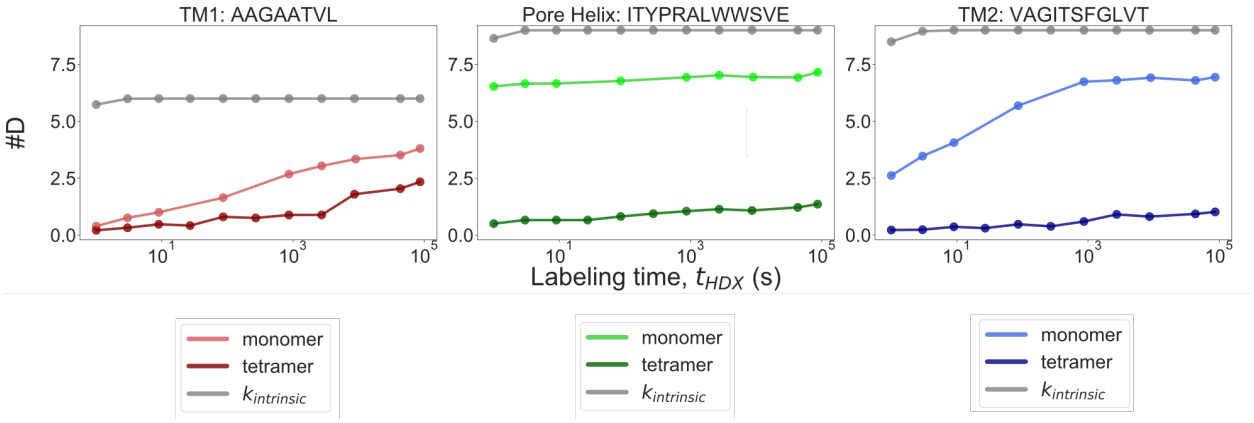

Figure 4.6: Comparison of deuterium uptake in the KcsA monomer and tetramer across 3 peptides from TM1, the pore helix, and TM2, overlaid on the theoretical exchange curves given by $k_{\text{intrinsic}}$.

There are several technical complications in attempting to quantify stability differences between tetramer and monomer beyond the inability to measure full uptake curves. The optimal HDX conditions were subtly different for monomer and tetramer experiments: both involved on-line protease digestion under the same flow rate and temperature, but the tetramer required an additional 5 minutes of digestion at room temperature with soluble pepsin. This may have resulted in greater back-exchange in the tetramer compared to the monomer. However, we repeated the tetramer HDX reaction with no soluble pepsin at 27 s of labeling, and while we observed much lower signal and many fewer peptides, the deuterium uptake in the few peptides with measurable signal was very close to the equivalent values at 27 s in the experiment with soluble pepsin reported in **Figure 4.5**. For example, in the three peptides from the tetramer in **Figure 4.6**, the average #D at 27 s without soluble pepsin was 0.39, 0.35, and 0.05, compared to 0.42, 0.66, and 0.05 with soluble pepsin, respectively.

If back-exchange were to change uptake behavior, then the calculated #D should be higher without soluble pepsin than with it. Since this is not the case, a comparison of monomer and tetramer uptake curves at pD 8.5 is reasonable.

Further, some TM2 peptides exhibited two classes or "bimodal" exchange behavior (**Figure 4.7**). For the peptide VAGITSFGLVT, the slowly-exchanging population had almost no

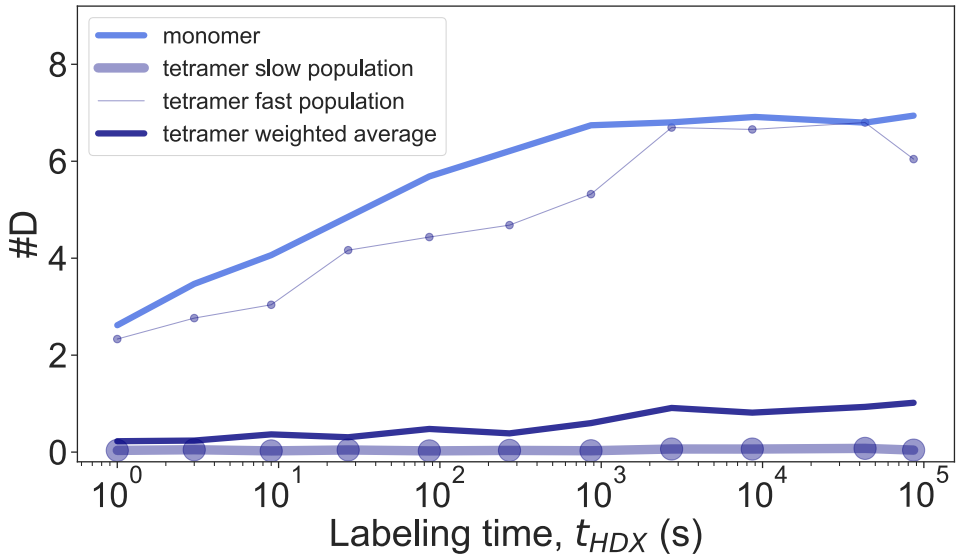

Figure 4.7: Tetrameric TM2 peptide "VAGITSFGLVT" exhibits bimodal behavior, with a slow population having no uptake and a fast population exchanging almost as quickly as in the monomer. The thickness of the lines and points in the fast and slow populations are scaled to their average size in the total population across all timepoints. These are overlaid on the plots of monomer and tetramer uptake, the latter a weighted average of the fast and slow populations.

D uptake, but accounted for 89.6% of the peptide population on average across all timepoints. This contrasts greatly with the fast population, which had very similar uptake as the monomer, but only accounted for 10.4% of the total population. This can be interpreted two ways: (1) There was significant unwanted carryover of protein in the LC system between runs, or (2) there were residual amounts of monomers in the tetrameric sample. The first scenario would result in a significant decrease in apparent deuterium uptake, as protein stuck in the LC between runs would likely back-exchange down to 0% deuterium and then elute in the subsequent run, effectively averaging that 0% population with the desired, labeled population from that run. This can happen passively as protein can stick to columns or

tubing and come out continuously, or this can occur when a plaque of protein forms in the LC and then is cleaved into peptides by soluble pepsin that is injected with the labeled protein sample in a new, subsequent run.

To evaluate the effect of carryover due to continuous sticking and elution, we measured the peptide signal from a blank run (i.e., no protein or buffers are injected into the LC-MS) following a high-signal labeled run. For the bimodal TM2 peptide VAGITSFGLVT, the measured #D in the blank run was 0.04 with signal $\mathcal{O}(7.0 \times 10^6)$ compared to 0.05 D in a protein-containing run (labeled with deuterium for 27 s) with signal $\mathcal{O}(4.5 \times 10^7)$. While the uptake was very similar between the blank and labeled experiments, the peptide signal was almost an order of magnitude greater for the labeled run, suggesting that continuous carryover did not significantly contribute to this peptide's average uptake. To evaluate the effect of soluble pepsin on carryover, we compared the #D uptake and total signal at 27 s of TM1 peptide AAGAATVL under an equivalent HDX experiment with and without soluble pepsin. Without soluble pepsin, we measured 0.39 D with signal $\mathcal{O}(3.5 \times 10^6)$, but with soluble pepsin we measured 0.42 D with signal $\mathcal{O}(6.0 \times 10^6)$. The lower signal of the experiment lacking soluble pepsin is not surprising since soluble pepsin is required for efficient proteolysis of the KcsA tetramer. If pepsin-induced carryover were significant, then a greater percentage of peptides in the experiment with soluble pepsin should have 0 D, lowering the average #D compared to the experiment without soluble pepsin. This was not observed, so soluble pepsin-based carryover is likely not the cause of the low uptake or observed bimodality in tetrameric KcsA. The second interpretation of the observed bimodality in the TM2 peptide VAGITSFGLVT is more likely, that there is a small population of monomers that accounts for $\sim$10% of the mass of the population and is not visible by SDS-PAGE. However, an additional experiment, in which soluble pepsin is injected into the LC system without KcsA while holding all other experimental conditions constant (i.e., quench and chase buffer), is necessary to definitively rule out any effect of carryover on native-state HDX measurements

of tetrameric KcsA.

To further characterize the extreme stability of the KcsA tetramer, we measured the native-state HDX of the tetramer in 4 M urea (**Figure 4.8**). Urea destabilized TM1 greatly, speeding up HDX both in the middle of the transmembrane helix and near the detergent-water interface preceding the turret. There was also a large increase in exchange in the loop between the SF and TM2. Surprisingly, there was a marked decrease in HDX in the M0 helix. We can compare the uptake curves of the M0 peptide LARLVKLLL and the SF loop peptide GDLYPVTL to examine the urea-induced HDX effects in more detail (**Figure 4.9**). Uptake in the M0 helix is significantly slowed in 4 M urea, while uptake in the SF loop is sped up moderately. However, to properly compare HDX in urea with HDX in water, measured uptake levels need to be scaled by a correction factor in order to account for the extensive interaction of urea with the protein backbone. It is well known that urea forms hydrogen bonds with backbone amide hydrogens and therefore slows HDX by approximately a factor of 2.[100] Correcting for this effect, we can compare the uptake of LARLVKLLL and GDLYPVTL in no urea with the uptake in 4 M urea, rescaled by a factor of 2 (**Figure 4.9** dotted lines). Even with this correction, the M0 peptide exhibits slower HDX in 4 M urea than in no urea, and the increase in HDX in the SF loop in the presence of urea is even more exaggerated. The decrease in HDX in the M0 helix is an unusual and unexpected effect. One possible interpretation is that urea causes TM1 to shift upward, exposing its C-terminal side to aqueous solvent and thus producing faster HDX. This is possible because this helix is capped only by a proline but lacks any aromatic residues to lock it in place at the membrane-water interface. Tyrosine 45 could lock TM1 in an upward conformation with this residue approaching the membrane-water interface, pulling the M0 helix partially into the membrane, potentially causing the linker between M0 and TM1 to become helical and protected. Further experiments would be necessary to evaluate the effect of urea on the structure of native KcsA.

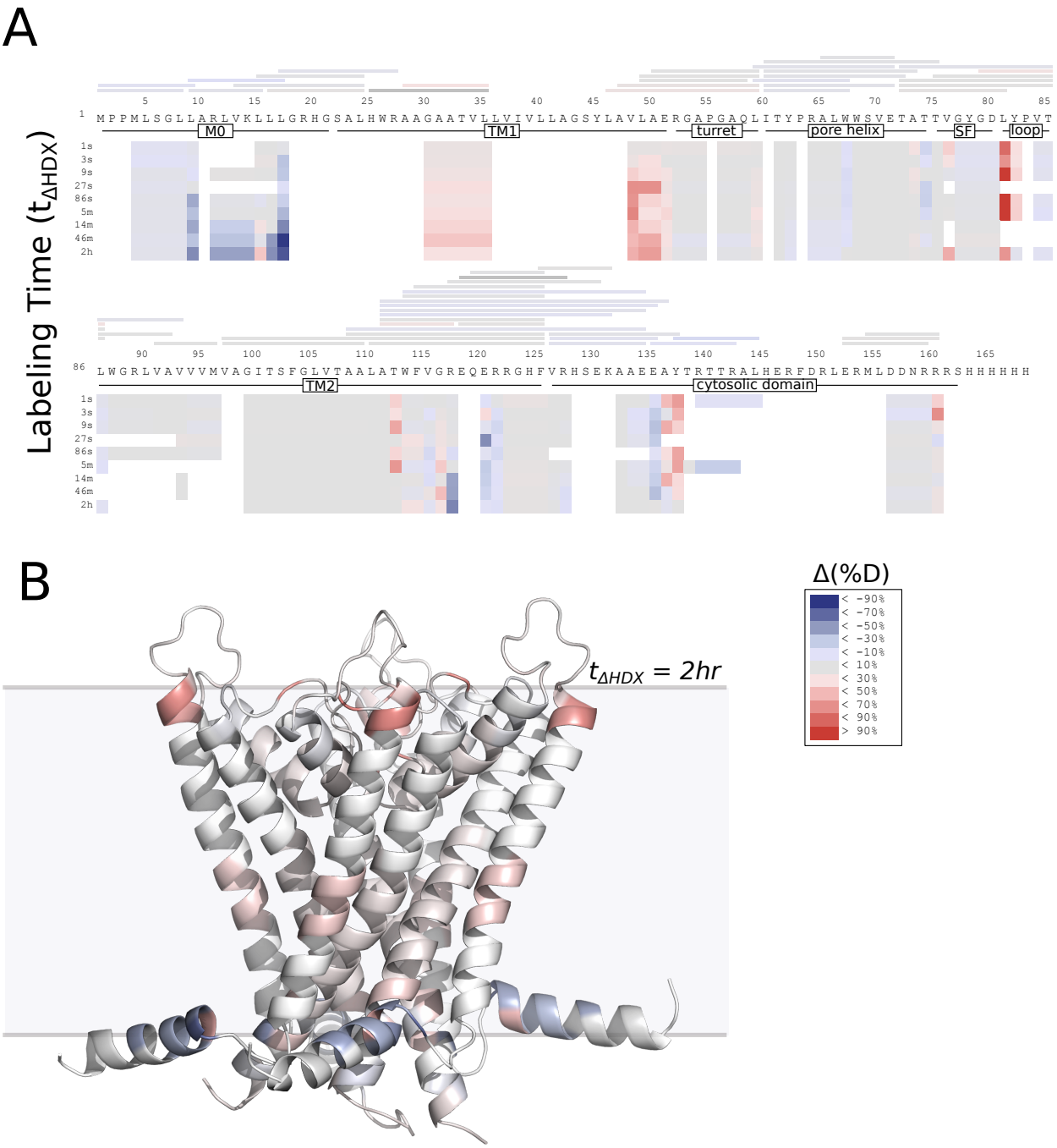

Figure 4.8: Differences in native-state HDX of KcsA tetramer in DDM without urea and with 4 M urea. **A.** Heatmap showing differences in percent deuteration (Δ%D), with red indicating more uptake in urea, blue indicating more uptake without urea, and grey indicating no change. Uptake differences are plotted on the sequence of the protein, with important structures annotated. Bars over the sequence show all measured overlapping peptides colored by average change in uptake. **B.** Cartoon representation of KcsA Δ125 tetramer colored by Δ%D at 2 hours of labeling. White indicates no data.

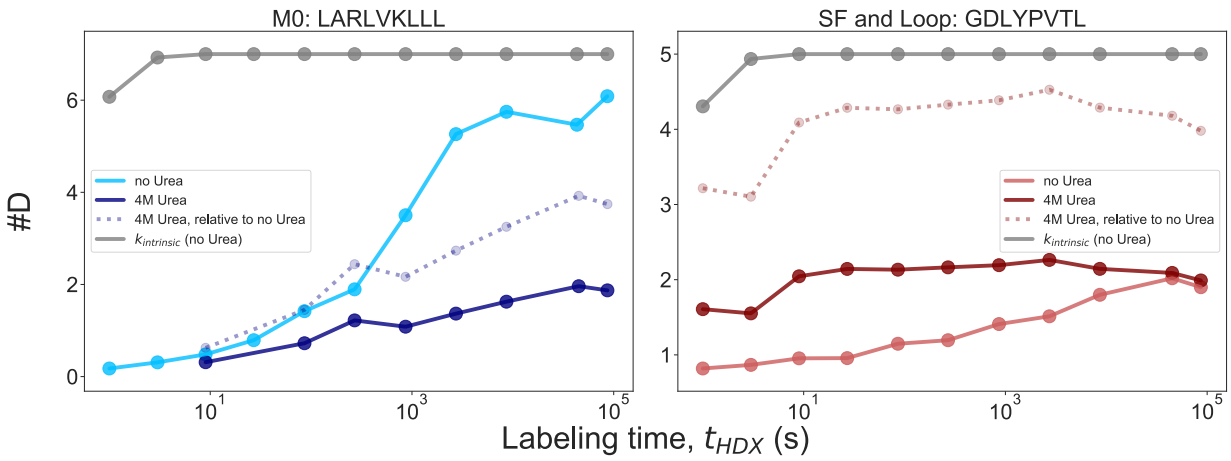

Figure 4.9: Changes in HDX in the presence of 4 M urea in two peptides in the KcsA tetramer, showing stabilization by urea in the M0 helix peptide LARLVKLLL and destabilization by urea in the SF loop peptide GDLYPVTL. Uptake curves are overlaid on the intrinsic exchange curve (grey) and an uptake curve corrected for the HDX-slowing effect of urea (dotted).

4.3 Ion-dependence of tetrameric stability is not observed with HDX.

Since the binding of selective ions K^+ and Rb^+ were observed to stabilize the tetrameric structure of KcsA so extensively in Chapter 3, we were interested in determining what specific parts of the channel were responsible for this stabilization. Accordingly, we measured native-state HDX of the KcsA tetramer in the presence of potassium ions to compare to the uptake observed in the presence of only sodium ions, reported above in **Figure 4.5**.

To our surprise, there was no significant difference in measured HDX for the KcsA tetramer in the presence of sodium or potassium (**Figure 4.10A**). We hoped to exaggerate any differences in HDX by measuring the effect of 4 M urea on the potassium-bound KcsA tetramer, but once again observed no difference in deuterium uptake at all (**Figure 4.10B**). This was unexpected, as such large differences in thermal stability between two states of a protein should be measurable by HDX. The reason for this may be the same reason why we cannot quantitatively measure ΔG_{fold} across the KcsA tetramer: Experimental constraints prevent us from sampling deuterium uptake for longer than 24 hours. Unpublished data

from Abigail Schroeter in the Sosnick Group suggest that another helical membrane protein, GlpG, requires weeks of incubation with deuterium buffer (at an equivalent pD) in order to observe full uptake of its transmembrane helices. Incubating KcsA in deuterium buffer past 24 hours results in aggregation, so these long measurements are not possible, though they may be necessary to observe the stabilization resulting from potassium or rubidium binding.

4.4 Discussion

In this chapter, we have presented native-state HDX measurements of the KcsA monomer and tetramer in DDM, in the presence of 4 M urea and in the presence of KCl. Monomer measurements were collected in a single replicate, but all tetramer measurements were averaged between 2 technical replicates.

We observed significant stabilization across KcsA tetramers compared to monomers. Despite being much less stable, the monomer is structured throughout, and exchanges much slower than the intrinsic HDX rate. This observation is consistent with existing studies of bacteriorhodopsin unfolding by single-molecule force spectroscopy that demonstrate stabilization of alpha helical transmembrane structures in membrane-embedded trimers compared to monomers.[154] While we only measured the native-state HDX of tetrameric KcsA in DDM, we would expect the stability of the KcsA tetramer in lipid to be even greater, as shown by SDS-PAGE in Chapter 3 (**Figure 3.1**). Therefore, we can conclude that during tetramerization, the KcsA monomer begins quite structured, but gains a significant amount of stability during folding to its native tetrameric state.

Native-state HDX of membrane proteins may not sample the same unfolded state that thermal unfolding or TFE denaturation achieve. This is supported by the strong dependence of bound ions on tetramer stability when measured by thermal unfolding in Chapter 3, compared to the complete lack of dependence of bound ions on tetramer stability when measured by native-state HDX-MS at room temperature in this chapter. Additionally, in

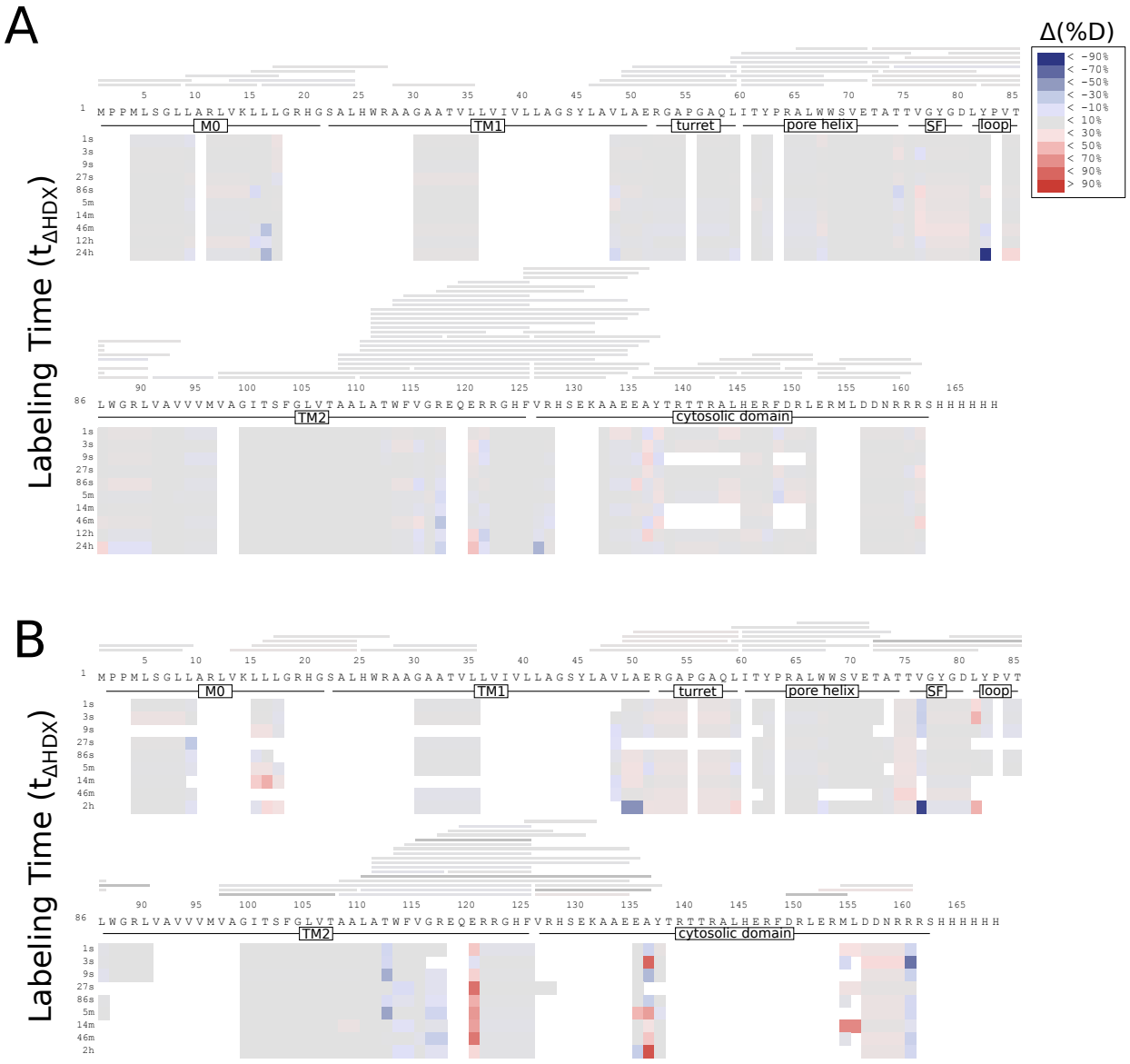

Figure 4.10: Potassium has no effect on the native-state HDX of tetrameric KcsA, with or without urea. **A.** Heatmap showing differences in deuterium uptake, Δ%D, between low potassium (100 mM NaCl) and high potassium (62.5 mM KCl, 100 mM NaCl) conditions. **B.** Heatmap showing differential deuterium uptake in 4 M urea between low potassium (100 mM NaCl) and high potassium (150 mM KCl, 100 mM NaCl) conditions. Color scale is the same in **A** and **B**, with red indicating greater uptake in the high potassium condition and blue indicating greater uptake in the low potassium condition.

Chapter 3, we observed melting temperatures of the water-soluble protein Cyt C around 85°C, compared to KcsA in DDM and NaCl, which melts at 61°C. From this, we might predict that the thermal stability of Cyt C would correspond to increased protection in native-state HDX compared to KcsA. However, in published work, many parts of Cyt C are fully exchanged by 100 s in pD 7.4.[66] While only small regions of Cyt C are not fully exchanged by 100,000 s, most of the KcsA tetramer is unexchanged at 100,000 s. For these differences to be consistent, HDX and thermal denaturation must access different unfolded states. To rationalize this, we consider the fact that membrane proteins must be solubilized in lipids or detergent. In order to unfold tetrameric KcsA into monomers in DDM, the detergent micelle must undergo fission. Membranes are easily perturbed by temperature, so at high temperatures during KcsA thermal denaturation, the energy barrier associated with micellar fission may be lowered to allow the channel to break into monomers. In contrast, at room temperature, where we measured HDX, there may be a higher barrier to micellar fission, leading KcsA to only rarely sample its monomeric state. Another explanation for the apparent inconsistency in melting temperatures and deuterium uptake in KcsA and Cyt C is also a membrane-based effect: The intrinsic exchange rate of any peptide in the membrane is necessarily lower than in bulk water. This is due to the depth-dependent decrease in the concentration of hydroxide ion (the HDX catalyst) in the interior of a bilayer or detergent micelle. It is highly unfavorable to bury a charged group in the membrane, so the effective intrinsic exchange rate must be decreased in the membrane[96,135]. Therefore, even if a buried portion of KcsA has the same stability as a portion of Cyt C, the effective $k_{\text{intrinsic}}$ will be lower in the membrane or detergent solubilizing KcsA compared to the aqueous solvent solubilizing Cyt C, which would result in comparatively lower deuterium uptake in KcsA.

Urea also induces different unfolding behavior in cytosolic and membrane proteins. In 4 M urea, we observed a destabilization of the TM1 helix of KcsA, especially near its C-terminal end, as well as destabilization in the loop between the SF and TM2. Unexpectedly,

we also measured significant stabilization of the M0 helix, which may be a result of increased secondary structure due to urea-induced upward motion of TM1. It is well known that urea induces its own protection from deuteration (by about a factor of 2) by hydrogen-bonding directly with the protein backbone.[100] However, this does not mean that the lack of any measured HDX changes in the rest of the protein necessarily indicates twofold destabilization by urea. This is because urea has a very low probability of entering the membrane and does not disrupt lipid tail packing, so very little urea is likely in contact with lipid-exposed regions of membrane proteins.[93,127] Therefore, in lipid-facing regions of KcsA exhibiting no measured change in HDX in the presence of urea, it is reasonable to conclude that these regions are not destabilized by urea. For the regions of KcsA that are destabilized by urea, it is notable that these do not occur at any inter-monomeric interfaces. This explains why urea alone is not observed to disassemble the KcsA tetramer (**Figure 3.1**). Perhaps the unfolding intermediate of KcsA observed at 50°C in Chapter 3 brings more of its inter-monomeric interfaces into contact with aqueous solvent, which could explain the urea-dependent stability of this species.

One should be wary of making any direct comparisons between the HDX measured in this chapter and the thermal stability of KcsA measured in Chapter 3 because all native-state HDX measurements were conducted in Tris buffer, which we showed significantly stabilizes tetrameric KcsA, at least at elevated temperatures (**Figure 3.3**). It is possible that measuring deuterium uptake in tetramers in phosphate buffer would yield more complete uptake curves that could resolve the differences in stability of tetrameric KcsA in potassium and sodium.

Lastly, the presence of a structured monomer with much greater flexibility than the native tetrameric species agrees with our previous work in which we observed a highly dynamic, monomeric KcsA species in nanodiscs by NMR and in all-atom MD simulations in lipids.[158] In the context of the "native assembly" model for folding, the monomers measured by native-

state HDX are flexible but structured. However, while they may retain some native-like structure, they must gain a tremendous amount of stability as they become tetramers. This suggests that the "native assembly" model, which assumes that monomers with native-like structure and stability are folding intermediates, is an unlikely mechanism for KcsA assembly. Rather, the extreme stability of the native state is only established by being locked into a tetramer.

CHAPTER 5

SITE-RESOLVED HYDROGEN-DEUTERIUM EXCHANGE PULSE-LABELING IDENTIFIES TETRAMERIZATION FOLDING PATHWAY IN A MEMBRANE PROTEIN FOR THE FIRST TIME

To determine the detailed mechanism for potassium channel assembly, it is necessary to observe changes in folding of individual structural elements of the channel. For this purpose, we have adapted hydrogen-deuterium exchange pulse-labeling, originally developed for the folding of soluble proteins, to membrane protein folding at the peptide level. Native-state HDX has been used recently to observe equilibrium dynamics of membrane proteins in lipid membranes, and around 10 years ago, HDX-MS pulse-labeling observed the folding of bacteriorhodopsin (bR) monomers from SDS into lipid bicelles.[89] However, that work only studied whole-protein changes in HDX during folding, so information about which specific parts of bR were folding was unattainable. Therefore, our work is innovative because we are the first to our knowledge to use HDX pulse-labeling to observe site-resolved changes in the hydrogen-bond network of a membrane protein undergoing folding and tetramerization in liposomes.

5.1 Adapting HDX-MS pulse-labeling for membrane protein folding in lipids

Measuring site-resolved changes in HDX in a membrane protein in liposomes (azolectin lipid SUVs) is challenging for many reasons including detergent-MS incompatibility, lipid removal, and recalcitrant proteolysis.

Ionic lipids and detergent are incompatible with MS analysis of peptides by electrospray

ionization since they co-elute with peptides off the LC and "steal" the ionizing charge required by the peptides for their flight and detection. Therefore, while in previous studies we have folded KcsA monomers from SDS into liposomes, I optimized a new purification protocol to produce KcsA monomers in DDM so that they could be folded into lipids from a non-ionic detergent. This purification protocol is detailed in Chapter 2, and was also used to generate the monomeric species of KcsA studied by native-state HDX-MS in Chapter 4.

Lipids present challenges not only in their ability to appropriate the ionizing charge from peptides during electrospray ionization, but also because they protect the protein from the proteolysis required to produce measurable peptides in the first place. Lipids also can foul the interior of the LC and MS and reduce instrument performance. We adapted a method using zirconium oxide resin to remove phospholipids from liposomes. Published studies have used ZrO_2 resin either in free suspension or packed into a column for phospholipid removal in native-state HDX studies of membrane proteins in lipids.[4,65] We observed that ZrO_2 binds not only lipids, but also protein and peptides, and that blocking excess free binding sites on ZrO_2 beads with bovine serum albumen (BSA) was required for peptide recovery with high signal, in agreement with recently-published work.[65] Unlike this work, however, we found that reproducible, high-signal detection of peptides from liposome-integrated KcsA required using a solution-suspension of ZrO_2, blocked with BSA for at least three hours, rinsed 5 times in isocratic buffer (0.1% FA in water, pH'd to 2.5 with TFA), and used for lipid removal within an hour of this last rinse. We also found that high amounts of non-ionic detergent (0.4% DDM) and a cocktail of denaturants (3 M urea, 1 M thiourea) were required in the acidic HDX quench buffer. This quench buffer had three main functions: (1) It stopped the HDX labeling reaction, (2) it prevented KcsA aggregation during lipid removal, and (3) it followed the sample through the LC system as a "chase" buffer to catch sticky and often elusive hydrophobic peptides for MS analysis. We found optimal proteolysis to occur for KcsA proteoliposomes in two digestion steps: (1) with soluble pepsin for 5 minutes at room

temperature and then (2) on-column in a hand-packed 1:1 pepsin:FPXIII (fungal pepsin from *Aspergillus saitoi*, type XIII) column at 20°C. Lastly, for long-term LC and MS maintenance, we eluted our sample from the analytical reverse-phase C18 column using methanol (with 0.1% FA) rather than acetonitrile.

This optimized preparation, summarized in **Figure 5.1**, is necessary in order to detect any peptides from KcsA tetramers in lipids, and allowed us to measure site-resolved changes in hydrogen bonded structure in a membrane protein for the first time. A more detailed protocol is described in Materials and Methods, Chapter 2. With this protocol, we were able to detect up to 26 unique peptides from a population of KcsA, 2.5 minutes after insertion into liposomes (**Figure 5.2**). In reality, at longer folding times, KcsA became even less accessible to proteolysis, but over 15.5 hours of folding, we were able to measure around 11 peptides reproducibly and with very high signal. We examine the behavior of those peptides during KcsA folding and tetramerization in detail below.

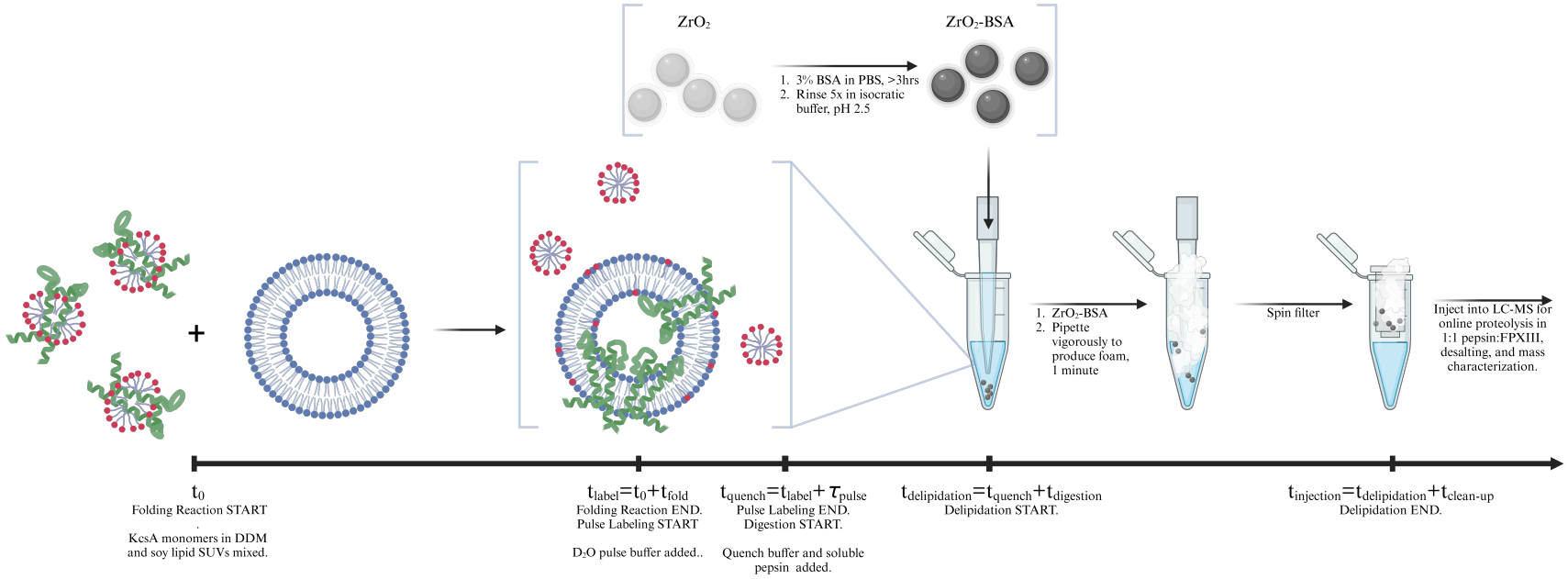

Figure 5.1: Workflow for KcsA folding with HDX Pulse-Labeling. Figure created with BioRender.com.

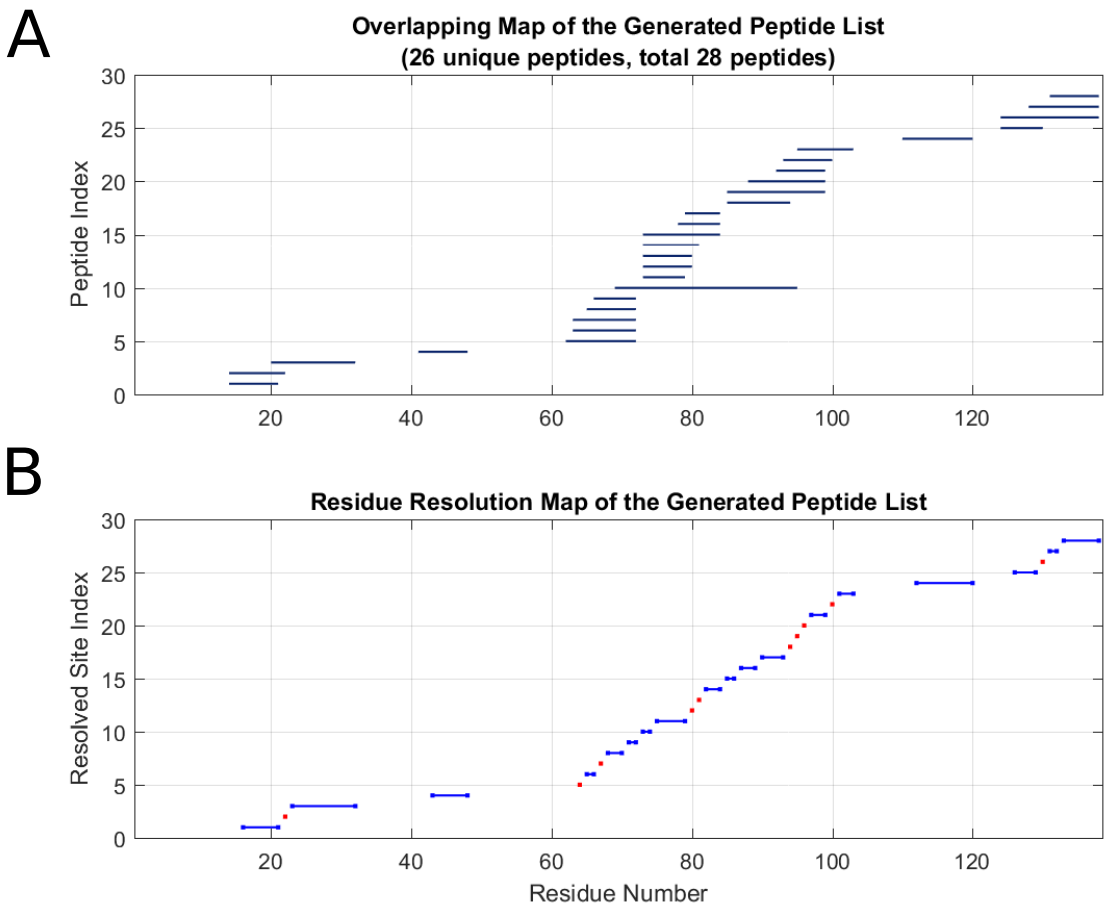

Figure 5.2: Peptide map of KcsA assembling from monomer in DDM to tetramer in azolectin lipid SUVs for 2.5 minutes, with optimized delipidation and proteolysis protocol for pulse-labeling. **A.** All peptides identified from MS-MS fragmentation spectra (blue bars indicate peptide length and location within the full sequence). **B.** Peptide and residue-level resolution indicated by red dots (single amino-acid resolution) and blue bars (longer peptide resolution), with no bar or dot indicating no coverage in that part of the sequence. At longer labeling times, even fewer high signal peptides were recovered.

5.2 Theoretical behavior of peptides in HDX pulse-labeling of membrane protein folding

For a given peptide in a pulse-labeling experiment studying KcsA folding and assembly, we consider three scenarios for changes in the average deuterium labeling during tetramerization: (1) If the peptide is from a part of the protein that is unfolded in the monomer and stays unfolded in the tetramer, then deuterium occupancy will be high in the monomer and remain

high throughout tetramerization (**Figure 5.3** top trace). (2) On the other hand, if the peptide is from a part of the protein that is folded in the monomer and remains folded in the tetramer, there will be low deuterium occupancy at all times during the assembly process (**Figure 5.3** bottom trace). (3) In the case where a peptide is from a part of the protein that has less secondary structure in the monomer than in the tetrammer, a decrease in deuterium occupancy will be seen (**Figure 5.3** middle trace). Of course, for membrane proteins, protection from HDX can arise not just from backbone hydrogen bond stability but also from the lipid bilayer. Therefore, a decrease in deuterium labeling of a peptide could also imply that it is becoming more buried in the bilayer over the course of tetramerization.

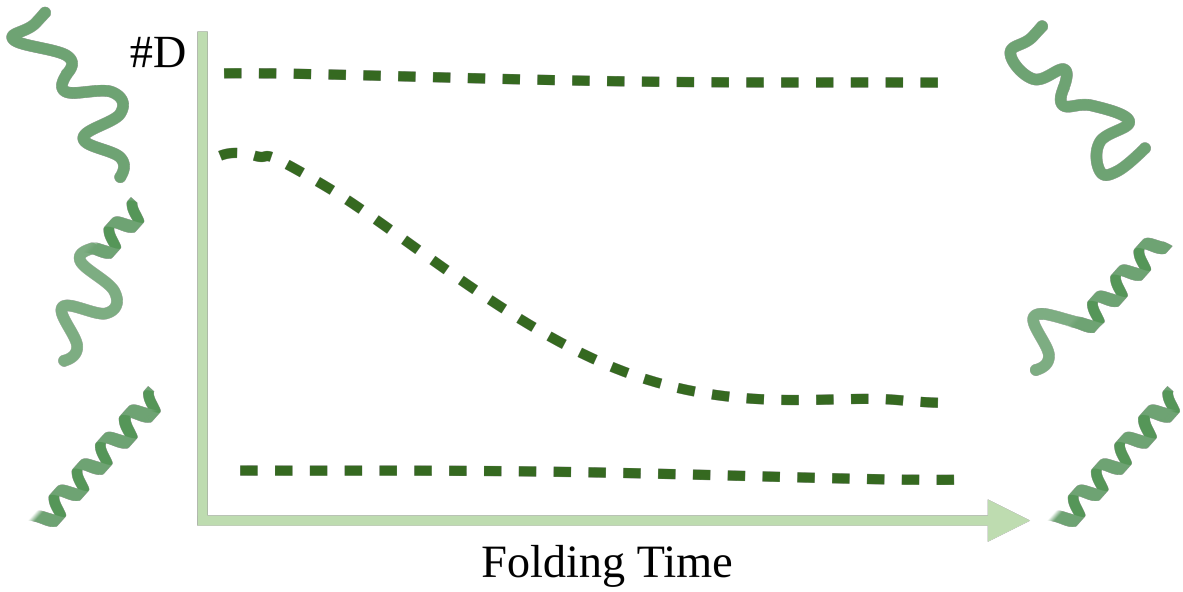

Figure 5.3: Possible scenarios for peptide-level HDX-MS pulse-labeling curves over the process of KcsA folding and assembly, from monomer in DDM on the left to tetramer in lipid on the right.

In reality, we only observe the latter two behaviors, peptides that fold over the course of tetramerization and peptides that remain stably folded throughout the process, as no measured peptide was fully unfolded in either the monomer or the tetramer. Although we are treating the monomer as our unfolded state, we know from native-state HDX that the monomer is already quite structured (**Figure 4.3**). Then if most parts of KcsA become even

more stable during tetramerization, we should not be surprised by the lack of any measured peptides with uniformly high deuterium labeling at all times during channel assembly. It is also conceivable that deuterium labeling could identify unfolding events, movement of helices out of the membrane and into aqueous solvent, or even non-monotonic behavior, but none of these trends were observed in any of the peptides during tetramerization.

This examination of peptide-level pulse-labeling behaviors treats the population of KcsA undergoing folding and tetramerization as homogeneous (unimodal) at each timepoint. This is reasonable for the peptide mass distributions in this pulse-labeling experiment, of which many can be fit well to single mass envelopes. However, some peptides, especially fast-folding peptides, are better fit with a bimodal model (**Figure 5.6**). This observation is consistent with previous pulse-labeling studies of fast-folding water-soluble proteins, which exhibit both unimodal and bimodal peptide mass distributions.[78,183]

Lastly, it is important to mention that we chose a pulse duration of 6 s, which is about 100 times the lifetime of an average unprotected amide hydrogen at pD 9.0 across all reported peptides ($< k_{\text{intrinsic}} >^{-1} \sim \ 0.06\ s$). Therefore, anytime a part of the KcsA backbone is unfolded and exposed to the labeling buffer during tetramerization, it will become deuterated.

5.3 Site-resolved changes in hydrogen-bonded structure during KcsA folding and tetramerization

In **Figure 5.4**, we present pulse-labeling curves for 9 peptides, pulsed at pD 9.0 for 6 s, extracted from a population of KcsA undergoing folding and tetramerization from monomers in DDM to tetramers in liposomes over 15.5 hours. These peptides span the following regions of KcsA: TM1, turret, pore helix, selectivity filter, and TM2. They exhibit different behaviors, with some peptides folding progressively during tetramerization (pore helix, selectivity filter, TM2) compared to others that retain similar folds during channel assembly (TM1, turret).

We are able to examine the contribution of the inner and outer halves of the pore he-

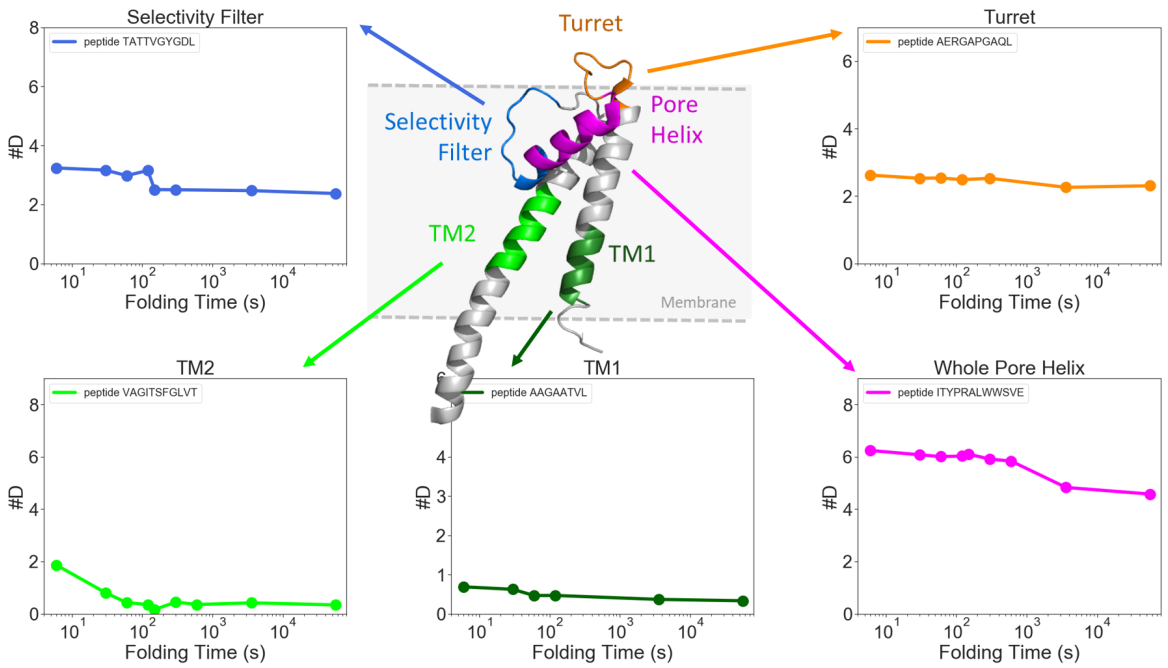

Figure 5.4: Site-resolved HDX pulse-labeling demonstrates diverse folding behaviors throughout the protein. Measurements were taken over 15.5 hours following initiation of insertion and tetramerization of DDM-solubilized KcsA monomers in liposomes (azolectin SUVs).

lix by examining the overlapping peptides LWWSVE (inner pore helix), ITYPRAL and ITYPRALW (outer pore helix), and ITYPRALWWSVE (whole pore helix). By "inner" and "outer" we are referring to the 3D location of each peptide with respect to the potassium conduction pathway in the center of the native tetramer. Both the inner and outer parts of the pore helix decrease occupancy by approximately 1 deuterium over 15.5 hours, implying that they each form on average about 1 hydrogen bond during tetramerization. This is consistent with the observation that the peptide containing the entire pore helix, ITYPRALWWSVE, loses about 2 deuterium atoms during channel tetramerization (**Figure 5.5**). Comparing the outer pore helix peptides ITYPRAL and ITYPRALW, we see a difference in deuterium occupancy of 0.8 D at t=0, which decreases to 0.3 D at 15.5 hours, suggesting that W67, the only residue of difference between these two peptides, contributes an average of approximately 0.5 hydrogen bonds formed during KcsA tetramerization.

Notably, the inner portion of the pore helix folds very fast compared to the outer por-

tion, with deuterium occupancy no longer changing about 1000 s after insertion into the membrane. In contrast, the outer part of the pore helix folds slower, with the peptide ITYPRALW still undergoing exchange after 1 hour.

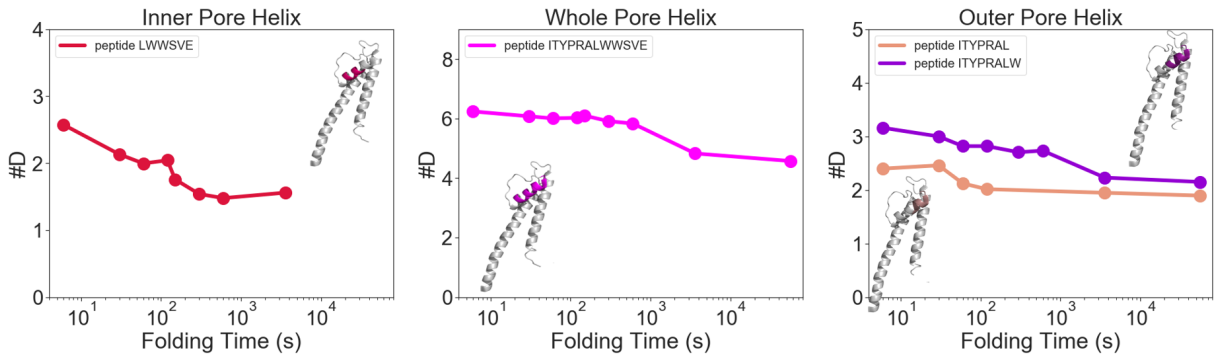

Figure 5.5: HDX pulse-labeling behavior in overlapping peptides from the KcsA pore helix. The inner portion of the pore helix folds faster than the outer pore helix.

Among other peptides examined in this study, the peptide VAGITSFGLVT from TM2 also folds very quickly, within 100 s of insertion into the membrane. This peptide contains both the putative channel opening hinge, G99, and the first glycine of a conserved glycine zipper, G104.[90,108,151,171]

Notably, peptides ITYPRALWWSVE from the pore helix and VAGITSFGLVT in TM2 have bimodal mass distributions, of which we have plotted only the quickly-exchanging population from ITYPRALWWSVE and the unimodal fit of VAGITSFGLVT in **Figures 5.4** and **5.5**. The full, bimodal behavior of these peptides is shown in **Figure 5.6**. For the pore helix peptide, this bimodality is likely not EX1-type HDX behavior since none of the constituent peptides from the inner or outer pore helix are bimodal. Also, if this were true EX1 behavior, we would expect the fraction of proteins in each population to change monotonically in time, but this is not the case (**Figure 5.6**, bottom left). In contrast, VAGITSFGLVT may be exchanging in the EX1 limit at fast folding times. However, since we only have one timepoint exhibiting bimodal behavior, we cannot conclude that this peptide is in the EX1 limit without additional data at shorter folding timepoints with higher temporal

resolution.

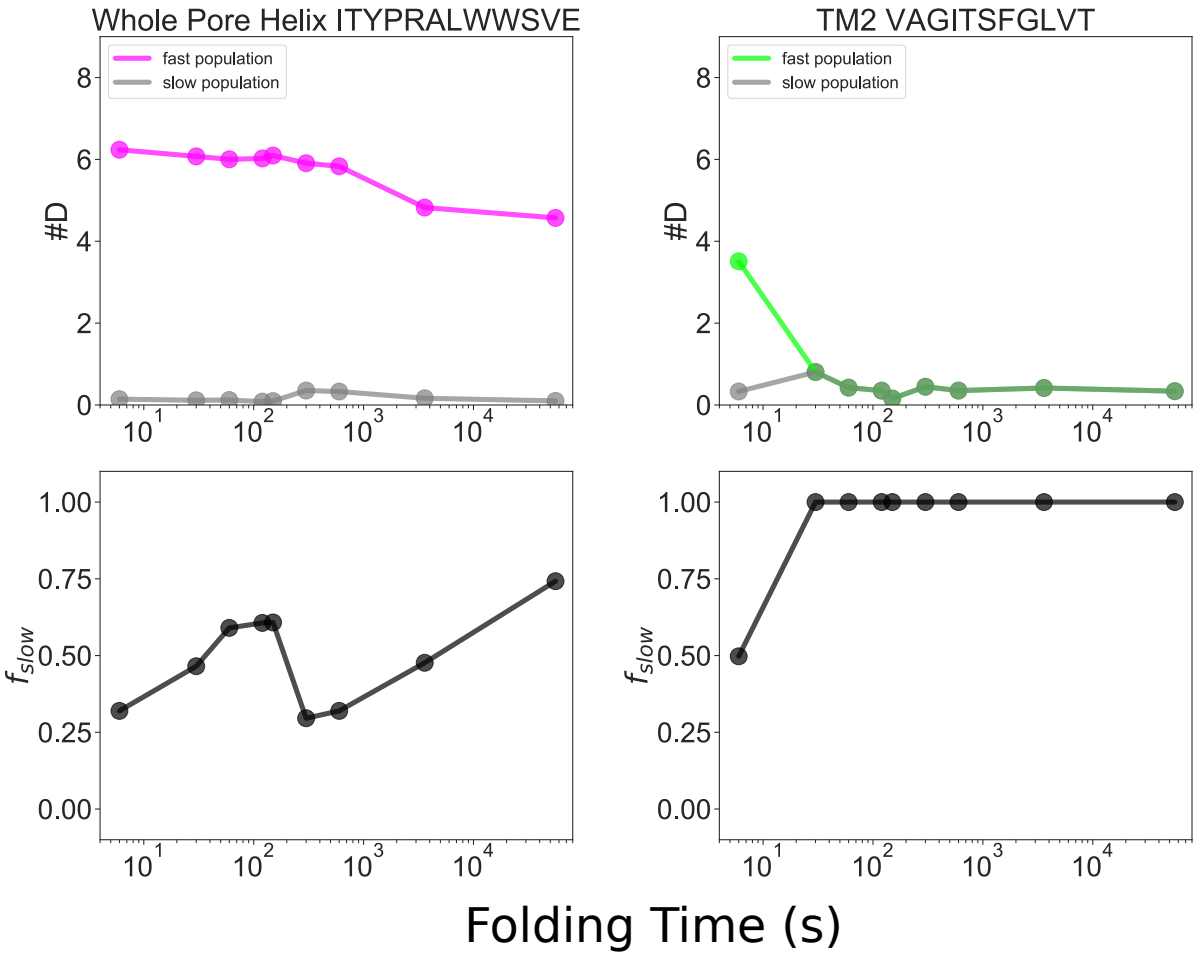

Figure 5.6: Bimodality in mass envelopes of two peptides during pulse-labeling. *Upper* plots show changes in deuterium occupancy in the fast and slow-exchanging populations of each peptide. *Lower* plots estimate the fraction of the KcsA particles in the slow-exchanging population over time.

Overall, these results suggest that the inner pore helix and center of TM2 in the vicinity of the glycine hinge fold quickly (within 1000 s and 100 s, respectively), followed by slower folding of the outer pore helix and selectivity filter during channel tetramerization.

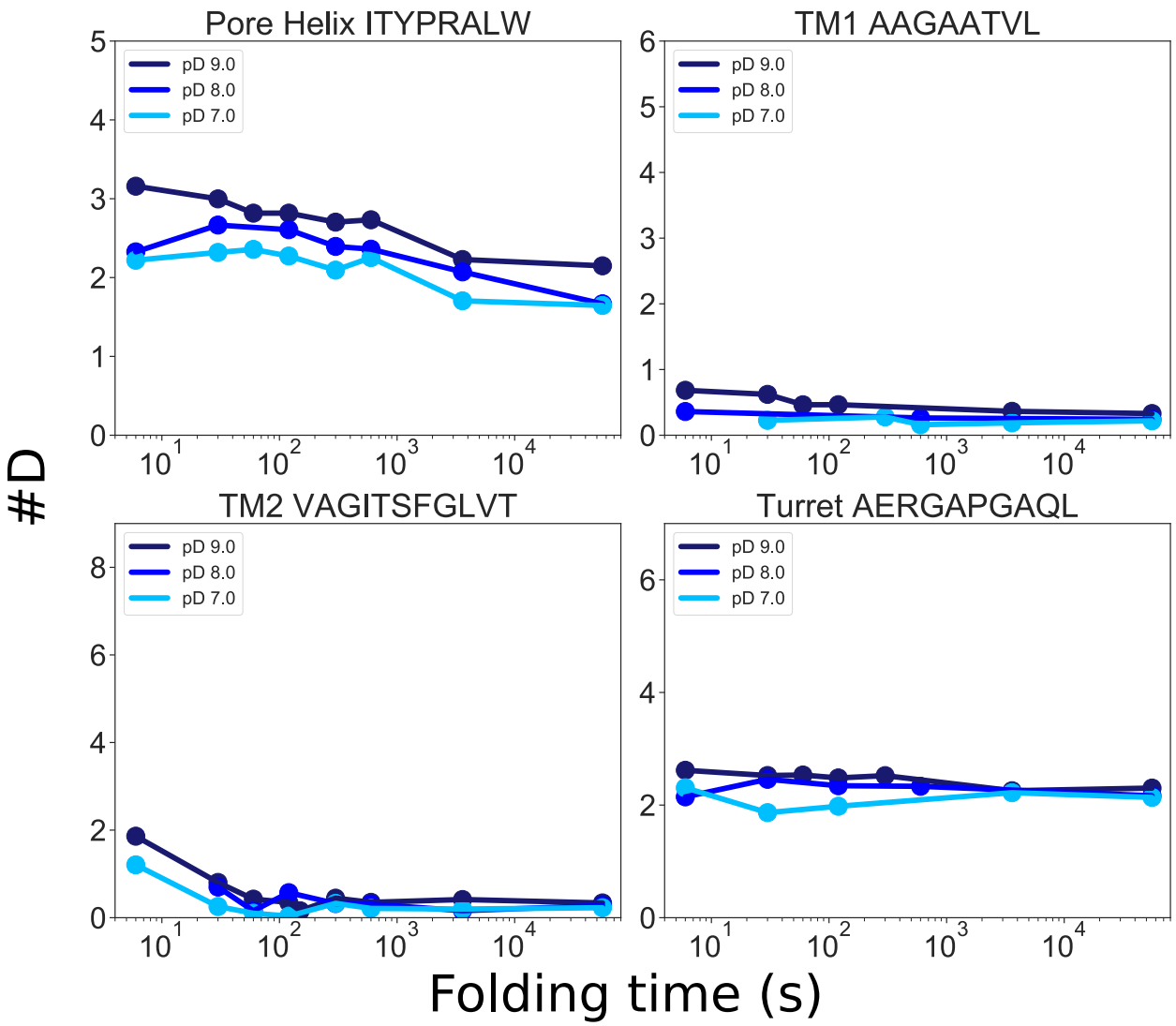

Figure 5.7: Stability-labeling of KcsA tetramerization at pD 7.0, 8.0, and 9.0 demonstrates diverse stability in folding intermediates at different sites in the protein.

5.4 Stability-labeling demonstrates stable tetramerization intermediates.

Our pulse-labeling experiment studying KcsA tetramerization with a pulse of pD 9.0 was repeated, but we applied labeling pulses of different strengths by changing the pD from 7.0 to 9.0. This variation of HDX pulse-labeling is termed "stability-labeling" since differences in deuterium uptake between different pulse strengths applied at the same folding time measure

the relative stability of the population at that given folding timepoint.[188] Here we highlight 4 representative peptides exhibiting interesting behavior from HDX stability-labeling (**Figure 5.7**).

The pore helix, throughout the entire tetramerization process, and early folding intermediates of TM2 have lower stability compared to other structures according to HDX. We conclude this from the marked differences in deuterium occupancy at all timepoints between pD 7, 8, and 9 in the pore helix, and between pD 7 and 9 in the TM2 peptide within 100 s of membrane insertion. In contrast, the HDX data indicate that intermediates of TM1, TM2 after 100s, and the turret are very stable, with equivalent pulse-labeling deuterium occupancies over all strengths of pulse. The regions of KcsA that exhibit less stable intermediates from stability-labeling are the same regions observed to be less stable in the native-state HDX of the monomer (**Figure 4.3**). Unexpectedly, these are not the same regions of the KcsA tetramer perturbed by 4 M urea (**Figure 4.8**). This suggests that the tetramerization intermediates of KcsA are more similar in stability to the monomeric state. Lastly, the slow populations of bimodal peptides are all unperturbed by different pDs, suggesting that the slow-exchanging population is extremely stable, perhaps being the folded tetrameric state.

Stability-labeling by varying pulse pD is particularly tricky difficult for KcsA, since it is a pH-gated channel that opens at low pH.[168] This means the range of pDs we choose must be small: We cannot go above pD 9 without risking neutralization of cationic residues. Likewise, below pD 7, the histidines may become protonated, while below pD 5 acidic amino acids in the intracellular gate of KcsA are neutralized. The restriction of pulse strength to between pD 7 and 9 necessarily leads to a small dynamic range in measured deuterium occupancy. Overall, we would expect more dynamic range in stability-labeling measurements if the monomer were less structured at the start of tetramerization, but since we know from native-state HDX that the monomer is already quite structured in DDM, the small changes in deuterium occupancy we see during tetramerization are expected.

Note that at pD 7, our pulse length of 6 s is just shorter than the average lifetime of an unprotected amide hydrogen in pD 7 pulse buffer. Therefore, it is possible that not every backbone opening event is captured by this pulse condition. Despite this, the pulse-labeling curves of each peptide at pD 7 appear to follow the same qualitative trends as those measured at pD 8 and 9, simply with a smaller changes in average deuteration over 15.5 hours of tetramerization.

5.5 Putting pulse-labeling in context

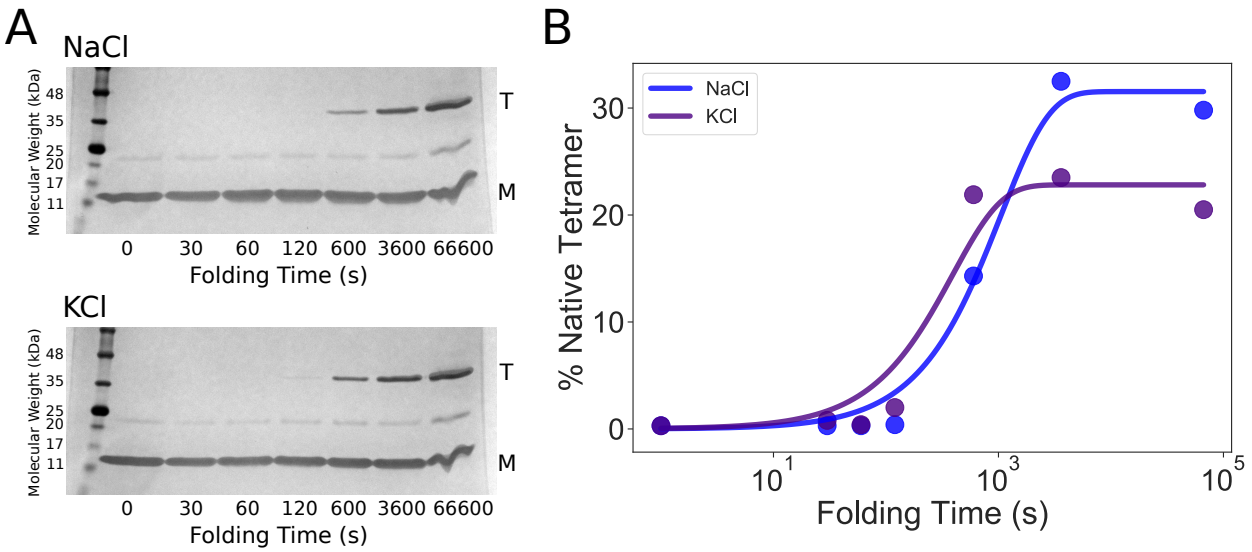

Figure 5.8: SDS-PAGE folding assay measures tetramerization kinetics in the presence of NaCl or KCl. Measurements were taken over 18.5 hours following initiation of insertion and tetramerization of DDM-solubilized KcsA monomers in liposomes, as in pulse-labeling measurements.

To extract mechanistic information from site-resolved HDX pulse-labeling, these data must be put in the context of other measurements. The most informative of these measurements is the SDS-PAGE folding assay that we have previously published. In that study, we made use of the extreme stability of the KcsA tetramer and measured the fraction of tetrameric species following mixing of SDS-solubilized monomers and azolectin SUVs, finding heterogeneous folding kinetics, with fast and slow rate constants of 40 ± 2 s and 1500 ± 100 s.[158] Here we adapt that protocol to study the tetramerization kinetics of KcsA

monomers from DDM micelles into azolectin SUVs (**Figure 5.8A**). Note that both the monomeric protein and the SUV samples used for this SDS-PAGE folding assay are from the same preparation as those used for the pulse-labeling experiments presented in this chapter. Quantifying these SDS-PAGE gels, and fitting the fraction tetramer to a single exponential fit, we only observe a slow-folding population with time constant 1050 ± 264 s (**Figure 5.8**). One benefit of folding from DDM is that we can now study the effect of folding in the presence of potassium ions, which is impossible in the presence of any SDS, in which potassium is insoluble. We find that the kinetics of KcsA folding in the presence of potassium is slightly faster than the kinetics of folding in only NaCl: We measure the folding rate constant of DDM-solubilized KcsA into azolectin SUVs in 300 mM potassium to be 393 ± 187 s.

Since the pulse-labeling experiments were conducted in the absence of potassium, we can compare the site-resolved changes in deuterium occupancy with the kinetics of tetramerization in NaCl. Interestingly, the fast-folding TM2 peptide VAGITSFGLVT is no longer changing deuterium levels after 100 s, a much shorter folding timescale than the tetramerization time constant in NaCl from SDS-PAGE. In contrast, the pore helix, turret, and selectivity filter are folding over the same timescales that tetramers are being detected by SDS-PAGE ($\sim$ 1000 s). Together, this suggests that the stabilization of the pore helix, SF, and turret are necessary for folding to the native tetramer, whereas the fast folding of TM2 observed in pulse-labeling does not represent folding to the native tetramer.

What structure could be forming so early in KcsA tetramerization? There are two possibilities: (1) The glycine zipper of KcsA could be forming a dimeric, trimeric, or tetrameric bundle very early, but without a properly folded pore helix, and this tetrameric structure may not be stable enough to run as a tetramer on SDS-PAGE. Alternatively, (2) TM2 is very flexible in monomers in DDM micelles, likely due to the hinge at G99, but may become fully stabilized and protected simply by insertion into the lipid membrane. It has been

shown that TM2 is very flexible in SDS micelles, even adopting a bent orientation.[26] This is in agreement with the uptake of TM2 in our native-state HDX measurements of the KcsA monomer (**Figure 4.3**). In fact, TM2 in the monomer is less stable than TM1. In agreement with this, in pulse-labeling, the TM2 peptide undergoes a large rapid increase in protection compared to TM1, which is very protected throughout tetramerization. Perhaps the consistent protection of TM1 comes from the presence of the M0 helix, which may lock TM1 into a rigid structure both in DDM and in liposomes, whereas TM2 only gains significant protection when it is inserted into a lipid membrane.

We also note that tetramerization of DDM-solubilized monomers inserting into azolectin SUVs does not go to completion, even after the 18.5 hours of folding measured by SDS-PAGE. Therefore, our pulse-labeling measurements are likely detecting a substantial population of monomer in lipid membrane or even monomer in detergent micelles. However, the only significant effect of this is that the magnitude of changes we observed by pulse-labeling are smaller than they would be if we folded to 100% tetramer.

We must also contextualize these pulse-labeling curves within the vast knowledge pool of KcsA structure-function studies. Many of these studies surround the pore helix and selectivity filter, as these are critical structures to channel inactivation. One such structure is the well-studied side-chain hydrogen-bond network including the "inactivation triad" of E71-D80-W67 with structural waters in this region, highly coupling the movements of the SF and the pore helix.[29,34,98,132,141,143] This hydrogen-bond network spans two peptides with very different pulse-labeling behaviors: the fast-folding inner pore helix peptide LWWSVE and the slow-folding selectivity filter (SF) peptide TATTVGYGDL. The difference in folding behaviors between the inner pore helix and the SF suggests that the inactivation network does not contribute much to folding of the pore helix region during channel tetramerization. It is possible that this network is already formed in the monomer, so it would not contribute to stability changes during tetramerization. Alternatively, this network may be weaker than

the forces stabilizing the inner pore helix. To fully evaluate the importance of the inactivation hydrogen-bond network on folding, it is necessary to measure tetramerization kinetics in an "open mutant" like E71V. If the presence of potassium ions speeds up folding (as we observe in **Figure 5.8**) by perturbing the selectivity filter and inactivation triad, then we would also expect the E71V variant to perturb folding kinetics significantly.

To ensure that the final folded state, measured by HDX pulse-labeling and our SDS-PAGE tetramerization assay, is the natively-folded KcsA tetramer, we compared the melting temperature of refolded KcsA to that of the KcsA tetramer purified in DDM and phosphate buffer from *e. coli* and reconstituted into the same azolectin SUVs. We confirmed that the two have the same thermal stability, with a melting point of the refolded tetramer being 91.0 ± 1.5 °C compared to 92.53 ± 1.0 °C of the reconstituted tetramer (**Figure 5.9**).

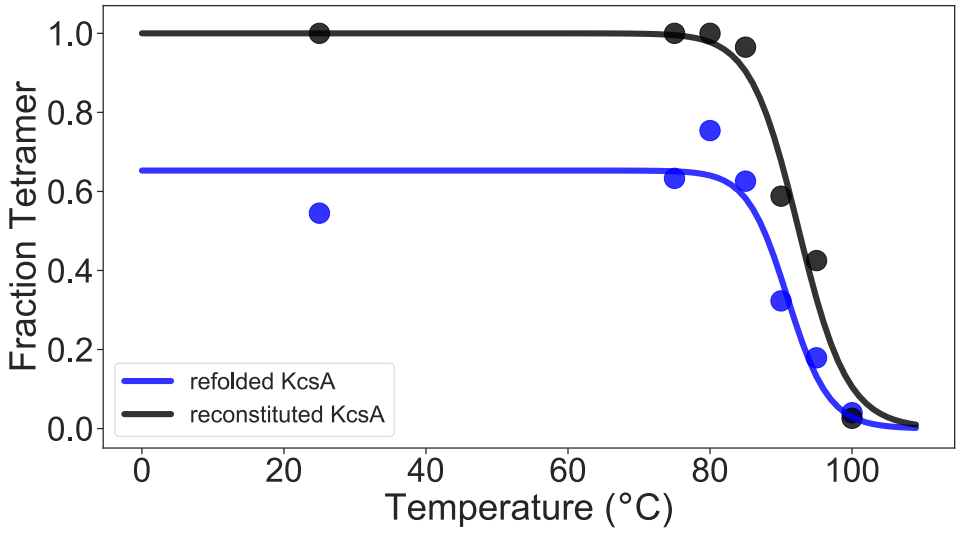

Figure 5.9: Thermal denaturation of refolded KcsA and reconstituted, purified KcsA demonstrates equivalent stability of the two species, suggesting that the refolded KcsA is the native tetrameric species.

Not only does this confirm that we are folding to the native tetrameric structure in pulse-labeling, but the existence of monomer in the refolded sample of KcsA (observed at 25°C on SDS-PAGE), with DDM micelles removed via incubation with Bio-Beads^{TM}, suggests that a substantial portion of the non-tetramerized KcsA after 15.5 hours of folding is monomers in lipid.

Lastly, we note that the vesicular structure of the lipids did not significantly change in the timeframe of a pulse-labeling experiment. Dynamic light scattering (DLS) measurements replicating the solvent conditions of pulse-labeling experiments suggest that the additive presence of DDM and KcsA perturbed the SUV structure much more than the 15.5 hours of incubation with detergents and protein (**Table 5.1**). In fact, under all buffer conditions tested, the average radius and polydispersity of the SUV sample increased only marginally between initial mixing and 15.5 hours of subsequent incubation. At either timepoint, the addition of DDM increased the average SUV radius and polydispersity only marginally, though the addition of KcsA monomers was a much larger perturbation, increasing both the radius and polydispersity substantially. These results would suggest that phosphate buffer or DDM did not cause significant SUV swelling or fusion, but the insertion of many KcsA monomers into each SUV caused significant liposome swelling.

	SUV + Phosphate Buffer		SUV + Phosphate-DDM Buffer		SUV + KcsA Monomer in Phosphate-DDM Buffer	
folding time (hr)	radius (nm)	polydispersity (%)	radius (nm)	polydispersity (%)	radius (nm)	polydispersity (%)
0	57.32 ± 8.06	20.07 ± 8.79	58.08 ± 5.86	21.45 ± 12.00	74.72 ± 11.53	45.03 ± 17.43
15.5	69.51 ± 9.56	23.83 ± 9.56	61.63 ± 3.80	25.74 ± 11.0	79.34 ± 11.17	55.93 ± 17.77

Table 5.1: DLS measurements of SUV size (radius) and polydispersity when mixed with experimental buffers containing DDM and KcsA monomers, immediately following mixing and after 15.5 hours.

5.6 Discussion

In this chapter, we presented what we believe to be the first site-resolved measurements from HDX pulse-labeling reported for a membrane protein folding and assembling into liposomes.

During tetramerization of DDM-solubilized KcsA monomers inserting into azolectin liposomes (SUVs), we observed changes in different hydrogen-bonded structures across the protein. The differences we observed were subtle, with changes in deuterium occupancy never exceeding 2 deuterium atoms for any peptide over the 15.5 hours measured. However, given the pre-existence of significant structure in the starting state, monomeric KcsA in DDM, this subtle change is not unexpected. Perhaps the large difference in measured native-state HDX stabilities between monomer and tetramer in Chapter 4 would suggest that the change in deuterium occupancy during tetramerization should be greater, but it is important to consider that pulse-labeling was conducted in phosphate buffer, while native-state HDX was measured in Tris. As Tris is known to greatly stabilize tetrameric KcsA (Chapter 3), it is likely that the stability differences between monomeric and tetrameric KcsA, measured by pulse-labeling in this chapter, are smaller than those in Tris, further making these subtle differences in deuterium occupancy expected.

Compared to our native-state HDX measurements of KcsA, as well as to most HDX studies of soluble and membrane proteins, we were only able to resolve a very small number of peptides during pulse-labeling. However, we are confident in the identity of these peptides, due to their high signal, often with counts of $\mathcal{O}(10^8)$, trustworthy fragmentation pattern by MS-MS, and by comparison of these peptides to their native-state equivalents whose identity is confirmed by similar uptake behavior in adjacent, overlapping peptides. The peptides we observe in HDX pulse-labeling, although few, span all regions of KcsA except the M0 helix, thereby allowing us to observe the folding behavior across many different structures within KcsA. Most notably, in the context of previous work that reported changes in deuterium occupancy in bR folding coarsely across the whole protein, our measurements represent

the first site-resolved HDX pulse-labeling of membrane protein folding in lipids to date. Therefore, despite the small number of measured peptides, this represents a significant step forward in studying membrane protein folding and dynamics.

The existence of a set of useful peptides is significant because we can interpret the changes in deuterium occupancy as changes in hydrogen bonds being formed or lost during KcsA tetramerization. A decrease of 1 deuterium measured by pulse-labeling corresponds to an average increase of 1 hydrogen bond across the ensemble of KcsA. Therefore, we really are observing site-resolved *folding* dynamics during the oligomerization of a membrane protein.

HDX stability-labeling measurements suggest that the pore helix and TM2 have less stable folding intermediates early in tetramerization, similar to native-state HDX measurements of the monomer in Chapter 4. Considering this fact alone, we may suspect a "native assembly model" for KcsA tetramerization. However, the fact that we observe any temporal changes in deuterium occupancy at all in our pulse-labeling measurements, and that the timescales of these changes are different in different parts of the protein argues against the native assembly model: natively-folded monomers coming together to form tetramers without much rearrangement is inconsistent with this pulse-labeling data. Additionally, we find from stability-labeling that the pore helix of KcsA remains less stable than other parts of the protein, even after 15.5 hours of tetramerization. This seems inconsistent with our native-state HDX measurements of the tetramer demonstrating extreme stability in the pore helix (**Figure 4.5**), but since our native-state HDX was measured in Tris buffer and our pulse-labeling HDX was measured in phosphate buffer, this inconsistency may be explained by the stabilization of KcsA by Tris buffer (**Figure 3.3**). Overall, from stability-labeling HDX, we found that the average population of KcsA at different timepoints during tetramerization — i.e., intermediate folding ensembles — was quite stable across many peptides. The pore helix was the least stable part of KcsA during tetramerization, and the TM2 peptide containing part of the glycine zipper was the only peptide observed to gain stability over

the course of tetramerization. Lastly, stability-labeling measurements can be treated almost as technical replicates, especially given the high stability of tetramerization intermediate ensembles. The same pulse-labeling behavior was observed across different pDs, except with smaller magnitudes in deuterium occupancy changes at lower pD pulses.

Comparing the timescales and magnitudes of deuterium occupancy changes, we propose a sequential model for KcsA folding and tetramerization: TM2 folds very quickly, around 100 s after membrane insertion, at the same time as fast folding of the inner portion of the pore helix, which is folded 1000 s after membrane insertion. The fast stabilization of TM2 may represent the initial formation of a tetrameric bundle of transmembrane helices around the glycine zipper or fast stabilization by the lipid bilayer. The inner portion of the pore helix is known to have high inherent helical propensity, as the inner pore helix of the closely-related potassium channel Kv1.3 was observed to have stable secondary structure cotranslationally.[54] Therefore, the fast folding we observe of the inner pore helix may reflect both the inherent high helical propensity of this structure and fast-forming initial contacts with neighboring monomers. This could then nucleate the slower folding of nearby structures (the outer half of the pore helix, selectivity filter, and turret). This model resembles the proposed "keystone" mechanism of folding, with fast formation of a transmembrane helix bundle and inner pore helix contacts followed by slower folding of the outer pore helix and selectivity filter. The slower-folding elements of the structure can be considered the keystone, added last in the folding of tetrameric KcsA to stabilize the native structure. Comparison of the fast TM2 stabilization with the slower tetramerization rate from SDS-PAGE, however, does not rule out a cooperative folding model in which all parts of the channel form native tetrameric structures simultaneously. Future experiments are necessary to evaluate the effects of pore helix helical propensity in lipids, anionic lipid binding to the monomer-monomer interface, and fast monomer insertion into a protein-dense phase on the mechanism of KcsA folding.[158]

CHAPTER 6

DISCUSSION AND DETAILED MODEL OF POTASSIUM CHANNEL FOLDING AND ASSEMBLY

This work is centered on uncovering the mechanism for potassium channel folding and assembly, but also speaks to many questions related to membrane protein folding, structure, and dynamics in general.

What is the unfolded state of a membrane protein? While the native, folded state of membrane proteins is extensively characterized by structural biology, the unfolded state of a membrane protein is not so easy to define. Water-soluble proteins have a well-studied unfolded state, or denatured state ensemble (DSE). The DSE is often dependent on solvent conditions or crowders as well as protein sequence, but most often the DSE of water-soluble proteins is approximated by denaturating the native state using chaotropic agents such as urea or guanidinium chloride, thermal denaturation, or force-based unfolding using atomic force microscopy (AFM) or optical tweezers.[62,81,117,131] As we observed in Chapter 3, traditional chaotropic denaturants are often too weak to fully unfold a membrane protein, so the DSE of membrane proteins is much less well characterized. The unfolded state of membrane proteins depends on additional factors arising from the membrane: membrane packing and defects, thickness, lateral tension, curvature, fluidity, and headgroup charge. All of these factors affect not only the DSE but also the dynamics of natively-folded membrane proteins, many of which undergo dynamic structural changes in response to membrane properties, including protein activation, channel opening, oligomerization, or formation of larger supramolecular protein complexes.[3,7,32,45,53,76,95,109]

These considerations have been discussed in the context of "good" and "poor" solvents. For water-soluble proteins, solvent quality is well-quantified by Flory coefficients.[11,52,73,149] However, due to the geometric constraints of membrane proteins in the bilayer, with unfolding events occurring both within and orthogonal to the plane of the bilayer, this formulation

is not readily applicable to describe the DSE of membrane proteins. However, qualitative descriptions of solvent quality are still informative: In general, the membrane acts as a good enough solvent to stabilize isolated hydrophobic transmembrane helices within the bilayer. However, the membrane is not a perfect solvent, or else transmembrane helices would never stably associate or form higher-order oligomers with water-filled cavities in the membrane like KcsA.

From pulse-labeling studies of KcsA tetramerization presented here as well as past studies of KcsA folding, the membrane appears to be a poor solvent for monomers, tetramers, and intermediate states.[158] Not only do transmembrane helices have to assemble into a stable transmembrane bundle, the interior of this bundle is a water-filled cavity. Additionally, KcsA is known to form supramolecular clusters during and after folding, with implications for folding and gating.[9,58,124,148,158,179] This would suggest that lipids are a relatively poor solvent for KcsA: The many charged and polar lipid-facing surfaces in the monomer favor a compact structure in the membrane, both in extremely stable tetramers and in large protein-dense phases during folding. In fact, lipids are such a poor solvent for TM2 that it forms a tight, helical bundle with the TM2 helices from adjacent monomers through a conserved glycine zipper, surrounding a water-filled cavity within the membrane that is a critical part of the potassium conduction pathway in the native tetramer.

Perhaps counterintuitively, the membrane can be considered a relatively good solvent for KcsA monomers: In DDM, monomers are highly prone to irreversible aggregation, likely through misfolding of their transmembrane helices in aqueous solvent, whereas when they are embedded in the lipid membrane, they are stably solvated and protected from aggregation. Additionally, in our *in vitro* KcsA folding experiments, in which monomers initially insert into azolectin SUVs and quickly form a protein-dense phase, the synthetic lipid membrane is still a good enough solvent to allow the rearrangements within the protein-dense phase necessary for correct monomer-monomer contacts to be made during tetramerization.

The nature of the unfolded state of a membrane protein is also highly dependent on the mechanism of unfolding.[51,53,77] Membrane beta barrels can often be fully denaturated in urea, from which they can be refolded into lipid membranes.[13,39,43] This is not often the case for an alpha helical membrane protein like KcsA, which we find is only moderately destabilized in urea, in TM1 and the small loop preceding TM2 (**Figure 4.8**), certainly not enough to disassemble the tetramer (**Figure 3.1**). Similarly, even 8% SDS is insufficient to disassemble the KcsA tetramer. However, the organic solvent TFE leads to tetramer disassembly at concentrations above 20% (v/v) and the KcsA tetramer breaks into monomers at 61°C in DDM, but is stabilized by lipids, melting at 93°C when reconstituted into SUVs. This is very curious considering that the melting point of Cyt C, a water-soluble protein, is over 80°C as measured by CD (**Figure 3.6**). This would imply that it is more stable than the DDM-solubilized KcsA tetramer. However, we observe extreme stability of the KcsA tetramer by native-state HDX at pD 8.5 at 25°C (**Figure 4.5**) compared to generally high uptake at short labeling times reported in Cyt C at pD 7.4 at 3°C.[66] This inconsistency suggests that proteins access different unfolded states transiently at low temperatures compared to near their melting temperatures. In this way, it seems that the DSE of Cyt C is very different than that of the KcsA tetramer in DDM at low temperatures. The KcsA tetramer almost never accesses the monomeric unfolded state at 25°C, but is almost entirely monomeric at 80°C, whereas Cyt C accesses its DSE frequently even at 3°C, leading to high uptake, despite its high melting point. The DSE of tetrameric KcsA at 25°C may only consist of small wiggles around its native structure that are exacerbated by 4 M urea (**Figure 4.8**). Larger unfolding events are not sampled in our native-state HDX experiments. In contrast, above 61°C, the DSE of KcsA in DDM is monomeric and very unstable, forming visible aggregates. The DSE of other helical membrane proteins is quite different, for example with GlpG accessing a partially expanded state of transmembrane helices, with one transmembrane helix that even reversibly leaves the membrane, partially shifting into aque-

ous solvent.[53] However, even in the case of GlpG, it was found that the mode of unfolding determines the precise forces necessary to reach the unfolded state.[51]

Lastly, the physiological context of cotranslational membrane protein folding must be considered when defining the folded and unfolded states of a membrane protein. Outer membrane beta barrels in bacteria, mitochondria, and chloroplasts are extruded as unfolded chains through translocation machinery into the periplasm where they are finally inserted and folded by additional chaperones in the outer membrane.[23,74,137] Therefore, the DSE of outer membrane beta barrels *in vivo* may resemble that of water-soluble proteins, a mostly extended chain that must be pulled through the inner membrane into the periplasm. In contrast, helical proteins are often translated directly into the membrane by a docked complex consisting of a ribosome and membrane chaperones. Translocated polypeptides, often already with significant helical structure in the translocon channel, are released laterally into the membrane.[99,164,176,181,182,186] Multiple copies of a helical membrane protein may be translated simultaneously from ribosomes docked on the same mRNA transcript, called polysomes.[56] This may facilitate oligomerization of separate monomers by their cotranslational proximity. Many cotranslational folding studies of helical membrane proteins measure the force required to arrest peptide formation at the ribosome-docked translocon.[36,37,40,54] In this case, the DSE of these helical membrane proteins is a partially formed peptide chain spanning the ribosome exit tunnel, the core of the translocon, and possibly several transmembrane helices that have already been released laterally into the membrane.

Therefore, it remains unclear how to best define the unfolded state of a membrane protein, yet this question remains so central to our understanding of membrane protein folding and dynamics. It seems that the DSE of a membrane protein is highly dependent on the protein itself, the membrane or membrane mimetic used to solubilize it, the mode of denaturation, and even on the method used to measure its stability and structure. What states are accessible to a membrane protein *in vitro*, in a detergent micelle, in a lipid membrane,

exposed to chemical denaturants or heat, or *in vivo* cotranslationally attached to ribosomes and chaperones? How are these states perturbed by solvent conditions, lipid composition and curvature, ligands, and other proteins within and peripheral to the membrane? For a multi-pass oligomeric helical membrane protein such as KcsA, should we define the unfolded state to be the monomeric state, or something with even less secondary structure, like the precipitated endpoint of a thermal melt? And how does the method of measurement affect the unfolded state we observe, since we measure very different unfolded states in native-state HDX compared to thermal denaturation of KcsA? These are all nontrivial questions that must be considered in any study of membrane protein folding and dynamics.

Throughout this study, we have been careful with our definitions of folded, unfolded, and intermediate states of KcsA, and while these definitions are subtly different in our thermal denaturation, *unfolding* studies, compared to our HDX pulse-labeling, *folding* studies, we have observed commonalities in structure and stability of monomeric, native tetrameric, and intermediate folding states, that all point to a keystone-like mechanism for potassium channel folding, which we believe to be the most detailed mechanism of the folding and oligomerization of an ion channel to date.

In Chapter 3, we observed a novel species of KcsA during thermal denaturation, at around 50°C, consisting of a tetrameric transmembrane helix bundle, but with displaced and dynamic pore helices that are more exposed to aqueous solvent than in the native state. This novel tetrameric species is metastable by our *Upside* CG-MD model, but is less stable than the native tetramer in TFE, and is uniquely sensitive to urea denaturation. While this species resembles our hypothesized "keystone" folding intermediate, we were not able to observe reversible folding from a similar, but less stable, 65°C state, so it remains unclear whether or not this state is accessed during the folding and assembly of KcsA. In Chapter 4, we measured site-resolved stabilities across KcsA using native-state HDX. We observed a monomeric species that is much less stable than the tetramer, but retains significant

secondary structure, especially in the transmembrane helices. However, the fact that these monomers must gain a tremendous amount of stability as they transition into tetramers argues against the "native assembly" model, which assumes that monomers with native-like structure and stability are folding intermediates. In Chapter 5, we adapted HDX pulse-labeling to a membrane protein undergoing oligomerization in liposomes with peptide-level resolution for the first time. We observed fast folding of TM2 and the inner half of the pore helix, followed by slower folding, on the same timescales as tetramerization measured by SDS-PAGE, for the outer pore helix, selectivity filter, and turret. The fast folding of the inner pore helix is likely due to the high helical propensity of this region, but it remains unclear whether the fast folding of TM2 is due to stabilization of this transmembrane helix by lipids during rapid membrane insertion or if it represents the fast folding of a tetrameric helical bundle around the glycine zipper.

Therefore, from pulse-labeling we cannot unambiguously determine the kinetics of transmembrane helix bundle formation. If the transmembrane bundle forms quickly, then this supports the "keystone" mechanism, but if the transmembrane bundle forms later, on the same timescales as outer pore helix, SF, and turret folding, then this supports a more "cooperative" model for KcsA assembly. At the very least, given the importance of the pore helix in the stability of the tetramer, which we learned from thermal denaturation experiments in Chapter 3, this structural unit — consisting of the pore helix, SF, and turret — which folds on the same timescales as native tetramers form, can be considered an architectural "keystone" of KcsA assembly, folding last and locking the tetramer into an extremely stably folded structure.

CHAPTER 7

FUTURE EXPERIMENTS

In this dissertation, I have presented a thorough study of KcsA unfolding and folding, through a combination of diverse experiments, simulation, and modeling. These involved the novel purification of a folding-competent KcsA monomer solubilized in DDM micelles as well as the adaptation of HDX pulse-labeling to study membrane protein folding and oligomerization in liposomes with peptide-level resolution for the first time. We have learned a sequential mechanism of KcsA unfolding, and measured the extreme stability of the DDM-solubilized KcsA tetramer in relation to a less stable, but structured monomer. During folding and assembly of the KcsA tetramer in liposomes, we observed from HDX pulse-labeling the fast folding of TM2 and the inner half of the pore helix, with the outer half of the pore helix, selectivity filter, and turret folding slower, on the same timescales as native tetramer formation measured by SDS-PAGE. In the context of the theoretical models for KcsA oligomerization presented in **Figure 1.2**, we can rule out the "native assembly" model due to the large difference in stabilities between monomers and tetramers measured by native-state HDX. However, we are unable to measure the kinetics of both TM2 helix tetramerization (along with the formation of a water-filled cavity surrounded by bundled TM2s) and the formation of inter-monomeric pore helix contacts, so we must remain agnostic to whether TM2 bundle formation forms first, as in the "keystone" model, or simultaneous with pore helix, selectivity filter, and turret folding, as in the "cooperative" folding model. To clarify the final details of this sequential folding and assembly mechanism, it is necessary to more fully understand the driving forces behind the fast folding of the inner pore helix and TM2.

First, we must measure the helical propensity of KcsA monomers in lipids. This result will indicate whether the fast folding of the inner pore helix as observed in pulse-labeling was a result of this peptide forming fast inter-monomeric contacts or rather increasing helicity rapidly upon insertion into the lipid bilayer, irrespective of coming into contact with other

monomers. Initial *Upside* simulations of partially-unfolded KcsA demonstrate high helical propensity in the pore helix (**Figure 7.1A**), in agreement with cotranslational arrested peptide force profiles of Kv1.3 which suggest high helical content in the inner pore helix of this highly conserved region.[54] Potentially, native tryptophan homo-FRET experiments could also clarify the timescales of tetrameric pore helix contact formation, as this technique has been applied to a single-W67 mutant of KcsA to measure subtle changes in W67-W67 distances in expanded and contracted states of the selectivity filter.[146]

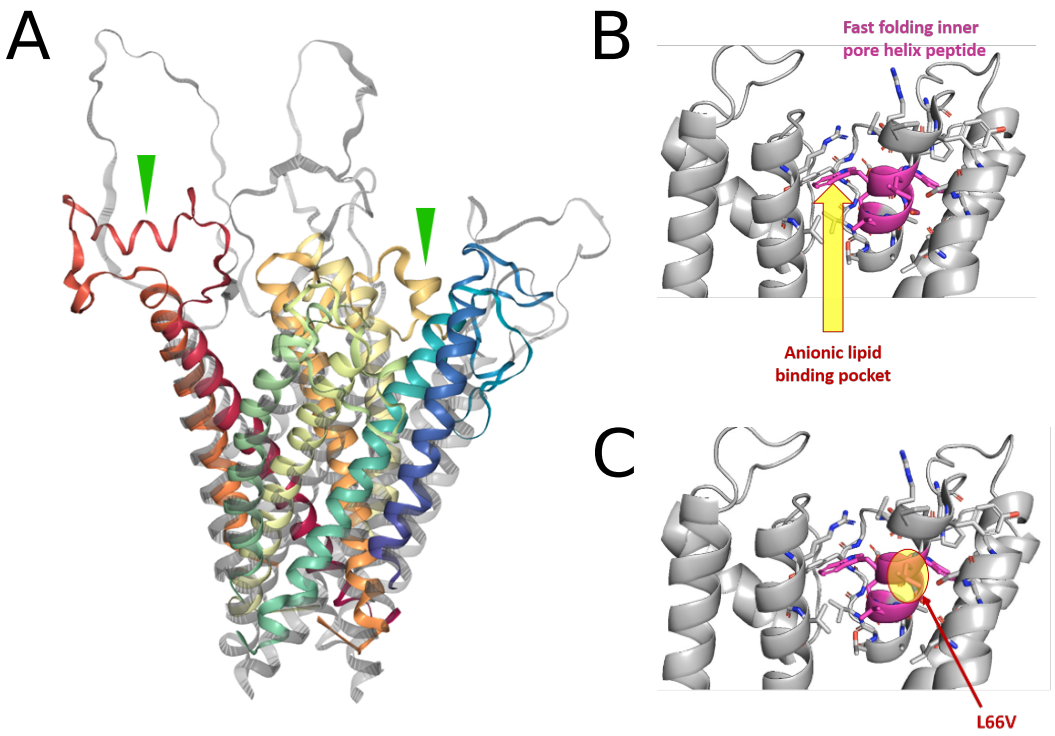

Figure 7.1: Future avenues to study pore helix folding. **A.** Constant temperature T=0.85 *kT* *Upside* simulation of a partially unfolded KcsA showing spontaneously-formed pore helix segments (green wedges). The grey outline shows the simulation starting state, containing no pore helix secondary structure. **B.** Location of the putative anionic binding pocket at the interface between the pore helix of one monomer and TM2 of the adjacent monomer. **C.** Location of the mutation L66V that leads to slow folding. In **B** and **C**, the inner pore helix peptide, LWWSVE, that folds quickly by HDX pulse-labeling, is highlighted in magenta. Structure from PDB 3EFF.

We may be able to understand pore helix folding kinetics more fully by studying the effect of chemical perturbations on channel formation. Unexpectedly, the pore helix is very protected at room temperature from water-soluble chaotropic agents like urea (**Figure 4.8**).

However, it remains unclear how urea affects the stability of the monomer. Therefore if the rate-limiting step of KcsA tetramerization resembles the monomer, urea (or the more hydrophobic chemical variant, thiourea) may slow folding kinetics by disrupting pore helix folding.

Additionally, the pore helix is known to form an anionic lipid binding pocket with TM2 of an adjacent monomer (**Figure 7.1B**).[9,143,148,170,174] The pulse-labeling folding experiments presented here were all carried out in azolectin SUVs, which contain approximately 7% PA by weight. Therefore, folding kinetics in the absence of anionic lipids has not been investigated, and if anionic lipid binding stabilizes a native-like inter-monomeric contact in the rate-limiting step of folding, then the absence of PA may slow tetramerization.

Lastly, we can perturb the pore helix by mutagenesis. We have expressed two pore helix mutants, KcsA L66V and L66E. L66E is equivalent to F383E of Kv1.3, a mutation shown to significantly destabilize the pore helix of Kv1.3.[40] The mutation of the same residue to a valine in L66V is equivalent to a mutation in the pore helix of hERG, L615V, that is one cause of the life-threatening arrythmia long-QT syndrome.[160] Mutational analysis of the pore helices can be tricky since this part is so critical for potassium channel formation, and while L66V expressed well in *e. coli*, the yield of L66E purification was so low that I was unable to study it. We found that KcsA L66V had the same thermal stability as WT (both in NaCl and KCl conditions), but refolded into azolectin SUVs much more slowly. After approximately 12 hours of folding, L66V produced only about 30% of the amount of tetramers as WT in that same time period measured by our SDS-PAGE refolding assay. This is curious because L66 natively faces the lipid bilayer and doesn't seem to be particularly important for side-chain packing in the structure of WT KcsA (**Figure 7.1C**). Further, the substitution of a L for V does not seem particularly perturbative, though perhaps either (1) this site is a critical protein-protein contact point in a folding intermediate that is significantly different from the native tetrameric structure, or (2) L66V perturbs the anionic lipid binding site, leading to

destabilization of important folding intermediates. Therefore, further study of pore helix mutant folding is a nontrivial endeavor, but would help elucidate the specific role of the pore helix in potassium channel tetramer formation.

The other large answered question raised by our HDX pulse-labeling experiments involves the rapid folding of the TM2 helix: Are we observing the glycine zipper, which our TM2 peptide contains, rapidly forming a tetrameric transmembrane helix bundle? Or is the rapid increase in secondary structure of this peptide instead a result of stabilization by the bilayer? We observe that TM2 in the KcsA monomer is structured, but remains very dynamic in our native-state HDX measurements, in agreement with published NMR studies of the KcsA monomer in SDS micelles, which observed a very flexible, bent TM2 structure.[26] While the SDS-solubilized state may be more disordered than the DDM-solubilized state, we observe markedly different stability in the tetramer, with TM2 exhibiting almost no deuterium uptake in our native-state HDX measurements in DDM. Since we know that the presence of lipids greatly increases the stability of the KcsA tetramer, it is unclear whether the fast folding of TM2 we observe in HDX pulse-labeling derives from rapid formation of an extremely stable tetrameric structure or simply from insertion into the lipid bilayer, which confers additional stability. When the tetrameric bundle of TM2 helices is formed natively, lipids must be displaced in the center of the tetramer to form a water-filled cavity. This is a conserved feature of many helical membrane protein bundles stabilized by a glycine zipper.[90] It is unclear whether this happens concurrently with or following tetrameric transmembrane helix bundle formation. However, future experiments may be able to take advantage of the water-filled cavity and measure TM2 water exposure during tetramerization as a proxy for transmembrane helix bundle formation. This can be done with synchrotron-based hydroxyl radical footprinting or with fast photochemical oxidation of proteins (FPOP). Both of these methods produce highly-reactive hydroxyl radicals, from water and hydrogen peroxide, respectively. These hydroxyl radicals react with nearby species, including protein side chain

groups. Similar to HDX-MS, the location of this labeling can be measured by proteolysis and MS.[63,64,185] An alternative version of FPOP optimized for membrane proteins and coupled with titanium dioxide nanoparticles instead labels only lipid-exposed residues.[163] Using either of these techniques to map changes in water or lipid-exposed area during KcsA tetramerization would clarify the timescales of formation of a bundle of TM2s with a water-filled pore. An alternative method to measure the timescales of water-cavity formation in KcsA would be to incubate liposomes with a fluorescently-tagged potassium channel toxin, such as quaternary ammonium (QA), that selectively binds the inner cavity of KcsA.[97] Then the liposome-bound fluorescent toxin can be separated from unbound toxin with centrifugation or size exclusion chromatography at different folding timepoints to measure the percent decrease in toxin in bulk solution. This would be a measure of the relative population of folded water cavities at each folding timepoint. Since QA binds the interior of the selectivity filter region, however, this may ultimately just be another measure of native channel formation. Additionally, this folding reaction would have to be conducted at low pH, ensuring that the intracellular gate of newly-formed tetramers is open and accessible to fluorescent toxin entry. Lastly, kinetics of tetrameric bundle formation can be studied by mutational perturbation of the two glycines in the fast-folding TM2 peptide. Replacing the glycine hinge, G99, would likely reduce the flexibility of the monomer, bringing the stability of TM2 in the monomer closer to its stability in the tetramer. Replacing the first glycine of the glycine zipper, G104 may slow folding or prevent tetramer formation at all. This latter variant may be difficult to study due to low expression levels.

There is also a third potential source of TM2 stability: the protein-dense phase. Since we know that the protein-dense forms rapidly, within 10 seconds, from monomers inserted into azolectin lipids from SDS micelles, it is possible that the fast folding of our TM2 peptide could reflect the stabilization resulting from increased lateral pressure from a protein-dense phase.[158] However, it is unknown how quickly the protein-dense phase forms when monomers

are inserted from DDM rather than SDS. We know that folding from DDM eliminates the fast-folding population observed when folding from SDS, so the timescales of protein-dense phase formation may also be perturbed. To evaluate this, we must measure the kinetics of protein-dense phase formation from DDM-solubilized monomers inserting into azolectin SUVs using a FRET assay with fluorophore-tagged (L86C) KcsA monomers as previously reported.[158]

Aside from questions arising directly from difficulties in the interpretation of HDX pulse-labeling, this study of KcsA folding and unfolding has opened up many new, intriguing questions and avenues for further study. Here, I present a brief motivation for each, as well as preliminary data where available.

It will be beneficial for future studies of KcsA folding from DDM-solubilized monomers to confirm not just that the refolded tetramer has the same stability as the native species, but also to confirm that the refolded protein is functional. This can be done by patch clamping the refolded channel, which has been used to confirm the functional conductance of refolded KvAP and KcsA in the past.[42,174] Alternatively, a fluorescent ion flux assay can be used to measure potassium currents in liposomes containing refolded KcsA.[162] It would be interesting to use either of these measures of potassium conductance to estimate rates of folding to the native, conductive tetramer. Of course, this will be complicated by the inherent inactivation rate of the channel, but in theory this effect should be negligible on measured folding rates at steady state, and the total current should reflect only newly-formed channels.[55] Note that the low-pH state of KcsA with an open intracellular gate, required for either patch clamping or an ion flux assay, was found to be much less stable than the closed channel at neutral pH in Chapter 3.

Currently, the field of HDX-MS references all of their uptake curves to intrinsic exchange rates of a solvent exposed amide proton in water.[6,28,130] Since we know that the DSE of membrane proteins is complex, it may be more useful to estimate the intrinsic exchange rates

of peptides in and near membranes. This will likely be a very difficult task, given the diversity of membranes and membrane-mimetics in which membrane-protein HDX is measured, and it remains unclear whether fully unfolded peptides with unsatisfied backbone hydrogen bonds can even exist in the hydrophobic core of lipid bilayers. However, calibrating this membrane-dependent intrinsic exchange rate will be critical for more meaningful estimations of folding free energies of membrane proteins by HDX in the future.

Additionally, an outstanding problem facing many groups studying very stable membrane proteins like KcsA and GlpG with native-state HDX is the requirement of very long labeling times for full deuterium uptake in the most stable, detergent-embedded transmembrane helices. In currently unpublished work, Abigail Schroeter of the Sosnick group found that parts of GlpG require weeks of incubation in deuterium buffer to reach the saturated, "all-D" uptake levels necessary to calculate EX2-limit folding free energies. However, we have found that labeling KcsA in DDM for longer than 24 hours at room temperature is impossible because of its tendency to aggregate. In order to measure full uptake curves for tetrameric KcsA, it may be necessary to use phosphate rather than Tris buffer, as we show the large stabilization of the KcsA by Tris in Chapter 3, and destabilizing the tetramer should produce greater uptake at shorter labeling times. Additionally, labeling may have to be carried out at low temperature, possibly with added glycerol or urea, to increase the shelf life and facilitate labeling timepoints on the scale of days or weeks. The KcsA tetramer may also be less stable in other detergents, which may decrease the labeling time necessary to measure full uptake curves.

While we reported here the site-resolved HDX pulse-labeling of KcsA folding in liposomes, we could only measure around 11 peptides with high confidence from KcsA. This pales in comparison to the number of peptides we measure in native-state HDX experiments, which is smaller yet than the average number of peptides for a water-soluble protein of the same length. Therefore, there is much work to be done to further optimize pulse-labeling in lipids

to obtain more peptides. This would produce even higher-resolution measurements, ideally providing single-residue-level resolution throughout the protein when fully optimized. As we have discussed, there are many barriers to the proteolysis, lipid removal, and detection of peptides required for site-resolved pulse-labeling in lipids, especially for smaller, extremely stable helical membrane proteins like KcsA. Further optimization for higher peptide coverage and overlap would likely require the study of new, acid-active proteases like nepenthesin II, as well as optimization of the physical and chemical properties of trap/desalting and analytical columns for more efficient separation of lipids and peptides as well as higher binding capacity to the more hydrophobic peptides from membrane proteins.[189]. Additionally, it would be beneficial to standardize the lipid removal process that involves frothing with zirconium oxide beads. Right now, physical agitation and aeration is conducted manually by pipetting rapidly with the pipette tip pushed against the side of the sample container. To standardize this process, it may be useful to machine a filtration device that simultaneously disturbs the membrane structure by mechanical force and maximizes the air-surfactant-liquid interface while mixing the quenched HDX solution with BSA-blocked zirconium oxide for maximum lipid removal. Perhaps a structure with tiny pores like a pumice stone could be incorporated into such a device. Lastly, the geometry and phospholipid-binding activity of the zirconium oxide resin can be optimized. Currently, the process of blocking zirconium oxide beads with BSA and then rinsing this resin multiple times with acidic isocratic buffer is time-consuming and produces a resin that does not last very long (only a few hours) before the BSA falls off. Better immobilization of BSA to the beads would improve the efficiency of this process, as would using a version of zirconium oxide that is less reactive and does not require BSA blocking for maximum peptide recovery. Ultimately, the higher the peptide recovery, the more site-resolved information about the folding process we would gain.

Nonetheless, we have created a valuable tool for understanding membrane protein folding in lipids at a peptide-level resolution. Therefore, future work should not only optimize this

process for KcsA, but also apply it to the folding of other membrane proteins. Of great interest to the field is the folding and tetramerization of potassium channels containing voltage sensors like KvAP. Pulse-labeling KvAP folding will come with added difficulties due to the high temperature dependence of its folding, conditions which are not particularly amenable to HDX.[114] Applying pulse-labeling to the folding of a domain-swapped voltage-gated channel like Kv1.2 may also be interesting, as it may suggest a mechanism for the formation of domain-swapped voltage sensing and pore domains that are a hallmark of many mammalian potassium channels. One particularly easy target for pulse-labeling would be the folding of outer membrane beta barrels. The unfolded states of these proteins are often fully soluble in urea and can be refolded simply by dilution into lipid bilayers.[13,39,43] Outer membrane beta barrel pulse labeling still requires lipid removal, but bypasses the need for detergents for protein stabilization (though detergents may still be necessary for full membrane solubilization during lipid removal). Additionally, the natively-folded states of beta barrel proteins have large water-soluble pores that may be more accessible to acidic proteases and may produce many more peptide fragments, allowing for much higher resolution in HDX. The ability of outer membrane beta barrels to become fully solubilized in urea suggests that the commonly used water-based intrinsic exchange rates are physically-meaningful references states for this class of protein.

While lipids are known to greatly affect the stability of KcsA, it is unknown how membrane properties affect the folding rate of KcsA. All experiments presented in this dissertation have used a heterogeneous mixture of lipids extracted from soy membranes (called "azolectin") that contains approximately 46% PC, 22% PE, 18% PI, 7% PA, with about 7% of headgroup composition unknown. The tail composition is not reported as well. We have conducted several folding experiments using purified lipids, and have found that KcsA requires unsaturated lipids to insert and tetramerize. This is consistent with the finding that no tetramers are formed in 100% DMPC, but 100% POPC is sufficient for tetramer

formation. However, old samples of POPC and azolectin (older than 1 week and not stored under inert argon gas) do not produce KcsA tetramers. This suggests that azolectin contains unsaturated lipids, and exposure to atomspheric oxygen for longer than a week oxidizes the unsaturated lipid tails, cleaving them, and leading to additional packing defects in the membrane that are incompatible with KcsA tetramer formation. It is unclear whether this affects the insertion or folding steps of *in vitro* tetramerization, so there is room for further work to investigate this. Additionally, membrane thickness is known to be a significant driver of protein-protein association in the membrane through the effect of hydrophobic mismatch.[20,67,88,119] Perturbing the association of KcsA monomers by varying the mismatch between the height of their hydrophobic core and the thickness of the membrane would likely change the tetramerization rate of the channel. Therefore, it would be interesting to measure changes in folding rates in liposomes of different bilayer thicknesses, holding headgroup identity and degree of unsaturation constant. Additionally, studying the effect of varying headgroup, membrane curvature (controlled by varying liposome size), lateral tension (controlled by incorporating lyso-lipids), and stiffness (from sterols) would inform our understanding of the membrane-based forces that drive KcsA folding and assembly.

A large amount of work remains to characterize the protein-dense phase and determine its effect on KcsA folding. We have previously observed a quickly-forming protein-dense phase during folding from SDS into azolectin SUVs using FRET spectroscopy of fluorophore-tagged KcsA undergoing insertion and folding. We find that this phase initially consists of monomers immediately following membrane insertion, but remains as monomers within the phase fold and tetramerize.[158] We have also conducted total internal reflection fluorescence (TIRF) microscopy to visualize these laterally-associated protein clusters (**Figure 7.2A**). However, until this point, every time we had observed the formation of a protein-dense phase, either by FRET or TIRF microscopy, there were fluorophores attached to KcsA. Because fluorophores can be very sticky, we wanted to know if the dense phase could be formed by KcsA in

the absence of fluorophores. To study this, we conducted fluid-cell AFM measurements in which we assembled empty supported lipid bilayers (SLBs) from azolectin lipids, and then added SDS-solubilized KcsA monomers, as in our standard refolding protocol. We observed the formation of tall features protruding from the SLB that likely correspond to clusters of several hundred KcsA monomers near the edges of the SLB patch (**Figure 7.2B** and **C**). We believe these clusters in general to be a liquid-like phase since diffusion and rearrangement of monomers must necessarily occur within the clusters to allow for folding and assembly of tetramers. Therefore, to measure the diffusion of particles within and outside the phase, it would be informative to use fluorescence recovery after photobleaching (FRAP). Additionally, TIRF microscopy can be paired with FRET to distinguish proteins diffusing within the dense phase from those floating freely in the bilayer. However, several key questions remain: Does the protein-dense phase have a function in folding? Do membrane proteins fold within a protein-dense phase in live cells?

We have observed that the rate of KcsA tetramerization is independent of the concentration of detergent-solubilized monomer in bulk solution.[158] However, KcsA folds within a protein-dense phase in the membrane. If the density of protein in this phase is always constant, which might be expected at a constant temperature and lipid composition, then we really have no control over the concentration of KcsA in the bilayer and cannot measure the effect of membrane-incorporated KcsA concentration on assembly rate. We hypothesize that the protein-dense phase functions to concentrate KcsA monomers in the bilayer, increasing the probability of productive collisions, and thus increasing the efficiency of tetramer assembly. Therefore, it is necessary to find conditions to perturb or even eliminate the formation of the protein-dense phase. Then we would be able to measure assembly rates in the absence of a dense phase. If the rate of tetramerization decreases in the absence of the dense phase, this would confirm our hypothesis that the dense phase increases the speed and efficiency of KcsA folding.

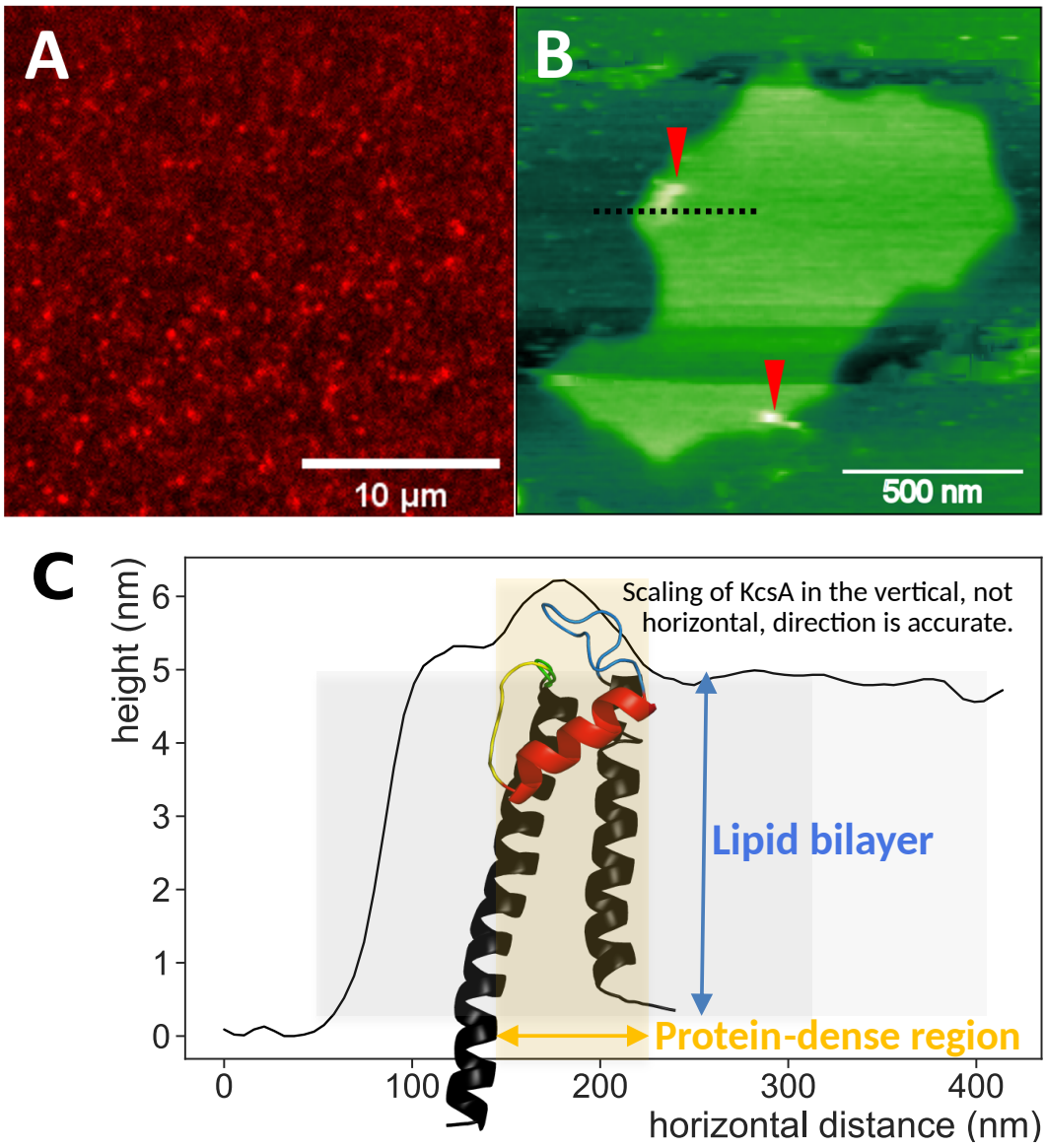

Figure 7.2: Potassium channel protein-dense phase. **A.** TIRFM of Alexa 594-labeled KcsA Δ125 clusters in azolectin GUVs. **B.** AFM height trace of putative KcsA Δ125 clusters (red wedges) in an azolectin supported lipid bilayer. **C.** Cross section along dotted line in **B** of protein-dense phase with overlaid monomer structure, with protein height (not width) to scale. KcsA concentrations in 0.5% SDS: **A.** 100 μM, **B.** 0.7 μM.

So far, our efforts to perturb the protein-dense phase while maintaining membrane integrity have not been successful: It is resistant to temperatures up to 80°C, but it remains unclear if lipid composition could drive dense phase dissociation. Therefore, additional FRET experiments should be conducted to examine the presence of any protein-dense phase

under membrane conditions of varying headgroup charge and tail length, as electrostatic interactions and hydrophobic mismatch may be significant drivers of protein-dense phase stability.

Another way to perturb the KcsA dense phase is to add a different protein into the same membrane as KcsA. Independently, it would be interesting to characterize the generalizability of this phase, and to see if another potassium channel, like KvAP or a completely different helical membrane protein like a proteolytically-dead variant of GlpG, can enter the protein-dense phase clusters formed by KcsA. If it can, then we will be able to control the concentration of KcsA in the dense phase by tuning the amount of secondary protein in the phase.

To further probe the generalizability of a protein-dense phase in membrane protein folding, it is necessary to investigate whether this phase exists in live cells within membranes where potassium channel folding occurs. In prokaryotes, this is the inner membrane, and in eukaryotes, this membrane is the endoplasmic reticulum (ER). Notably, the ER membrane is much thinner than the plasma membrane of a eukaryotic cell, and the membrane thickness of each compartment of the secretory pathway increases in the direction of the plasma membrane.[123] Therefore, we hypothesize that hydrophobic mismatch, potentially resulting in the formation of a protein-dense phase, could be a significant driving force for oligomeric protein folding and assembly *in vivo*. Measuring real concentrations of membrane proteins in live cells is very difficult, and often requires cotranslationally expressing a fluorescent protein attached to the protein of interest. For a protein like KcsA, with monomers that have a very small cross-sectional footprint in the membrane, attaching a bulky, protein-based fluorophore will be difficult and may even disrupt the *in vivo* assembly of KcsA by sterically trapping the protein in an unfolded, monomeric state.

Understanding the role of the protein-dense phase in folding would be aided significantly by molecular modeling. However, existing models are either poorly parametrized and

over-stabilize protein-protein interactions like the Martini CG model, or are too coarsely parametrized like Ising-based models for membrane protein association that lack the detail necessary to evaluate the role of specfic protein-protein interactions on macroscopic phase behavior.[2,92,105–107] Therefore, there is a need for a new CG force field to bridge length scales between large material properties of the protein-dense phase and the specific intermolecular interactions in the membrane that contribute to protein clustering. For example, CG Martini lipid interactions are well parametrized as are *Upside* protein interactions. Therefore, Martini lipids could be added to our *Upside* force field. This would be an improvement from the current implicit membrane potential in *Upside* for the simulation of any protein that has lipid-specific behavior, but also could facilitate the simulation of large clusters of proteins in a realistic lipid membrane. Alternatively, a CG model could be created from scratch to model protein-dense phase behavior in the membrane. We have briefly studied a model in which we represent KcsA monomers by circles undergoing simple rotational (but not translational) diffusion. By defining an arc on the surface of the idealized circular monomer as the native, inter-monomeric binding interface, we can calculate the mean first passage time for tetramer formation under these conditions. For example, if the average time for a full rotation of one monomer is 20 μs and the folding window on each monomer is an arc spanning 10°, then the mean first passage time of tetramer formation is approximately 1 s. This model can be expanded to include translational diffusion as well as probabilistic treatment of multiple folding-competent or non-competent states of each monomer. Formation of a protein-dense phase can be modeled in 2 ways: (1) energetically, by defining an interaction energy term between monomers, or (2) by enforcing different translational diffusion inside and outside clusters, which can be parametrized by FRAP measurements of KcsA diffusion inside and outside the protein-dense phase.

While there are undoubtedly many interesting new avenues for future studies on membrane protein HDX and characterization of protein-dense phases during membrane protein

assembly, this work represents a significant step forward in our understanding of membrane protein folding, especially the folding of potassium channel pore domains, which are highly conserved across all biology. We have developed new methods to purify refolding-competent KcsA monomers in DDM, and adapted HDX pulse-labeling to study the folding of a membrane protein in liposomes with peptide-level resolution for the first time. We learned many factors that influence KcsA stability and the path-dependent nature of the DSE of KcsA. While the precise sequence of events driving KcsA folding and assembly remain hidden, we were able to measure the dynamics of hydrogen bond formation across many structural elements of KcsA, observing rapid folding of TM2 and the inner pore helix followed by slower folding of more external structures. These external structures consist of the outer pore helix, selectivity filter, and turret, which we observe to fold on the same timescales as native tetramers are formed, suggesting that these structures act as an architectural "keystone" that is added last to stabilize the tetramer into its native fold.

REFERENCES

[1] Suraj Adhikary, Daniel J. Deredge, Anu Nagarajan, Lucy R. Forrest, Patrick L. Wintrode, and Satinder K. Singh. Conformational dynamics of a neurotransmitter: Sodium symporter in a lipid bilayer. *Proceedings of the National Academy of Sciences of the United States of America*, 114(10):E1786–E1795, 3 2017.

[2] Riccardo Alessandri, Paulo C.T. Souza, Sebastian Thallmair, Manuel N. Melo, Alex H. De Vries, and Siewert J. Marrink. Pitfalls of the Martini Model. *Journal of Chemical Theory and Computation*, 15(10):5448–5460, 2019.

[3] Veerappan Anbazhagan and Dirk Schneider. The membrane environment modulates self-association of the human GpA TM domain—Implications for membrane protein folding and transmembrane signaling. *Biochimica et Biophysica Acta (BBA) - Biomembranes*, 1798(10):1899–1907, 10 2010.

[4] Kyle W. Anderson, Elyssia S. Gallagher, and Jeffrey W. Hudgens. Automated Removal of Phospholipids from Membrane Proteins for H/D Exchange Mass Spectrometry Workflows. *Analytical Chemistry*, 90(11):6409–6412, 6 2018.

[5] Minkyung Baek, Frank DiMaio, Ivan Anishchenko, Justas Dauparas, Sergey Ovchinnikov, Gyu Rie Lee, Jue Wang, Qian Cong, Lisa N. Kinch, R. Dustin Schaeffer, Claudia Millán, Hahnbeom Park, Carson Adams, Caleb R. Glassman, Andy DeGiovanni, Jose H. Pereira, Andria V. Rodrigues, Alberdina A. Van Dijk, Ana C. Ebrecht, Diederik J. Opperman, Theo Sagmeister, Christoph Buhlheller, Tea Pavkov-Keller, Manoj K. Rathinaswamy, Udit Dalwadi, Calvin K. Yip, John E. Burke, K. Christopher Garcia, Nick V. Grishin, Paul D. Adams, Randy J. Read, and David Baker. Accurate prediction of protein structures and interactions using a three-track neural network. *Science*, 373(6557):871–876, 8 2021.

[6] Yawen Bai, John S. Milne, Leland Mayne, and S. Walter Englander. Primary structure effects on peptide group hydrogen exchange. *Proteins: Structure, Function, and Bioinformatics*, 17(1):75–86, 9 1993.

[7] Stephanie Ballweg, Erdinc Sezgin, Milka Doktorova, Roberto Covino, John Reinhard, Dorith Wunnicke, Inga Hänelt, Ilya Levental, Gerhard Hummer, and Robert Ernst. Regulation of lipid saturation without sensing membrane fluidity. *Nature Communications 2020 11:1*, 11(1):1–13, 2 2020.

[8] Francisco N. Barrera, M. Lourdes Renart, M. Luisa Molina, José A. Poveda, José A. Encinar, Asia M. Fernández, José L. Neira, and José M. González-Ros. Unfolding and refolding in vitro of a tetrameric, α-helical membrane protein: The prokaryotic potassium channel KcsA. *Biochemistry*, 44(43):14344–14352, 2005.

[9] Francisco N. Barrera, M. Lourdes Renart, José A. Poveda, Ben De Kruijff, J. Antoinette Killian, and José M. González-Ros. Protein self-assembly and lipid binding in the folding of the potassium channel KcsA. *Biochemistry*, 47(7):2123–2133, 2 2008.

[10] Tobias Baumgart, Adam T. Hammond, Prabuddha Sengupta, Samuel T. Hess, David A. Holowka, Barbara A. Baird, and Watt W. Webb. Large-scale fluid/fluid phase separation of proteins and lipids in giant plasma membrane vesicles. *Proceedings of the National Academy of Sciences of the United States of America*, 104(9):3165–3170, 2 2007.

[11] Robert B. Best. Emerging consensus on the collapse of unfolded and intrinsically disordered proteins in water. *Current Opinion in Structural Biology*, 60:27–38, 2 2020.

[12] Paula J. Booth. The trials and tribulations of membrane protein folding in vitro. *Biochimica et Biophysica Acta (BBA) - Biomembranes*, 1610(1):51–56, 2 2003.

[13] Paula J. Booth and Jane Clarke. Membrane protein folding makes the transition. *Proceedings of the National Academy of Sciences of the United States of America*, 107(9):3947–3948, 3 2010.

[14] Peter Bross, Brage S Andresen, Thomas J Corydon, and Niels Gregersen. Protein Misfolding and Degradation in Genetic Disease. *eLS*, 2 2011.

[15] Sandi Brudar and Barbara Hribar-Lee. Effect of buffer on protein stability in aqueous solutions: A simple protein aggregation model. *Journal of Physical Chemistry B*, 125(10):2504–2512, 3 2021.

[16] Gwen R. Buel and Kylie J. Walters. Can AlphaFold2 predict the impact of missense mutations on structure? *Nature Structural & Molecular Biology 2022 29:1*, 29(1):1–2, 1 2022.

[17] Laura S. Busenlehner, Simona G. Codreanu, Peter J. Holm, Priyaranjan Bhakat, Hans Hebert, Ralf Morgenstern, and Richard N. Armstrong. Stress sensor triggers conformational response of the integral membrane protein microsomal glutathione transferase 1. *Biochemistry*, 43(35):11145–11152, 9 2004.

[18] Antonello Calcutta, Christian M. Jessen, Manja Annette Behrens, Cristiano L.P. Oliveira, Maria Lourdes Renart, José M. González-Ros, Daniel E. Otzen, Jan Skov Pedersen, Anders Malmendal, and Niels Chr Nielsen. Mapping of unfolding states of integral helical membrane proteins by GPS-NMR and scattering techniques: TFE-induced unfolding of KcsA in DDM surfactant. *Biochimica et Biophysica Acta (BBA) - Biomembranes*, 1818(9):2290–2301, 9 2012.

[19] Juan C. Canul-Tec, Reda Assal, Erica Cirri, Pierre Legrand, Sébastien Brier, Julia Chamot-Rooke, and Nicolas Reyes. Structure and allosteric inhibition of excitatory amino acid transporter 1. *Nature 2016 544:7651*, 544(7651):446–451, 4 2017.

[20] Rahul Chadda, Nathan Bernhardt, Elizabeth G. Kelley, Susana C.M. Teixeira, Kacie Griffith, Alejandro Gil-Ley, Tuğba N. Öztürk, Lauren E. Hughes, Ana Forsythe, Venkatramanan Krishnamani, José D. Faraldo-Gómez, and Janice L. Robertson. Membrane transporter dimerization driven by differential lipid solvation energetics of dissociated and associated states. *eLife*, 10, 4 2021.

[21] Rahul Chadda, Lucy Cliff, Marley Brimberry, and Janice L. Robertson. A model-free method for measuring dimerization free energies of CLC-ec1 in lipid bilayers. *Journal of General Physiology*, 150(2):355–365, 2 2018.

[22] Rahul Chadda, Venkatramanan Krishnamani, Kacey Mersch, Jason Wong, Marley Brimberry, Ankita Chadda, Ludmila Kolmakova-Partensky, Larry J. Friedman, Jeff Gelles, and Janice L. Robertson. The dimerization equilibrium of a CLC CL-/ H+ antiporter in lipid bilayers. *eLife*, 5(AUGUST), 8 2016.

[23] Deepti Chaturvedi and Radhakrishnan Mahalakshmi. Transmembrane β-barrels: Evolution, folding and energetics. *Biochimica et biophysica acta. Biomembranes*, 1859(12):2467, 12 2017.

[24] Tapan K. Chaudhuri and Subhankar Paul. Protein-misfolding diseases and chaperone-based therapeutic approaches. *The FEBS Journal*, 273(7):1331–1349, 4 2006.

[25] Shi Jie Chen, Mubashir Hassan, Robert L. Jernigan, Kejue Jia, Daisuke Kihara, Andrzej Kloczkowski, Sergei Kotelnikov, Dima Kozakov, Jie Liang, Adam Liwo, Silvina Matysiak, Jarek Meller, Cristian Micheletti, Julie C. Mitchell, Sayantan Mondal, Ruth Nussinov, Kei Ichi Okazaki, Dzmitry Padhorny, Jeffrey Skolnick, Tobin R. Sosnick, George Stan, Ilya Vakser, Xiaoqin Zou, and George D. Rose. Protein folds vs. protein folding: Differing questions, different challenges. *Proceedings of the National Academy of Sciences of the United States of America*, 120(1):2214423119, 1 2023.

[26] Jordan H. Chill, John M. Louis, Frank Delaglio, and Ad Bax. Local and global structure of the monomeric subunit of the potassium channel KcsA probed by NMR. *Biochimica et biophysica acta*, 1768(12):3260, 12 2007.

[27] Ratul Chowdhury, Nazim Bouatta, Surojit Biswas, Christina Floristean, Anant Kharkar, Koushik Roy, Charlotte Rochereau, Gustaf Ahdritz, Joanna Zhang, George M. Church, Peter K. Sorger, and Mohammed AlQuraishi. Single-sequence protein structure prediction using a language model and deep learning. *Nature Biotechnology 2022 40:11*, 40(11):1617–1623, 10 2022.

[28] Gregory P. Connelly, Yawen Bai, Mei-Fen -F Jeng, and S. Walter Englander. Isotope effects in peptide group hydrogen exchange. *Proteins: Structure, Function, and Bioinformatics*, 17(1):87–92, 9 1993.

[29] Julio F. Cordero-Morales, Vishwanath Jogini, Sudha Chakrapani, and Eduardo Perozo. A Multipoint Hydrogen-Bond Network Underlying KcsA C-Type Inactivation. *Biophysical Journal*, 100(10):2387, 5 2011.

[30] Robin A. Corey, Zainab Ahdash, Anokhi Shah, Euan Pyle, William J. Allen, Tomas Fessl, Janet E. Lovett, Argyris Politis, and Ian Collinson. ATP-induced asymmetric pre-protein folding as a driver of protein translocation through the sec machinery. *eLife*, 8:1–25, 9 2019.

[31] Karolina Corin and James U Bowie. How physical forces drive the process of helical membrane protein folding. *EMBO reports*, 23(3):e53025, 3 2022.

[32] C. D. Cox, N. Bavi, and B. Martinac. Origin of the Force: The Force-From-Lipids Principle Applied to Piezo Channels. *Current Topics in Membranes*, 79:59–96, 1 2017.

[33] Lidia Cristian, James D. Lear, and William F. DeGrado. Use of thiol-disulfide equilibria to measure the energetics of assembly of transmembrane helices in phospholipid bilayers. *Proceedings of the National Academy of Sciences of the United States of America*, 100(25):14772–14777, 12 2003.

[34] Luis G. Cuello, D. Marien Cortes, and Eduardo Perozo. The gating cycle of a K+ channel at atomic resolution. *eLife*, 6, 11 2017.

[35] Paul Curnow, Natalie D. Di Bartolo, Kathleen M. Moreton, Oluseye O. Ajoje, Nicholas P. Saggese, and Paula J. Booth. Stable folding core in the folding transition state of an α-helical integral membrane protein. *Proceedings of the National Academy of Sciences of the United States of America*, 108(34):14133–14138, 8 2011.

[36] Florian Cymer, Rickard Hedman, Nurzian Ismail, and Gunnar Von Heijne. Exploration of the arrest peptide sequence space reveals arrest-enhanced variants. *Journal of Biological Chemistry*, 290(16):10208–10215, 4 2015.

[37] Florian Cymer and Gunnar Von Heijne. Cotranslational folding of membrane proteins probed by arrest-peptide- mediated force measurements. *Proceedings of the National Academy of Sciences of the United States of America*, 110(36):14640–14645, 9 2013.

[38] Annemieke Dalen, Martin Laan, Arnold J.M. Driessen, J. Antoinette Killian, and Ben Kruijff. Components required for membrane assembly of newly synthesized K+ channel KcsA. *FEBS Letters*, 511(1-3):51–58, 1 2002.

[39] Emily J. Danoff and Karen G. Fleming. Membrane defects accelerate outer membrane β-barrel protein folding. *Biochemistry*, 54(2):97–99, 1 2015.

[40] Erin Delaney, Pooja Khanna, Li Wei Tu, John M. Robinson, and Carol Deutsch. Determinants of pore folding in potassium channel biogenesis. *Proceedings of the National Academy of Sciences of the United States of America*, 111(12):4620–4625, 2014.

[41] Emily Deutsch, Aubrey V. Weigel, Elizabeth J. Akin, Phil Fox, Gentry Hansen, Christopher J. Haberkorn, Rob Loftus, Diego Krapf, and Michael M. Tamkun. Kv2.1 cell surface clusters are insertion platforms for ion channel delivery to the plasma membrane. *Molecular Biology of the Cell*, 23(15):2917–2929, 2012.

[42] Prasanna K. Devaraneni, Jordan J. Devereaux, and Francis I. Valiyaveetil. In vitro folding of K vAP, a voltage-gated K + channel. *Biochemistry*, 50(48):10442–10450, 12 2011.

[43] Taylor Devlin, Dagan C. Marx, Michaela A. Roskopf, Quenton R. Bubb, Ashlee M. Plummer, and Karen G. Fleming. FkpA enhances membrane protein folding using an extensive interaction surface. *Protein Science*, 32(4):e4592, 4 2023.

[44] Nguyen Minh Duc, Yang Du, Thor S. Thorsen, Su Youn Lee, Cheng Zhang, Hideaki Kato, Brian K. Kobilka, and Ka Young Chung. Effective application of bicelles for conformational analysis of G protein-coupled receptors by hydrogen/deuterium exchange mass spectrometry. *Journal of the American Society for Mass Spectrometry*, 26(5):808–817, 5 2015.

[45] Krisna C. Duong-Ly, Vikas Nanda, William F. DeGrado, and Kathleen P. Howard. The conformation of the pore region of the M2 proton channel depends on lipid bilayer environment. *Protein Science*, 14(4):856–861, 4 2005.

[46] R. A. Durst and B. R. Staples. Tris/Tris·HCl: A Standard Buffer for Use in the Physiologic pH Range. *Clinical Chemistry*, 18(3):206–208, 3 1972.

[47] Martin Lorenz Eisinger, Aline Ricarda Dörrbaum, Hartmut Michel, Etana Padan, and Julian David Langer. Ligand-induced conformational dynamics of the Escherichia coli Na+/H+ antiporter NhaA revealed by hydrogen/deuterium exchange mass spectrometry. *Proceedings of the National Academy of Sciences of the United States of America*, 114(44):11691–11696, 10 2017.

[48] Martin Lorenz Eisinger, Laiyin Nie, Aline Ricarda Dörrbaum, Julian David Langer, and Hartmut Michel. The Xenobiotic Extrusion Mechanism of the MATE Transporter NorM_PS from Pseudomonas stutzeri. *Journal of Molecular Biology*, 430(9):1311–1323, 4 2018.

[49] Donald M. Engelman, Yang Chen, Chen Ni Chin, A. Rachael Curran, Ann M. Dixon, Allison D. Dupuy, Albert S. Lee, Ursula Lehnert, Erin E. Matthews, Yana K. Reshetnyak, Alessandro Senes, and Jean Luc Popot. Membrane protein folding: beyond the two stage model. *FEBS Letters*, 555(1):122–125, 11 2003.

[50] Melanie Ernst, Esam A. Orabi, Randy B. Stockbridge, José D. Faraldo-Gómez, and Janice L. Robertson. Dimerization mechanism of an inverted-topology ion channel in membranes. *bioRxiv*, page 2023.01.27.525942, 1 2023.

[51] Nabil F. Faruk, Xiangda Peng, and Tobin R. Sosnick. Factors That Control the Force Needed to Unfold a Membrane Protein in Silico Depend on the Mode of Denaturation. *International Journal of Molecular Sciences*, 24(3):2654, 2 2023.

[52] Gustavo Fuertes, Niccolò Banterle, Kiersten M. Ruff, Aritra Chowdhury, Davide Mercadante, Christine Koehler, Michael Kachala, Gemma Estrada Girona, Sigrid Milles, Ankur Mishra, Patrick R. Onck, Frauke Gräter, Santiago Esteban-Martín, Rohit V. Pappu, Dmitri I. Svergun, and Edward A. Lemke. Decoupling of size and shape fluctuations in heteropolymeric sequences reconciles discrepancies in SAXS vs. FRET

measurements. *Proceedings of the National Academy of Sciences of the United States of America*, 114(31):E6342–E6351, 8 2017.

[53] Kristen A. Gaffney, Ruiqiong Guo, Michael D. Bridges, Shaima Muhammednazaar, Daoyang Chen, Miyeon Kim, Zhongyu Yang, Anthony L. Schilmiller, Nabil F. Faruk, Xiangda Peng, A. Daniel Jones, Kelly H. Kim, Liangliang Sun, Wayne L. Hubbell, Tobin R. Sosnick, and Heedeok Hong. Lipid bilayer induces contraction of the denatured state ensemble of a helical-bundle membrane protein. *Proceedings of the National Academy of Sciences of the United States of America*, 119(1):e2109169119, 1 2022.

[54] Christine Gajewski, Alper Dagcan, Benoit Roux, and Carol Deutsch. Biogenesis of the pore architecture of a voltage-gated potassium channel. *Proceedings of the National Academy of Sciences of the United States of America*, 108(8):3240–3245, 2011.

[55] Lizhi Gao, Xianqiang Mi, Vesa Paajanen, Kun Wang, and Zheng Fan. Activation-coupled inactivation in the bacterial potassium channel KcsA. *Proceedings of the National Academy of Sciences of the United States of America*, 102(49):17630–17635, 12 2005.

[56] Max Gemmer, Marten L. Chaillet, Joyce van Loenhout, Rodrigo Cuevas Arenas, Dimitrios Vismpas, Mariska Gröllers-Mulderij, Fujiet A. Koh, Pascal Albanese, Richard A. Scheltema, Stuart C. Howes, Abhay Kotecha, Juliette Fedry, and Friedrich Förster. Visualization of translation and protein biogenesis at the ER membrane. *Nature 2023 614:7946*, 614(7946):160–167, 1 2023.

[57] Moshe Giladi, Liat Van Dijk, Bosmat Refaeli, Lior Almagor, Reuben Hiller, Petr Man, Eric Forest, and Daniel Khananshvili. Dynamic distinctions in the Na+/Ca2+ exchanger adopting the inward- and outward-facing conformational states. *The Journal of Biological Chemistry*, 292(29):12311, 7 2017.

[58] A. Marcela Giudici, M. Luisa Molina, José L. Ayala, Estefanía Montoya, M. Lourdes Renart, Asia M. Fernández, José A. Encinar, Antonio V. Ferrer-Montiel, José A. Poveda, and José M. González-Ros. Detergent-labile, supramolecular assemblies of KcsA: Relative abundance and interactions involved. *Biochimica et Biophysica Acta - Biomembranes*, 1828(2):193–200, 2 2013.

[59] Ana Marcela Giudici, Maria Lourdes Renart, Clara Díaz-García, Andrés Morales, José Antonio Poveda, and José Manuel González-Ros. Accessibility of Cations to the Selectivity Filter of KcsA in the Inactivated State: An Equilibrium Binding Study. *International Journal of Molecular Sciences Article*, 2019.

[60] Casper A. Goverde, Benedict Wolf, Hamed Khakzad, Stéphane Rosset, and Bruno E. Correia. De novo protein design by inversion of the AlphaFold structure prediction network. *Protein Science : A Publication of the Protein Society*, 32(6), 6 2023.

[61] Norma J. Greenfield. Using circular dichroism spectra to estimate protein secondary structure. *Nature protocols*, 1(6):2876, 1 2006.

[62] Emily J. Guinn and Susan Marqusee. Exploring the denatured state ensemble by single-molecule chemo-mechanical unfolding: the effect of force, temperature and urea. *Journal of molecular biology*, 430(4):450, 2 2018.

[63] Sayan Gupta, Richard Celestre, Christopher J. Petzold, Mark R. Chance, and Corie Ralston. Development of a microsecond X-ray protein footprinting facility at the Advanced Light Source. *Journal of Synchrotron Radiation*, 21(4):690–699, 7 2014.

[64] Sayan Gupta, Jun Feng, Leanne Jade G. Chan, Christopher J. Petzold, and Corie Y. Ralston. Synchrotron X-ray footprinting as a method to visualize water in proteins. *Journal of Synchrotron Radiation*, 23(Pt 5):1056, 9 2016.

[65] Dietmar Hammerschmid, Valeria Calvaresi, Chloe Bailey, Benjamin Russell Lewis, Argyris Politis, Michael Morris, Laetitia Denbigh, Malcolm Anderson, and Eamonn Reading. Chromatographic Phospholipid Trapping for Automated H/D Exchange Mass Spectrometry of Membrane Protein–Lipid Assemblies. *Analytical Chemistry*, 18:54, 2 2023.

[66] Yoshitomo Hamuro and Terry Zhang. High-Resolution HDX-MS of Cytochrome c Using Pepsin/Fungal Protease Type XIII Mixed Bed Column. *Journal of the American Society for Mass Spectrometry*, 30(2):227–234, 2 2019.

[67] Binhan Hao, Wenjie Zhou, and Steven M. Theg. Hydrophobic mismatch is a key factor in protein transport across lipid bilayer membranes via the Tat pathway. *The Journal of biological chemistry*, 298(7), 7 2022.

[68] Nicola J. Harris, Grant A. Pellowe, Laura R. Blackholly, Samuel Gulaidi-Breen, Heather E. Findlay, and Paula J. Booth. Methods to study folding of alpha-helical membrane proteins in lipids. *Open biology*, 12(7), 7 2022.

[69] Christine M. Hebling, Christopher R. Morgan, Darrel W. Stafford, James W. Jorgenson, Kasper D. Rand, and John R. Engen. Conformational analysis of membrane proteins in phospholipid bilayer nanodiscs by hydrogen exchange mass spectrometry. *Analytical chemistry*, 82(13):5415, 7 2010.

[70] Jan Hegermann, Jens Overbeck, and Hildgund Schrempf. In vivo monitoring of the potassium channel KcsA in Streptomyces lividans hyphae using immunoelectron microscopy and energy-filtering transmission electron microscopy. *Microbiology*, 152(9):2831–2841, 9 2006.

[71] J. Michael Henderson, Alan J. Waring, Frances Separovic, and Ka Yee C. Lee. Antimicrobial Peptides Share a Common Interaction Driven by Membrane Line Tension Reduction. *Biophysical Journal*, 111(10):2176–2189, 11 2016.

[72] Ken ichiro Higashi, Shigeo Suzuki, Hiroshi Fujii, and Yutaka Kirino. Preparation and Some Properties of Giant Liposomes and Proteoliposomes. *The Journal of Biochemistry*, 101(2):433–440, 2 1987.

[73] Hagen Hofmann, Andrea Soranno, Alessandro Borgia, Klaus Gast, Daniel Nettels, and Benjamin Schuler. Polymer scaling laws of unfolded and intrinsically disordered proteins quantified with single-molecule spectroscopy. *Proceedings of the National Academy of Sciences of the United States of America*, 109(40):16155–16160, 10 2012.

[74] Alexandra I.C. Höhr, Sebastian P. Straub, Bettina Warscheid, Thomas Becker, and Nils Wiedemann. Assembly of β-barrel proteins in the mitochondrial outer membrane. *Biochimica et Biophysica Acta (BBA) - Molecular Cell Research*, 1853(1):74–88, 1 2015.

[75] Heedeok Hong. Toward understanding driving forces in membrane protein folding, 12 2014.

[76] Heedeok Hong and James U. Bowie. Dramatic destabilization of transmembrane helix interactions by features of natural membrane environments. *Journal of the American Chemical Society*, 133(29):11389–11398, 7 2011.

[77] Heedeok Hong, Hyun Kyu Choi, and Tae Young Yoon. Untangling the complexity of membrane protein folding. *Current opinion in structural biology*, 72:237, 2 2022.

[78] Wenbing Hu, Benjamin T. Walters, Zhong Yuan Kan, Leland Mayne, Laura E. Rosen, Susan Marqusee, and S. Walter Englander. Stepwise protein folding at near amino acid resolution by hydrogen exchange and mass spectrometry. *Proceedings of the National Academy of Sciences of the United States of America*, 110(19):7684–7689, 5 2013.

[79] K. S. Huang, H. Bayley, M. J. Liao, E. London, and H. G. Khorana. Refolding of an integral membrane protein. Denaturation, renaturation, and reconstitution of intact bacteriorhodopsin and two proteolytic fragments. *Journal of Biological Chemistry*, 256(8):3802–3809, 4 1981.

[80] Mohammad Shahedul Islam, Md Abul Kashem Mia, Mohammad Shamsur Rahman, Mohammad Shamsul Arefin, Pranab Kumar Dhar, and Takeshi Koshiba. Frequent contiguous pattern mining over biological sequences of protein misfolded diseases. *BMC Bioinformatics*, 22(1):1–28, 12 2021.

[81] Jaby Jacob, Bryan Krantz, Robin S. Dothager, P. Thiyagarajan, and Tobin R. Sosnick. Early Collapse is not an Obligate Step in Protein Folding. *Journal of Molecular Biology*, 338(2):369–382, 4 2004.

[82] David R. Jacobson and Thomas T. Perkins. Free-energy changes of bacteriorhodopsin point mutants measured by single-molecule force spectroscopy. *Proceedings of the National Academy of Sciences of the United States of America*, 118(13):e2020083118, 3 2021.

[83] Mavis Jiarong Li, Miklos Guttman, and William M. Atkins. Conformational dynamics of P-glycoprotein in lipid nanodiscs and detergent micelles reveal complex motions on a wide time scale. *The Journal of Biological Chemistry*, 293(17):6297, 4 2018.

[84] John Jumper, Richard Evans, Alexander Pritzel, Tim Green, Michael Figurnov, Olaf Ronneberger, Kathryn Tunyasuvunakool, Russ Bates, Augustin Žídek, Anna Potapenko, Alex Bridgland, Clemens Meyer, Simon A.A. Kohl, Andrew J. Ballard, Andrew Cowie, Bernardino Romera-Paredes, Stanislav Nikolov, Rishub Jain, Jonas Adler, Trevor Back, Stig Petersen, David Reiman, Ellen Clancy, Michal Zielinski, Martin Steinegger, Michalina Pacholska, Tamas Berghammer, Sebastian Bodenstein, David Silver, Oriol Vinyals, Andrew W. Senior, Koray Kavukcuoglu, Pushmeet Kohli, and Demis Hassabis. Highly accurate protein structure prediction with AlphaFold. *Nature 2021 596:7873*, 596(7873):583–589, 7 2021.

[85] John M. Jumper, Nabil F. Faruk, Karl F. Freed, and Tobin R. Sosnick. Trajectory-based training enables protein simulations with accurate folding and Boltzmann ensembles in cpu-hours. *PLOS Computational Biology*, 14(12):e1006578, 12 2018.

[86] Zhong Yuan Kan, Benjamin T. Walters, Leland Mayne, and S. Walter Englander. Protein hydrogen exchange at residue resolution by proteolytic fragmentation mass spectrometry analysis. *Proceedings of the National Academy of Sciences*, 110(41):16438–16443, 10 2013.

[87] Zhong Yuan Kan, Xiang Ye, John J. Skinner, Leland Mayne, and S. Walter Englander. ExMS2: An Integrated Solution for Hydrogen-Deuterium Exchange Mass Spectrometry Data Analysis. *Analytical Chemistry*, 91(11):7474–7481, 6 2019.

[88] Shachi Katira, Kranthi K. Mandadapu, Suriyanarayanan Vaikuntanathan, Berend Smit, and David Chandler. Pre-transition effects mediate forces of assembly between transmembrane proteins. *eLife*, 5(FEBRUARY2016), 2 2016.

[89] Anil Khanal, Yan Pan, Leonid S. Brown, and Lars Konermann. Pulsed hydrogen/deuterium exchange mass spectrometry for time-resolved membrane protein folding studies. *Journal of Mass Spectrometry*, 47(12):1620–1626, 12 2012.

[90] Sanguk Kim, Tae Joon Jeon, Amit Oberai, Duan Yang, Jacob J. Schmidt, and James U. Bowie. Transmembrane glycine zippers: Physiological and pathological roles in membrane proteins. *Proceedings of the National Academy of Sciences of the United States of America*, 102(40):14278–14283, 10 2005.

[91] Seoyoon Kim, Daehyo Lee, W. C. Bhashini Wijesinghe, and Duyoung Min. Robust membrane protein tweezers reveal the folding speed limit of helical membrane proteins. *eLife*, 12, 2023.

[92] Ofer Kimchi, Sarah L. Veatch, and Benjamin B. Machta. Ion channels can be allosterically regulated by membrane domains near a de-mixing critical point. *Journal of General Physiology*, 150(12):1769–1777, 12 2018.

[93] Janet D. Klein, Mitsi A. Blount, and Jeff M. Sands. Molecular Mechanisms of Urea Transport in Health and Disease. *Pflugers Archiv : European journal of physiology*, 464(6):561, 2012.

[94] Ann Kathrin Kniggendorf, David Schmidt, Bernhard Roth, Oliver Plettenburg, and Carsten Zeilinger. pH-Dependent Conformational Changes of KcsA Tetramer and Monomer Probed by Raman Spectroscopy. *International Journal of Molecular Sciences*, 20(11), 6 2019.

[95] Nozomu Kono, Niko Amin-Wetzel, and David Ron. Generic membrane-spanning features endow IRE1α with responsiveness to membrane aberrancy. *Molecular Biology of the Cell*, 28(17):2318–2332, 8 2017.

[96] Themis Lazaridis, John M. Leveritt, and Leo Pebenito. Implicit membrane treatment of buried charged groups: Application to peptide translocation across lipid bilayers. *Biochimica et Biophysica Acta (BBA) - Biomembranes*, 1838(9):2149–2159, 9 2014.

[97] Michael J. Lenaeus, Dylan Burdette, Tobias Wagner, Pamela J. Focia, and Adrian Gross. Structures of KcsA in complex with symmetrical quaternary ammonium compounds reveal a hydrophobic binding site. *Biochemistry*, 53(32):5365–5373, 8 2014.

[98] Jing Li, Jared Ostmeyer, Luis G. Cuello, Eduardo Perozo, and Benoît Roux. Rapid constriction of the selectivity filter underlies C-type inactivation in the KcsA potassium channel. *The Journal of general physiology*, 150(10):1408–1420, 10 2018.

[99] Long Li, Eunyong Park, Jing Jing Ling, Jessica Ingram, Hidde Ploegh, and Tom A. Rapoport. Crystal structure of a substrate-engaged SecY protein-translocation channel. *Nature 2016 531:7594*, 531(7594):395–399, 3 2016.

[100] Woon Ki Lim, Jörg Rösgen, and S. Walter Englander. Urea, but not guanidinium, destabilizes proteins by forming hydrogen bonds to the peptide group. *Proceedings of the National Academy of Sciences of the United States of America*, 106(8):2595–2600, 2 2009.

[101] Xiaoxuan Lin, Adam M. Zmyslowski, Isabelle A. Gagnon, Robert K. Nakamoto, and Tobin R. Sosnick. Development of in vivo HDX-MS with applications to a TonB-dependent transporter and other proteins. *Protein Science*, 31(9):e4402, 9 2022.

[102] Heng Liu, Hee Ryung Kim, R. N.V.Krishna Deepak, Lei Wang, Ka Young Chung, Hao Fan, Zhiyi Wei, and Cheng Zhang. Orthosteric and allosteric action of the C5a receptor antagonists. *Nature Structural & Molecular Biology 2018 25:6*, 25(6):472–481, 6 2018.

[103] Steve W Lockless, Ming Zhou, and Roderick MacKinnon. Structural and Thermodynamic Properties of Selective Ion Binding in a K+ Channel. *PLoS Biology*, 5(5):e121, 5 2007.

[104] E. London and H. G. Khorana. Denaturation and renaturation of bacteriorhodopsin in detergents and lipid-detergent mixtures. *Journal of Biological Chemistry*, 257(12):7003–7011, 6 1982.

[105] Benjamin B. Machta, Ellyn Gray, Mariam Nouri, Nicola L.C. McCarthy, Erin M. Gray, Ann L. Miller, Nicholas J. Brooks, and Sarah L. Veatch. Conditions that Stabilize Membrane Domains Also Antagonize n-Alcohol Anesthesia. *Biophysical Journal*, 111(3):537–545, 8 2016.

[106] Benjamin B. Machta, Stefanos Papanikolaou, James P. Sethna, and Sarah L. Veatch. Minimal model of plasma membrane heterogeneity requires coupling cortical actin to criticality. *Biophysical Journal*, 100(7):1668–1677, 2011.

[107] Benjamin B. Machta, Sarah L. Veatch, and James P. Sethna. Critical casimir forces in cellular membranes. *Physical Review Letters*, 109(13):1–5, 2012.

[108] Elhanan Magidovich and Ofer Yifrach. Conserved gating hinge in ligand- and voltage-dependent K+ channels. *Biochemistry*, 43(42):13242–13247, 10 2004.

[109] Justin T. Marinko, Hui Huang, Wesley D. Penn, John A. Capra, Jonathan P. Schlebach, and Charles R. Sanders. Folding and Misfolding of Human Membrane Proteins in Health and Disease: From Single Molecules to Cellular Proteostasis. *Chemical Reviews*, 119(9):5537–5606, 5 2019.

[110] Chloe Martens and Argyris Politis. A glimpse into the molecular mechanism of integral membrane proteins through hydrogen–deuterium exchange mass spectrometry. *Protein Science*, 29(6):1285–1301, 6 2020.

[111] Chloe Martens, Mrinal Shekhar, Antoni J. Borysik, Andy M. Lau, Eamonn Reading, Emad Tajkhorshid, Paula J. Booth, and Argyris Politis. Direct protein-lipid interactions shape the conformational landscape of secondary transporters. *Nature Communications*, 9(1):1–12, 12 2018.

[112] Chloe Martens, Mrinal Shekhar, Andy M. Lau, Emad Tajkhorshid, and Argyris Politis. Integrating Hydrogen-Deuterium exchange mass spectrometry with Molecular Dynamics simulations to probe lipid-modulated conformational changes in membrane proteins. *Nature Protocols*, 14(11):3183, 11 2019.

[113] John M. McBride, Konstantin Polev, Amirbek Abdirasulov, Vladimir Reinharz, Bartosz A. Grzybowski, and Tsvi Tlusty. AlphaFold2 can predict single-mutation effects on structure and phenotype. *bioRxiv*, page 2022.04.14.488301, 6 2023.

[114] Sarah K. McDonald, Talya S. Levitz, and Francis I. Valiyaveetil. A Shared Mechanism for the Folding of Voltage-Gated K + Channels. *Biochemistry*, 58(12):1660–1671, 3 2019.

[115] Shahid Mehmood, Carmen Domene, Eric Forest, and Jean Michel Jault. Dynamics of a bacterial multidrug ABC transporter in the inward- and outward-facing conformations. *Proceedings of the National Academy of Sciences of the United States of America*, 109(27):10832–10836, 7 2012.

[116] Joshua Meier, Roshan Rao, Robert Verkuil, Jason Liu, Tom Sercu, and Alex Rives. Language models enable zero-shot prediction of the effects of mutations on protein function. In M Ranzato, A Beygelzimer, Y Dauphin, P S Liang, and J Wortman Vaughan, editors, *Advances in Neural Information Processing Systems*, volume 34, pages 29287–29303. Curran Associates, Inc., 2021.

[117] Wenli Meng, Bowu Luan, Nicholas Lyle, Rohit V. Pappu, and Daniel P. Raleigh. The denatured state ensemble contains significant local and long-range structure under native conditions: Analysis of the N-terminal domain of ribosomal protein L9. *Biochemistry*, 52(15):2662–2671, 4 2013.

[118] Patrick S. Merkle, Kamil Gotfryd, Michel A. Cuendet, Katrine Z. Leth-Espensen, Ulrik Gether, Claus J. Loland, and Kasper D. Rand. Substrate-modulated unwinding of transmembrane helices in the NSS transporter LeuT. *Science Advances*, 4(5), 5 2018.

[119] Dragomir Milovanovic, Alf Honigmann, Seiichi Koike, Fabian Göttfert, Gesa Pähler, Meike Junius, Stefan Müllar, Ulf DIederichsen, Andreas Janshoff, Helmut Grubmüller, Herre J. Risselada, Christian Eggeling, Stefan W. Hell, Geert Van Den Bogaart, and Reinhard Jahn. Hydrophobic mismatch sorts SNARE proteins into distinct membrane domains. *Nature Communications 2015 6:1*, 6(1):1–10, 1 2015.

[120] Duyoung Min, Robert E. Jefferson, James U. Bowie, and Tae Young Yoon. Mapping the energy landscape for second-stage folding of a single membrane protein. *Nature Chemical Biology 2015 11:12*, 11(12):981–987, 10 2015.

[121] Shintaro Minami, Naohiro Kobayashi, Toshihiko Sugiki, Toshio Nagashima, Toshimichi Fujiwara, Rie Tatsumi-Koga, George Chikenji, and Nobuyasu Koga. Exploration of novel $\alpha\beta$-protein folds through de novo design. *Nature Structural & Molecular Biology 2023*, 118(3):1–9, 7 2023.

[122] A. E. Mirsky and Linus Pauling. On the Structure of Native, Denatured, and Coagulated Proteins. *Proceedings of the National Academy of Sciences*, 22(7):439–447, 7 1936.

[123] Kakoli Mitra, Iban Ubarretxena-Belandia, Tomohiko Taguchi, Graham Warren, and Donald M. Engelman. Modulation of the bilayer thickness of exocytic pathway membranes by membrane proteins rather than cholesterol. *Proceedings of the National Academy of Sciences of the United States of America*, 101(12):4083, 3 2004.

[124] Maria L. Molina, Francisco N. Barrera, Asia M. Fernández, Jose A. Poveda, Maria L. Renart, Jose A. Encinar, Gloria Riquelme, and Jose M. González-Ros. Clustering and coupled gating modulate the activity in KcsA, a potassium channel model. *Journal of Biological Chemistry*, 281(27):18837–18848, 7 2006.

[125] C. Preston Moon and Karen G. Fleming. Using tryptophan fluorescence to measure the stability of membrane proteins folded in liposomes. *Methods in enzymology*, 492:189, 2011.

[126] Peter B. Moore, Wayne A. Hendrickson, Richard Henderson, and Axel T. Brunger. The protein-folding problem: Not yet solved. *Science*, 375(6580):507, 2 2022.

[127] J. Mueller, J. S.L. Oliveira, R. Barker, M. Trapp, A. Schroeter, G. Brezesinski, and R. H.H. Neubert. The effect of urea and taurine as hydrophilic penetration enhancers on stratum corneum lipid models. *Biochimica et biophysica acta*, 1858(9):2006–2018, 9 2016.

[128] J. K. Nagy, W. L. Lonzer, and C. R. Sanders. Kinetic study of folding and misfolding of diacylglycerol kinase in model membranes. *Biochemistry*, 40(30):8971–8980, 7 2001.

[129] Alice Nevone, Giampaolo Merlini, and Mario Nuvolone. Treating Protein Misfolding Diseases: Therapeutic Successes Against Systemic Amyloidoses. *Frontiers in Pharmacology*, 11:557149, 7 2020.

[130] David Nguyen, Leland Mayne, Michael C. Phillips, and S. Walter Englander. Reference parameters for protein hydrogen exchange rates. *Journal of the American Society for Mass Spectrometry*, 29(9):1936, 9 2018.

[131] C. Nick Pace, Roy W. Alston, and Kevin L. Shaw. Charge-charge interactions influence the denatured state ensemble and contribute to protein stability. *Protein Science : A Publication of the Protein Society*, 9(7):1395, 2000.

[132] Jared Ostmeyer, Sudha Chakrapani, Albert C. Pan, Eduardo Perozo, and Benoît Roux. Recovery from slow inactivation in K+ channels is controlled by water molecules. *Nature*, 501(7465):121–124, 2013.

[133] John P. Overington, Bissan Al-Lazikani, and Andrew L. Hopkins. How many drug targets are there? *Nature Reviews Drug Discovery 2006 5:12*, 5(12):993–996, 12 2006.

[134] Marina A. Pak, Karina A. Markhieva, Mariia S. Novikova, Dmitry S. Petrov, Ilya S. Vorobyev, Ekaterina S. Maksimova, Fyodor A. Kondrashov, and Dmitry N. Ivankov. Using AlphaFold to predict the impact of single mutations on protein stability and function. *PLOS ONE*, 18(3):e0282689, 3 2023.

[135] Adrian Parsegian. Energy of an Ion crossing a Low Dielectric Membrane: Solutions to Four Relevant Electrostatic Problems. *Nature 1969 221:5183*, 221(5183):844–846, 1969.

[136] Wojciech Paslawski, Ove K. Lillelund, Julie Veje Kristensen, Nicholas P. Schafer, Rosanna P. Baker, Sinisa Urban, and Daniel E. Otzen. Cooperative folding of a polytopic α-helical membrane protein involves a compact N-terminal nucleus and nonnative loops. *Proceedings of the National Academy of Sciences of the United States of America*, 112(26):7978–7983, 6 2015.

[137] Olga Pavlova, Janine H. Peterson, Raffaele Ieva, and Harris D. Bernstein. Mechanistic link between β barrel assembly and the initiation of autotransporter secretion. *Proceedings of the National Academy of Sciences of the United States of America*, 110(10):E938–E947, 3 2013.

[138] Robin Pearce, Xiaoqiang Huang, Gilbert S. Omenn, and Yang Zhang. De novo protein fold design through sequence-independent fragment assembly simulations. *Proceedings of the National Academy of Sciences of the United States of America*, 120(4):e2208275120, 1 2023.

[139] Joana Pereira, Adam J. Simpkin, Marcus D. Hartmann, Daniel J. Rigden, Ronan M. Keegan, and Andrei N. Lupas. High-accuracy protein structure prediction in CASP14. *Proteins: Structure, Function, and Bioinformatics*, 89(12):1687–1699, 12 2021.

[140] Paul Pfeiffer, Alexei V. Egorov, Franziska Lorenz, Jan Hendrik Schleimer, Andreas Draguhn, and Susanne Schreiber. Clusters of cooperative ion channels enable a membrane-potential-based mechanism for short-term memory. *eLife*, 9, 2 2020.

[141] Stephan A Pless, Jason D Galpin, Ana P Niciforovic, Harley T Kurata, and Christopher A Ahern. Hydrogen bonds as molecular timers for slow inactivation in voltage-gated potassium channels. *eLife*, 2, 12 2013.

[142] Jean Luc Popot, Sue Ellen Gerchman, and Donald M. Engelman. Refolding of bacteriorhodopsin in lipid bilayers: A thermodynamically controlled two-stage process. *Journal of Molecular Biology*, 198(4):655–676, 12 1987.

[143] José A. Poveda, A. Marcela Giudici, M. Lourdes Renart, Oscar Millet, Andrés Morales, José M. González-Ros, Victoria Oakes, Simone Furini, and Carmen Domene. Modulation of the potassium channel KcsA by anionic phospholipids: Role of arginines at the non-annular lipid binding sites. *Biochimica et Biophysica Acta (BBA) - Biomembranes*, 1861(10):183029, 10 2019.

[144] Eamonn Reading, Zoe Hall, Chloe Martens, Tabasom Haghighi, Heather Findlay, Zainab Ahdash, Argyris Politis, and Paula J. Booth. Interrogating Membrane Protein Conformational Dynamics within Native Lipid Compositions. *Angewandte Chemie - International Edition*, 56(49):15654–15657, 12 2017.

[145] M. L. Renart, I. Triano, J. A. Poveda, J. A. Encinar, A. M. Fernández, A. V. Ferrer-Montiel, J. Gómez, and J. M. González Ros. Ion binding to KcsA: Implications in ion selectivity and channel gating. *Biochemistry*, 49(44):9480–9487, 2010.

[146] M. Lourdes Renart, A. Marcela Giudici, José A. Poveda, Aleksander Fedorov, Mário N. Berberan-Santos, Manuel Prieto, Clara Díaz-García, José M. González-Ros, and Ana Coutinho. Conformational plasticity in the KcsA potassium channel pore helix revealed by homo-FRET studies. *Scientific Reports*, 9(1):1–13, 12 2019.

[147] María L. Renart, Francisco N. Barrera, María L. Molina, José A. Encinar, José A. Poveda, Asia M. Fernández, Javier Gómez, and Jose M. González-Ros. Effects of conducting and blocking ions on the structure and stability of the potassium channel KcsA. *Journal of Biological Chemistry*, 281(40):29905–29915, 10 2006.

[148] María Lourdes Renart, Ana Marcela Giudici, Clara Díaz-García, María Luisa Molina, Andrés Morales, José M. González-Ros, and José Antonio Poveda. Modulation of function, structure and clustering of K+ channels by lipids: Lessons learnt from KcsA, 4 2020.

[149] Joshua A. Riback, Micayla A. Bowman, Adam M. Zmyslowski, Catherine R. Knoverek, John M. Jumper, James R. Hinshaw, Emily B. Kaye, Karl F. Freed, Patricia L. Clark, and Tobin R. Sosnick. Innovative scattering analysis shows that hydrophobic disordered proteins are expanded in water. *Science*, 358(6360):238–241, 10 2017.

[150] Ahmed Rohaim, Li Dong Gong, Jing Li, Huan Rui, Lydia Blachowicz, and Benoît Roux. Open and Closed Structures of a Barium-Blocked Potassium Channel. *Journal of Molecular Biology*, 432(17):4783–4798, 8 2020.

[151] Avia Rosenhouse-Dantsker and Diomedes E. Logothetis. New Roles for a Key Glycine and Its Neighboring Residue in Potassium Channel Gating. *Biophysical Journal*, 91(8):2860, 10 2006.

[152] Mason Rouches, Sarah L. Veatch, and Benjamin B. Machta. Surface densities prewet a near-critical membrane. *Proceedings of the National Academy of Sciences of the United States of America*, 118(40):e2103401118, 10 2021.

[153] Charles R. Sanders and Jeffrey K. Myers. Disease-Related Misassembly of Membrane Proteins. *https://doi.org/10.1146/annurev.biophys.33.110502.140348*, 33:25–51, 5 2004.

[154] K. Tanuj Sapra, Hüseyin Besir, Dieter Oesterhelt, and Daniel J. Muller. Characterizing Molecular Interactions in Different Bacteriorhodopsin Assemblies by Single-molecule Force Spectroscopy. *Journal of Molecular Biology*, 355(4):640–650, 1 2006.

[155] Sarah A. Shelby, Ivan Castello-Serrano, Kathleen C. Wisser, Ilya Levental, and Sarah L. Veatch. Membrane phase separation drives responsive assembly of receptor signaling domains. *Nature Chemical Biology 2023 19:6*, 19(6):750–758, 3 2023.

[156] Zakhar O. Shenkarev, Ekaterina N. Lyukmanova, Ivan O. Butenko, Lada E. Petrovskaya, Alexander S. Paramonov, Mikhail A. Shulepko, Oksana V. Nekrasova, Mikhail P. Kirpichnikov, and Alexander S. Arseniev. Lipid–protein nanodiscs promote in vitro folding of transmembrane domains of multi-helical and multimeric membrane proteins. *Biochimica et Biophysica Acta (BBA) - Biomembranes*, 1828(2):776–784, 2 2013.

[157] Seishi Shimizu and Kentaro Shimizu. Alcohol denaturation: Thermodynamic theory of peptide unit solvation. *Journal of the American Chemical Society*, 121(11):2387–2394, 3 1999.

[158] Kevin C. Song, Andrew V. Molina, Ruofan Chen, Isabelle A. Gagnon, Young Hoon Koh, Benoît Roux, and Tobin R. Sosnick. Folding and misfolding of potassium channel monomers during assembly and tetramerization. *Proceedings of the National Academy of Sciences*, 118(34):e2103674118, 8 2021.

[159] Yuan Song, Richard L. Schowen, Ronald T. Borchardt, and Elizabeth M. Topp. Formaldehyde production by Tris buffer in peptide formulations at elevated temperature. *Journal of Pharmaceutical Sciences*, 90(8):1198–1203, 8 2001.

[160] Igor Splawski, Jiaxiang Shen, Katherine W. Timothy, Michael H. Lehmann, Silvia Priori, Jennifer L. Robinson, Arthur J. Moss, Peter J. Schwartz, Jeffrey A. Towbin, G. Michael Vincent, and Mark T. Keating. Spectrum of Mutations in Long-QT Syndrome Genes. *Circulation*, 102(10):1178–1185, 9 2000.

[161] Xiaolei Su, Jonathon A. Ditlev, Enfu Hui, Wenmin Xing, Sudeep Banjade, Julia Okrut, David S. King, Jack Taunton, Michael K. Rosen, and Ronald D. Vale. Phase separation of signaling molecules promotes T cell receptor signal transduction. *Science*, 352(6285):595–599, 4 2016.

[162] Zhenwei Su, Emily C. Brown, Weiwei Wang, and Roderick MacKinnon. Novel cell-free high-throughput screening method for pharmacological tools targeting K+ channels. *Proceedings of the National Academy of Sciences of the United States of America*, 113(20):5748–5753, 5 2016.

[163] Jie Sun, Xiaoran Roger Liu, Shuang Li, Peng He, Weikai Li, and Michael L. Gross. Nanoparticles and photochemistry for native-like transmembrane protein footprinting. *Nature Communications 2021 12:1*, 12(1):1–10, 12 2021.

[164] Arunkumar Sundaram, Melvin Yamsek, Frank Zhong, Yogesh Hooda, Ramanujan S. Hegde, and Robert J. Keenan. Substrate-driven assembly of a translocon for multipass membrane proteins. *Nature 2022 611:7934*, 611(7934):167–172, 10 2022.

[165] Sandra Tan, Tong Tan Hwee, and Maxey C.M. Chung. Membrane proteins and membrane proteomics. *PROTEOMICS*, 8(19):3924–3932, 10 2008.

[166] Chad D. Tatko, Vikas Nanda, James D. Lear, and William F. DeGrado. Polar networks control oligomeric assembly in membranes. *Journal of the American Chemical Society*, 128(13):4170–4171, 4 2006.

[167] Rooban Thavarajah, Vidya Kazhiyur Mudimbaimannar, Joshua Elizabeth, Umadevi Krishnamohan Rao, and Kannan Ranganathan. Chemical and physical basics of routine formaldehyde fixation. *Journal of Oral and Maxillofacial Pathology : JOMFP*, 16(3):400, 9 2012.

[168] Ameer N. Thompson, David J. Posson, Pirooz V. Parsa, and Crina M. Nimigean. Molecular mechanism of pH sensing in KcsA potassium channels. *Proceedings of the National Academy of Sciences of the United States of America*, 105(19):6900–6905, 5 2008.

[169] H. Holden Thorp. Proteins, proteins everywhere. *Science*, 374(6574):1415, 12 2021.

[170] I. Triano, F. N. Barrera, M. L. Renart, M. L. Molina, G. Fernández-Ballester, J. A. Poveda, A. M. Fernández, J. A. Encinar, A. V. Ferrer-Montiel, D. Otzen, and J. M. González-Ros. Occupancy of nonannular lipid binding sites on KcsA greatly increases the stability of the tetrameric protein. *Biochemistry*, 49(25):5397–5404, 6 2010.

[171] Serdar Uysal, Luis G. Cuello, D. Marien Cortes, Shohei Koide, Anthony A. Kossiakoff, and Eduardo Perozo. Mechanism of activation gating in the full-length KcsA K + channel. *Proceedings of the National Academy of Sciences of the United States of America*, 108(29):11896–11899, 7 2011.

[172] Siavash Vahidi, Yumin Bi, Stanley D. Dunn, and Lars Konermann. Load-dependent destabilization of the γ-rotor shaft in FOF1 ATP synthase revealed by hydrogen/deuterium-exchange mass spectrometry. *Proceedings of the National Academy of Sciences of the United States of America*, 113(9):2412–2417, 3 2016.

[173] Francis I. Valiyaveetil, Roderick MacKinnon, and Tom W. Muir. Semisynthesis and folding of the potassium channel KcsA. *Journal of the American Chemical Society*, 124(31):9113–9120, 8 2002.

[174] Francis I. Valiyaveetil, Yufeng Zhou, and Roderick MacKinnon. Lipids in the structure, folding, and function of the KcsA K+ channel. *Biochemistry*, 41(35):10771–10777, 9 2002.

[175] Annemieke Van Dalen, Sander Hegger, J. Antoinette Killian, and Ben De Kruijff. Influence of lipids on membrane assembly and stability of the potassium channel KcsA. *FEBS Letters*, 525(1-3):33–38, 8 2002.

[176] Bert Van Den Berg, William M. Clemons, Ian Collinson, Yorgo Modis, Enno Hartmann, Stephen C. Harrison, and Tom A. Rapoport. X-ray structure of a protein-conducting channel. *Nature 2004 427:6969*, 427(6969):36–44, 12 2003.

[177] Wade D. Van Horn and Charles R. Sanders. Prokaryotic Diacylglycerol Kinase and Undecaprenol Kinase. *Annual review of biophysics*, 41(1):81, 6 2012.

[178] Anbazhagan Veerappan, Florian Cymer, Noreen Klein, and Dirk Schneider. The tetrameric α-helical membrane protein GlpF unfolds via a dimeric folding intermediate. *Biochemistry*, 50(47):10223–10230, 11 2011.

[179] Koen M. Visscher, João Medeiros-Silva, Deni Mance, João P.G.L.M. Rodrigues, Mark Daniëls, Alexandre M.J.J. Bonvin, Marc Baldus, and Markus Weingarth. Supramolecular Organization and Functional Implications of K+ Channel Clusters in Membranes. *Angewandte Chemie - International Edition*, 56(43):13222–13227, 2017.

[180] Gunnar Von Heijne. Membrane-protein topology. *Nature Reviews Molecular Cell Biology 2006 7:12*, 7(12):909–918, 12 2006.

[181] Rebecca M. Voorhees, Israel S. Fernández, Sjors H.W. Scheres, and Ramanujan S. Hegde. Structure of the mammalian ribosome-Sec61 complex to 3.4 Å resolution. *Cell*, 157(7):1632–1643, 6 2014.

[182] Rebecca M. Voorhees and Ramanujan S. Hegde. Structure of the Sec61 channel opened by a signal sequence. *Science*, 351(6268):88–89, 1 2016.

[183] Benjamin T. Walters, Leland Mayne, James R. Hinshaw, Tobin R. Sosnick, and S. Walter Englander. Folding of a large protein at high structural resolution. *Proceedings of the National Academy of Sciences of the United States of America*, 110(47):18898–18903, 11 2013.

[184] Zongan Wang, John M. Jumper, Karl F. Freed, and Tobin R. Sosnick. On the Interpretation of Force-Induced Unfolding Studies of Membrane Proteins Using Fast Simulations. *Biophysical Journal*, 117(8):1429–1441, 2019.

[185] Thomas G. Watkinson, Antonio N. Calabrese, James R. Ault, Sheena E. Radford, and Alison E. Ashcroft. FPOP-LC-MS/MS Suggests Differences in Interaction Sites of Amphipols and Detergents with Outer Membrane Proteins. *Journal of the American Society for Mass Spectrometry*, 28(1):50–55, 1 2017.

[186] Paul Whitley, Brayan Grau, James C. Gumbart, Luis Martínez-Gil, and Ismael Mingarro. Folding and Insertion of Transmembrane Helices at the ER. *International Journal of Molecular Sciences*, 22(23):12778, 12 2021.

[187] Qian Xiao, Ceara K. McAtee, and Xiaolei Su. Phase separation in immune signalling. *Nature Reviews Immunology*, 22(3):188–199, 2022.

[188] Y. Xu, L. Mayne, and S. W. Englander. Evidence for an unfolding and refolding pathway in cytochrome c. *Nature Structural Biology 1998 5:9*, 5(9):774–778, 1998.

[189] Menglin Yang, Morgan Hoeppner, Martial Rey, Alan Kadek, Petr Man, and David C. Schriemer. Recombinant Nepenthesin II for Hydrogen/Deuterium Exchange Mass Spectrometry. *Analytical Chemistry*, 87(13):6681–6687, 7 2015.

[190] Cui Ye, Zhaoshuai Wang, Wei Lu, and Yinan Wei. Unfolding study of a trimeric membrane protein AcrB. *Protein Science*, 23(7):897–905, 7 2014.

[191] Xi Zhang, Ellen Y.T. Chien, Michael J. Chalmers, Bruce D. Pascal, Jovylyn Gatchalian, Raymond C. Stevens, and Patrick R. Griffin. Dynamics of the β2-adrenergic G-protein coupled receptor revealed by hydrogen-deuterium exchange. *Analytical chemistry*, 82(3):1100, 2 2010.